2007

# Structure and Mobility through Capillary Electrophoresis

John T. Williams

# STRUCTURE AND MOBILITY THROUGH CAPILLARY ELECTROPHORESIS

A Dissertation

Submitted to the Bayer School

of Natural and Environmental Sciences

Duquesne University

In partial fulfillment of the requirements for

The degree of Doctor of Philosophy

By

John T. Williams

December 2007

STRUCTURE AND MOBILITY THROUGH

CAPILLARY ELECTROPHORESIS

By

John T. Williams

Approved July 11, 2007

| | |
|---|---|
| Dr. Mitchell E. Johnson<br>Associate Professor of Chemistry<br>and Biochemistry<br>(Dissertation Director) | Dr. Partha Basu<br>Associate Professor of Chemistry<br>and Biochemistry<br>(Committee Member) |
| Dr. Charles T. Dameron<br>Associate Professor of Chemistry<br>and Biochemistry<br>(Committee Member) | Dr. David Gallaher Jr.<br>Associate Professor of Chemistry<br>(External Member) |
| Dr. David W. Seybert<br>Dean, Bayer School of Natural and<br>Environmental Sciences<br>Professor of Chemistry and Biochemistry | Dr. Jeffry D. Madura<br>Chair, Department of Chemistry and<br>Biochemistry<br>Professor of Chemistry and Biochemistry |

# ABSTRACT


STRUCTURE AND MOBILITY THROUGH

CAPILLARY ELECTROPHORESIS

By

John T. Williams

December 2007

Dissertation Supervised by Dr. Mitchell E. Johnson

No. of Pages in Text:140

Through the modification of capillary coating procedures electroosmotic flow was controlled without altering the buffer properties. Aqueous buffers of differing ionic strengths were utilized in order to develop a better understanding of the surface properties of nanocrystalline lattices known as quantum dots. Secondary determination of nanocrystal surface properties was determined through the use of a zetasizer.

Non-aqueous buffers were utilized in order to determine the effect of the coating on aseparation of hydrophobic, biologically relevant fatty acids. A dynamic capillary surface coat was compared to a successive multiple ionic layer (SMIL) polymeric coat in reguards to resolution and stability. The SMIL coat was further modified to improve resolution in non-aqueous analysis of fatty acids.

Laser induced fluorescence detection was utilized for detection of fluorescently tagged fatty acids. The labeling reaction was studied in order to determine the low concentration limit of the labeling reaction. This reaction was then utilized to label an extraction of free fatty acids from bovine omentum. The electrophoretic technique was utilized to separate the extract to identify fatty acid composition.

# ACKNOWLEDGMENT

Most importantly I would like to thank God for guiding and sustaining me through the years. Yet again you have proven that truly everything is possible.

To my wife Ciara I would like to thank for her understanding over the years. Without your love and support driving me I would not be completing this document. Thank you also for humoring me when I get fired up over some aspect of the research and need to talk it out.

I would like to thank my advisor Dr. Mitch Johnson for guiding my work throughout my time in graduate school. Many times I have wondered how you are able to tell the future about how something may not work as well as I sometimes hope it would. Thank you for allowing me to work in the lab with the best toys in the department.

I would like to thank my committee members for reading my work throughout my graduate school career and for their generous help when it was needed. I greatly appreciate the help given to me during the time Mitch was on sabbatical.

To the Johnson group both past and present I say thank you to as well. To Jason Stokes, Tara Carpenter, and Tamanna Sultana thank you for their help getting me on my feet and learning how the department works. To Kristin Adams, thank you for many conversations about numerous instrumental problems that we somehow inherit from other graduate students. Brian Kail, even though not directly a part of the Johnson group your angle on problems over the years has proven priceless.

Finally, a special thanks is reserved for the Bayer School of Natural and Environmental Sciences for their generous financial support.

## 1.1 TABLE OF CONTENTS

Page

LIST OF TABLES

LIST OF FIGURES

# Chapter 1

# Development of a Separation Method for Rapid Determination of Quantum Dot Size and Surface Properties

## 1.1 Introduction

Quantum dot nanocrystals research has received significant development in the last decade for purposes ranging from biological labeling to size reduction of computer components [1, 2]. Both applications are possible through utilizing the nanocrystals' semi-conductor properties. The greatest area of growth in quantum dot research is that of the biological labeling research. Applications within nanocrystal research has primarily involved using quantum dots to label specific organelles of live cells within an organism [3]. Traditionally, organic dyes have been used in labeling experiments due to the wide variety of dyes available, yet organic dyes have several major drawbacks. Drawbacks in using organic dyes include structural changes in the dye causing photobleaching of the dye molecule when exposed to light, toxicity of the dye, and limited chemical stability of either the dye or dye/analyte conjugates [4]. Quantum dots are attractive labeling agents due to the wide variety of coats that can be applied to the surface of the nanocrystals [5,

6]. By altering the surface of the crystal, customizing a dot to have a specific property is possible. Properties such as solubility and toxicity can be altered without changing the optical properties to a great extent. Nontoxic coats such as peptides have been applied to nanocrystals to specifically bind the nanocrystal to desired locations and also to reduce the crystal's effect on the cell [7, 8].

Emission in a quantum dot is controlled through the size of the nanocrystal. Structural integrity of quantum dots while excited is far superior to organic dyes and therefore is far more photostable than organic dyes [9]. Optical properties such as excitation and emission wavelengths are controlled by the crystalline lattice size and the existence of any impurities within the core of the nanocrystal. Briefly, excitation of a particle will occur when enough energy is introduced into a system for an electron to be excited from the ground energy state (where all single particle valence orbitals are occupied and conduction band orbitals remain unoccupied) to an excited state (where a conduction band orbital becomes filled and a valence orbital is unoccupied). This is homologous to fluorescence in an organic dye, an electron moving from a highest occupied molecular orbitals (HOMO) to the lowest unoccupied molecular orbital (Figure 1). In either scenario, this addition of energy creates an electron in an excited state and a 'hole' in the lower energy state which together referred to as an electron-hole pair.

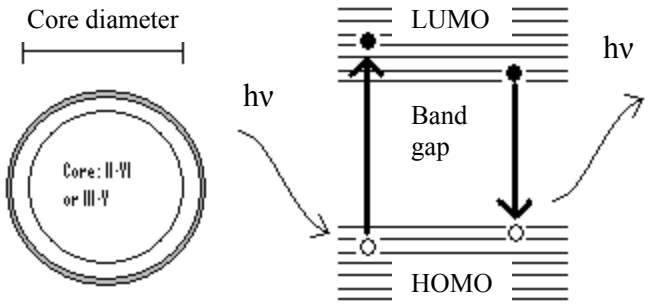


Figure 1. Size dependent fluorescence in a quantum dot is dependant on the core diameter being smaller than the exciton radius

In a nanocrystal, the excited electron "orbital" is confined by the size and shape of the crystalline lattice, and this confinement limits the distance between the excited electron and the 'hole'. The electron-hole pair is then referred to as the Bohr exciton radii and is defined by equation (1) where r is the distance between the electron and the corresponding hole, ε is the dielectric constant of the semiconductor, $m_r$ is the reduced mass of the electron-hole pair and e is the charge of an electron [10-12]. It is assumed that the nanocrystal is spherical for reasons of simplicity. TEM images have shown dots to be spherical in nature but the size of the crystal makes determination difficult [13]. When the excited electron falls back into the lower state fluorescence can occur. The excitation and emission energy corresponding to a crystal lattice is set by the band gap between the energy states. Energy will be altered from the expected bulk properties when a nanocrystal reaches a size close to the Bohr radius. The change in its band gap energy is shown in equation (2) where $E_g$ is the band gap energy, R is the quantum dot radii, $m_e$ is the mass of an electron, and $m_h$ is the mass of the hole. One of the largest advantages of quantum dot usage as biological tags, as their spectral properties are determined by their crystal size. A crystal with small dimensions (below the Bohr exciton radii) will cause confinement of the excited electron [14]. Due to this reason, the

(1) $$r = \frac{\varepsilon h^2}{\pi m_r e^2}$$

(2) $$E_g(quantumdot) = E_g(bulk) + (\frac{h^2}{8R^2})(\frac{1}{m_e} + \frac{1}{m_h}) - \frac{1.8e^2}{4\pi\varepsilon_0\varepsilon R}$$

crystal can absorb at any wavelength shorter than a threshold wavelength controlled by the crystal size. This property has shown itself to be useful in labeling experiments where different parts of cells are labeled with different size dots and then excited by a

single wavelength [3, 4, 15]. Both species of dots were seen to emit at their individual wavelengths.

Coatings that are used on nanocrystals are varied and not very well characterized when referring to the effect of the buffer in an aqueous system on the dot coating[16, 17]. The surface coverage of individual coats, how strongly the coat is bound to the crystals and the effect of the coat on both the optical properties and stability of the structure are topics currently under investigation in several labs [18, 19]. The chemical properties of these surface coats are key elements in determining the toxicity and solubility of dots however, the surface coats need to be characterized carefully with regard to surface coverage and chemical integrity. Without well defined surface properties, key information about the toxicity and solubility could prove problematic. In this study, information relating to the surface coverage and how the surface is affected by surrounding buffer was found.

### 1.1.1 Background of capillary electrophoresis

Capillary zone electrophoresis is a separation technique based on electrophoretic mobilities of analytes as they are driven by the electric field in the capillary. By exploiting the electrostatic properties of the species being separated, capillary electrophoresis has inherent advantages over chromatographic techniques, which exploit properties such as polarity and volatility. These advantages include increased number of theoretical plates due to a flat flow profile (Figure 2). By modifying the forces involved in capillary electrophoresis a system can be controlled to a greater extent and open up a wide range of applications including new analyte types, fast throughput and microscaling.

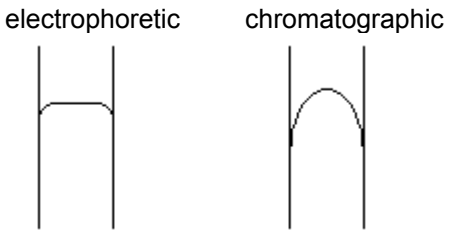


Figure 2. Flow profiles of electrophoretic and chromatographic systems

Electrophoretic mobility ($\mu_{ep}$) is the property of a given analyte. Any analyte will have its own inherent mobility when placed in an electric field in a given buffer. This mobility is the product of several components. First, the charge of the analyte in solution under an applied electric field will cause the analyte to migrate towards the capillary pole of opposite charge (equation 3). The mobility that is given by the charge is tempered by its effective size, or hydrated radius, within the solvent or buffer that the analyte is in.

Electroosmotic flow (EOF) is the bulk flow in electrophoresis arising from the charge on the capillary surface. While there are significant differences, EOF in electrophoresis is analogous to the pump in high performance liquid chromatography (HPLC) systems. This 'pump' utilized in CE has some major advantages over pressure driven pumps in that there are no moving parts and flow is constant after the initial momentum is gained. This creates a stable system for analytes to be separated without the need of the constraints that bulky pumps require.

The forces that will affect the EOF are primarily contained in the properties of the solvent used in the separation. There are three primary methods of altering the EOF in aqueous systems; changing the pH balance (Figure 3) (i.e., the potential differential between a surface and the bulk solution (zeta potential)), viscosity (Figure 4), and concentration of the buffer. The unfortunate aspect of manipulation of these three properties is that not only will concentration changes affect the EOF, but it will also affect electrophoretic mobility (EP) (equations 3-5), possibly to the detriment of the

(3) $$v_i = (\mu_{ep} + \mu_{eof})E$$

(4) $$\mu_{eof} = (\frac{\varepsilon_0}{4\pi\eta})\xi$$

(5) $$\mu_{ep} = \frac{q}{6\pi\eta r}$$

$\mu_{ep}$ = electrophoretic mobility
$\mu_{eof}$ = eletroosmotic mobility
$\xi$ = capillary zeta potential
$\eta$ = solvent viscosity
$\varepsilon$ = dielectric constant
$r$ = solvated radius
$q$ = analyte charge

separation. Alteration of the buffer pH can cause the analyte to protonate or deprotonate. By protonating or deprotonating the analyte of interest there will be a great affect on the EP of the analyte but could also potentially cause the analyte being studied to deteriorate. Altering the buffer concentration will cause the electronic double layer on both the capillary and colloidal analytes to be reduced or expanded (Figure 5). While this alteration can by beneficial to some separations, i.e. separations where the effect of buffer concentration will alter the EP to a greater extent than the alteration of the EOF, this is not always the case and it involves the undesirable alteration of two separate factors in the separation. Viscosity alterations can potentially be used to improve a separation, but careful attention to ionic strengths and Joule heating are necessary.

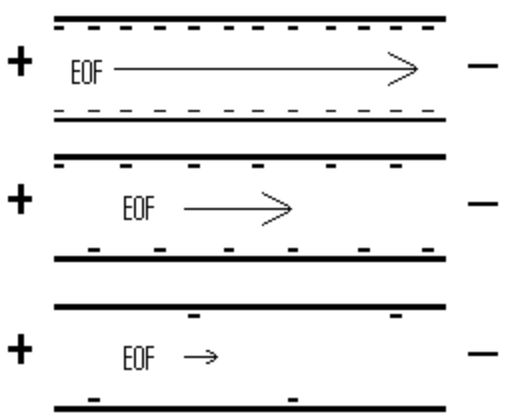


Figure 3. Effect of pH on EOF in a bare silica capillary: Top, high, pH; center, neutral pH; bottom, low pH

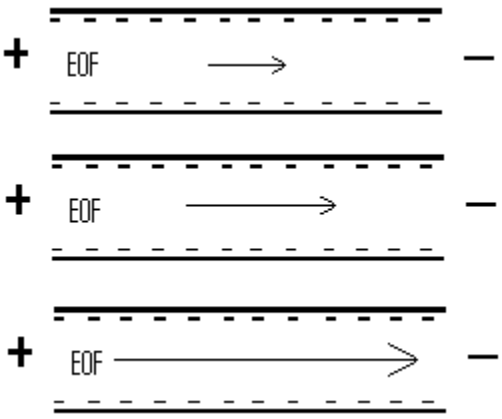


Figure 4. Effect of viscosity on EOF: Top, High viscosity; Bottom Low viscosity

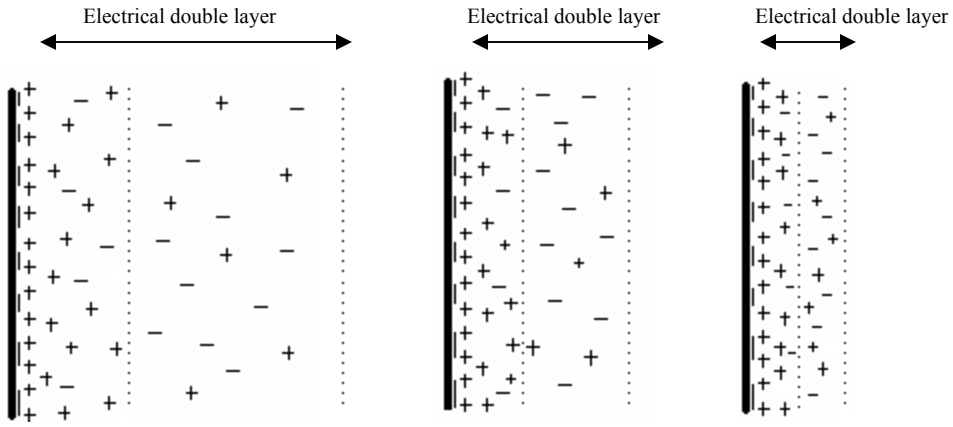


Figure 5. Raising buffer ionic strength will decrease the electronic double layer thickness. Left, dilute buffer (low ionic strength); right concentrated buffer (high ionic strength). Dotted lines indicate planes of zero potential (Helmholz planes)

A fourth method of altering EOF within a capillary is to alter the charge on the capillary by coating the capillary with a reagent that will modify the surface properties. The advantage of this method is that the EP is generally not affected by changes in wall coating (Equations 3-5, page 6). Careful attention to the modification method is needed to ensure that this is the case as analytes can potentially adhere to wall coatings. Disadvantages to coating methods can include difficult reactions when applying a coating to the surface of a capillary by using anhydrous, viscous, or hygroscopic solvents. Also, there is a chance of degradation of wall coatings over time, which will alter EOF and reduce reproducibility of separations in a coated capillary.

### 1.1.2 CE separation of charged particles

Capillary electrophoresis of charged particles has been an area that has become well understood over the last 40 years [20, 21]. The development of the field of colloidal material separations has led to an understanding of the forces involved in the electrophoretic separation of charged particles. Equation (5) describes the mobility of a

charged hard spherical particle in a buffer solution in that the factor $6\pi\eta R$ describes the translational friction coefficient. Equation 5, and the field in general, arose from the study of particles which are of similar scale to quantum dots (micometer to nanometer in diameter) and will by useful in this domain, but will not be useful when describing very large molecules such as proteins or very small particles such as small organic molecules.

One problem that has been known to arise when electrophoretic observation of particles on the scale of a quantum dots, or when observing larger colloidal material, is that the size of the particle can affect the separation to a greater extent than in small organic molecules or ions. A species may have a variety of properties which can cause electrophoretic heterogeneity (EH). In essence, the electric field surrounding the particle is non-uniform, causing a change in the expected electrophoretic mobility. Band broadening can occur and adversely effect in any separation attempted potentially causing the addition of separate species of the same colloid which are structurally identical, but have slightly different surface charges. A change differential within a particle will become apparent within the peak shape of any separated analytes and has been known to extend to the point of causing separate peaks for structurally identical species within an electropherogram [22]. The EH effect in colloidal systems is a major difference between an electrophoretic separation of larger particles and a separation of molecular compounds which will have a point charge, and therefore have homogenous electrophoretic mobilities.

When an electric field is applied to a larger particle in solution, such as what is found in a colloidal separation, the particle will migrate depending on its charge and size. The nature of this movement is well established for smaller particles in the literature and

equations that describe the motion of particles under an electric field (equation 6) can be found in many textbooks [23]. Briefly, Equation 6 describes the force applied through the electric field and the charge of the particle itself. In a larger particle the frictional forces that retard the migration of the particle are described by Equation 7 and include the viscosity of the solvent (η) the size of the particle (*a*) and the velocity of the particle due to the electrophoretic mobility of the particle ($\mu_{ep}$). With an electric charge applied to a capillary, the size of the colloid and the density of the charge on the surface has the potential to deform. This deformation can shield the colloid potentially causing a difference in the particle's $\mu_{ep}$. Equation 8 defines the particles electric double layer. A double layer describes the concentration of ions that will be high at the surface of the particle. This charged layer will be reduced to the ionic concentration of the bulk solvent as the distance from the particle increases. The double layer is identical to the diffuse double layer that is attributed to the capillary itself, but is not stationary. Due to the charged layer extending out into the buffer a shielding force is found. The relationship between particle zeta potential, charge and size are described in equation 9. This force is referred to as a shielding force due to its ability to alter the apparent charge of the particle and therefore alter the mobility from what the total surface charge of the particle would be. Effectively, the diffuse double layer will cause a reduction in mobility by reducing

(6) $$F_E = qE$$

(7) $$F_F = 6\pi\eta a\mu_{ep}$$

(8) $$\kappa = 2^{1/2} Ne(\varepsilon_0 \varepsilon RT)^{-1/2} I^{1/2}$$

(9) $$F_S = (\varepsilon\zeta a - q)E$$

$q$ = particle charge
$E$ = electric field
$\eta$ = viscosity
$a$ = stokes radius
$\varepsilon$ = dielectric constant
$\mu_{ep}$ = electrophoretic mobility
$\varepsilon_0$ = permittivity of free space
$\zeta$ = zeta potential

the effective charge on the particle (q in equation 6). The reduction in charge due to the diffuse double layer has been shown to drastically alter the separations of particles, such as dendrimers, under electrophoretic conditions [24]. Several groups have found that the retarding forces can be dominating within a separation of colloids and similar sized particles and it is well established that the effect is altered by pH and ionic strength of the surrounding buffer [21, 24-26].

## 1.2 Experimental

### 1.2.1 Laser induced fluorescence

Detection of analytes separated by capillary zone electrophoresis can present a challenge in that there are a wide variety of detection systems available, but few that can detect at the low concentration that is needed to avoid overloading a capillary. Common detection systems include absorbance, fluorescence, and electrical conductivity. CE has also been coupled to mass spectrometry in order to gain structural information on the analyte. Among these detection methods, fluorescence detection is ideal for applications involving quantum dots. The semiconducting nature of the nanocrystals creates a property that is easily distinguishable from solvent background through the use of fluorescence excitation/emission. Detection limits can be further decreased by utilizing laser induced fluorescence (LIF). A decrease in detection limit can only be realized if there is tight control over the excitation radiation in terms of intensity and wavelength control.

### 1.2.2 Instrumentation

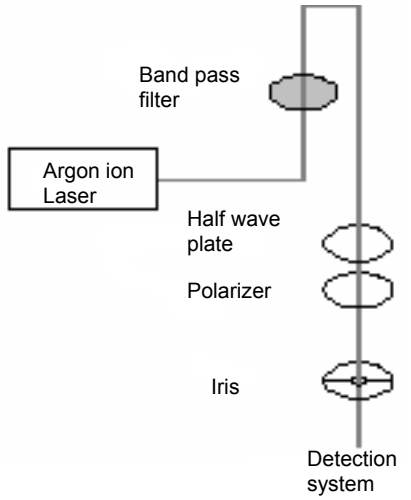


Figure 6. Excitation optics

Decreasing the background is important in laser induced fluorescence. This is done by controlling the laser intensity, wavelength and focus. In Figure 6, the setup for control over the excitation can be seen. The 488.0 nm beam is emitted from an air cooled argon ion laser (American Laser LS1000) and the height and angle are adjusted by reflecting through a series of high optical quality mirrors (not explicitly shown on Figure 6). To reject other laser lines and minimize broadband plasma background, a XL06 narrow bandpass filter (Omega Optical, Brattlebro, VT) is placed into the beam. A half-wave plate (Karl Lambert, Chicago IL.) is used in conjunction with a polarizer (Karl Lambert) to control the intensity of the beam along with controlling the polarization of the light. One problem that is caused by these adjustments is that, regardless of the quality of the optics, the beam will reflect partially off of each optical surface. Commonly called 'ghosts', these reflections can cause an increased background from stray light. To lessen the effect of these ghosts, an iris is placed in the beam. The beam is then reflected into a 505DRLP dichroic filter (Omega Optical, Brattleboro, VT) and into the capillary through a microscope objective (Fluor 40, Nikon, Tokyo Japan).

The fused silica capillary with dimensions of 50 μm internal diameter (ID), 350 μm outer diameter (OD) and 65 cm in length is prepared for detection by the pyrolyze of a 1 cm portion of the polyimide coating at 35 cm from the injection point. Removal of the coating can be done by two methods. The first is to use a low intensity flame such as

a butane torch. The second is to apply hot sulfuric acid drop wise to the capillary portion to be exposed. This will expose bare silica and decrease the flexibility of that section of the capillary. The capillary is affixed to a microscope slide using epoxy in order to ensure the capillary does shift out of the detection alignment when placed on the microscope stage.

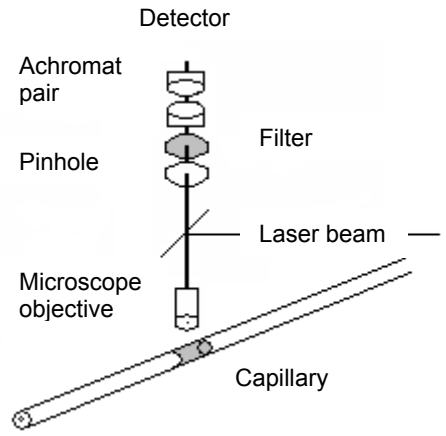

Figure 7. Detection optics

A portion of the fluorescence emitted from the capillary will travel through the detection optics and to the detector (Figure 7). The focused light from the objective was passed through a 100 μm pinhole (Melles Griot, Irvine CA) to remove potential 'ghosts'. In order to filter out the Rayleigh scattering and the laser light reflected back from the capillary a long pass filter (525DRLP, Omega Optical) was added. Several filters were tried for this purpose, as the fluorescence of several different species of nanocrystal were used, and each had a specific fluorescence (more below). The remaining fluorescence was focused by an achromat pair (CVI laser corporation) onto the active area of a photon-counting, avalanche diode detector (SPCM-AQ-131, EG&G Optoelectronics Canada, Vaudreuil, Quebec). Data was collected on a Pentium II PC through a multi-channel scalar card and the readings were through MCS software (MCS II, Oxford Tennelec/Nucleus, Oak Ridge, TN).

A Zetasizer 3000 (Malvern Instruments) was used to find the hydrodynamic radius through dynamic light scattering (zeta size) and surface potential (zeta potential) of both the quantum dots and the microspheres. Zeta size is a measurement of the particle

size based on its movement in a buffer. This instrument uses dynamic light scattering to find the Brownian motion and calculate the particle size distribution. Zeta potential is a measurement describing a particles electrophoretic mobility in a buffer. The Zetasizer 3000 uses the laser Doppler effect to detect particles moving electrophoretically in a quartz channel.

### 1.2.3 Buffers and reagents

Borate buffer used in the experiments was made by combining boric acid (Acros Organics) with borax (Acros Organics) to the desired pH. The ionic strength was adjusted through dilution and addition of NaCl (Fisher). Coumarin 334 laser dye (Acros Organics) was used to measure direction and magnitude of EOF in the separations. All water used for buffers was double filtered through a Nanopure water system (Barnstead) to 18 MΩ cm and all buffers were filtered through 0.2 μm membrane filters.

In order to find a method for the determination of the mobility of quantum dots, a model separation system was developed for the determination of the mobility of latex microspheres. The mobility of the microspheres was determined in two different methods, free zone capillary electrophoresis, and a zeta-sizing instrument.

Polymer latex microspheres were obtained from Polysciences, Inc. (Warrington, PA). The full description of the particles, sold as Fluoresbrite brand, can be obtained from the manufacturer's website (www.polysciences.com). In short, these particles were spherical particles with diameters ranging from 500 nm to 100 nm. The particles were terminated on the surface with carboxylate groups or, for the natural latex spheres, with sulfonate groups. The two surfaces were utilized in order to determine the effect of

surface charge density with differing buffer ionic strength and pH on particle mobility. Injection concentrations for the microspheres were at 25 ppm solid content. This method caused the larger particles to have lower concentrations (352 nm particles had 1.7 pM concentration and the 100 nM particles had 76 nM concentration). All solutions within the electrophoresis experiments contained 10 nM coumarin 334 as a neutral marker for determining electroosmotic flow.

Quantum dots that were used in the experiments were purchased from Evident Technologies. Two series of nanocrystals were purchased, one that was stabilized through tri-octylphosphine oxide (TOPO) which gave rise to the series being insoluble in aqueous buffer. The other series was coated in a water soluble coating that the manufacturer specifications indicate was acid functionalized. Detailed information on either coating was not available due to proprietary information that was not made available.

Both series of quantum dots had a similar structure. The crystals were said to be 'core-shell' quantum dots. This refers to the crystal structure of the individual dots in that the dot had a core of a semiconducting material and this core was surrounded by a layer of another crystal with a slightly larger band gap. The final layer on the nanocrystals is the functionalized coating that gives rise to the solubility properties discussed above. The crystals that were purchased for these experiments consisted of a core of cadmium selenide and a shell of zinc sulfide. The dots fluoresced at wavelengths that depended on the size of the core crystal lattice. Three TOPO caped nanocrystals were observed, these included the Andirondack Green (2.1 nm diameter, emission 520 nm), Catskill Green (2.4 nm diameter, 540 nm emission) and Hops Yellow (2.6 nm

diameter, 560 nm emission) dots. Aqueous soluble dots included Andirondack Green, Catskill Green, Hops Yellow, Birch Yellow (3.2 nm diameter, 570 nm emission) and Forest Orange (4 nm diameter, 590 nm emission). The full diameter of the total crystal was unknown in either series.

## 1.3 Results and discussion

Microspheres were injected at the positive pole (anode) of uncoated fused silica capillaries. The microspheres migrated toward the negative pole (cathode) and separated based on their size and their surface charge. The order of elution is key in identifying the

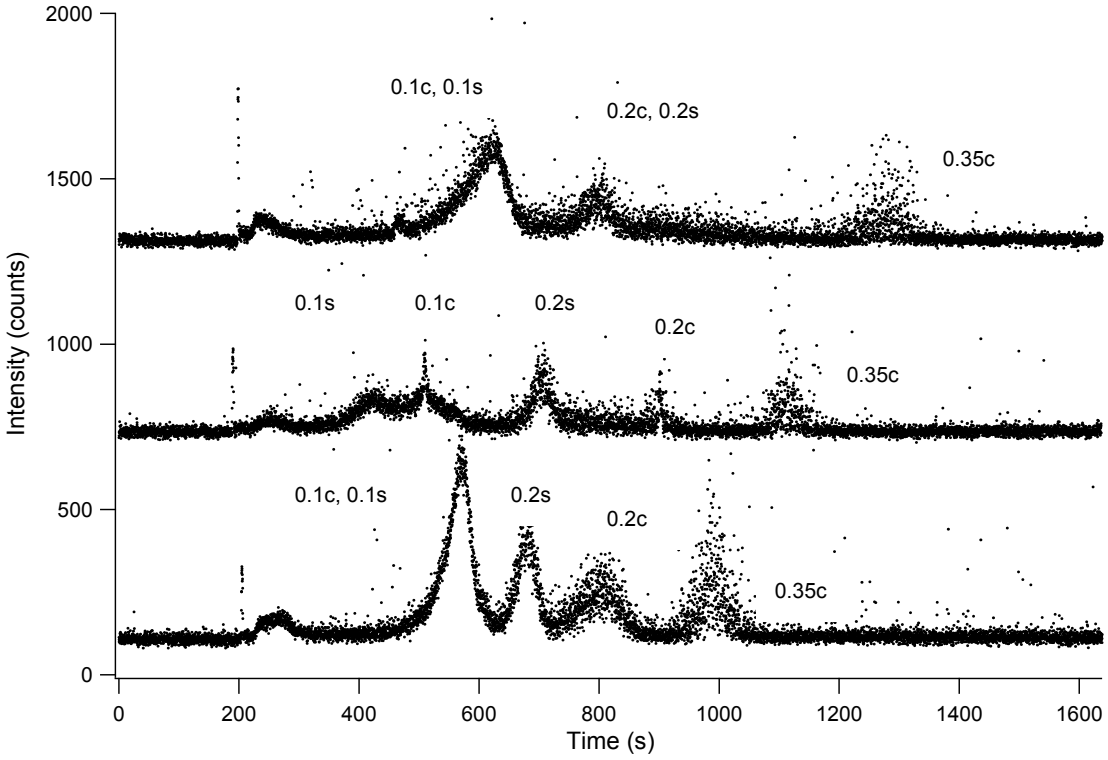


Figure 8. Microsphere separations showing change in total ionic strength. top I=0.010, center I=0.015, bottom I=0.020 Borate buffer pH = 9.2, 5s 5kV electrokinetic injections, capillary ID = 50μm; excitation at 488 nm 50 μW laser power. Number indicates particle size in μm, letter corresponds to carboxylates or sulfonated surfaces. Subsequent traces are shown with an offset.

mobilities within any separation and this separation is no different. Larger microspheres were found to elute later than the smaller microspheres (Figure 8). This indicates that the EOF velocity is possibly in the same direction of the EP velocity of the spheres. Although the surface properties are not entirely known due to intellectual property rights owned by Polysciences, what is known about them is that the surface groups are terminated with either a carboxylate coat or a sulfate group. With the high pH (9.2), the surface of the spheres has a net negative charge. As a secondary observation against this interpretation, the EP intrinsic to the spheres cannot be in the same direction as the EOF due to the fact that the neutral marker, coumarin 334, migrates faster than the spheres. Although the dye will be governed by a slightly different separation mechanism than the spheres, the primary difference between the two separation mechanisms is that there is less of a frictional component to the dye separation mechanism. This indicates that the EP velocity of the spheres is opposite to the EOF.

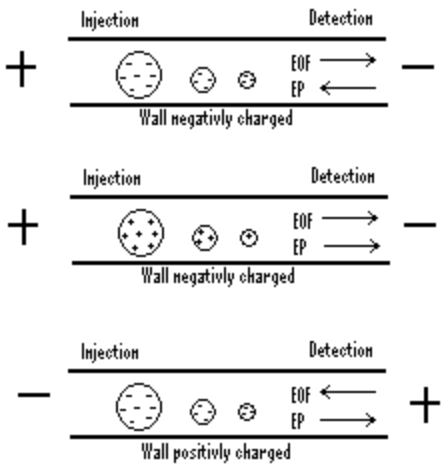


Figure 9. Three possible scenarios for the explanations of the order of migration of microspheres

The remaining scenario left for interpretation of the separations (shown in Figure 9) is that the EOF velocity is from anode to cathode and the EP velocity of the spheres is in the opposite direction. The conclusion that can be drawn from this observation is that the EP of the larger spheres would be larger than the EP of the smaller spheres. This is likely due to a higher charge density on the larger spheres, coupled with a relatively small change in hydrodynamic radii and low viscosity of the buffer used for separation.

Secondary confirmation of this increase in negative surface charge is desirable and is discussed below.

The apparent mobility of the spheres in the separation is the vector sum of the EOF velocity and the EP velocity. It is established that the EP velocity is one primary factor that will yield a separation. In order to understand the effect of the EP, the equations outlined in equation 1-3 (page 6) are not sufficient. This is due to the electric double layer on the particles themselves. This effect is explained in depth in [25] but briefly, Figure 10 shows a picture depicting a colloidal particle in a solution with an applied electric field. The charge of that particle will be affected by the applied electric field to cause the particle to migrate to either the cathode or anode depending on the charge of the particle. In the case of microspheres, this would be towards that positively charged anode at higher pH when the carboxylate groups deprotonate. Due to this movement, the particle will have a frictional force of an opposite direction to the direction of its migration.

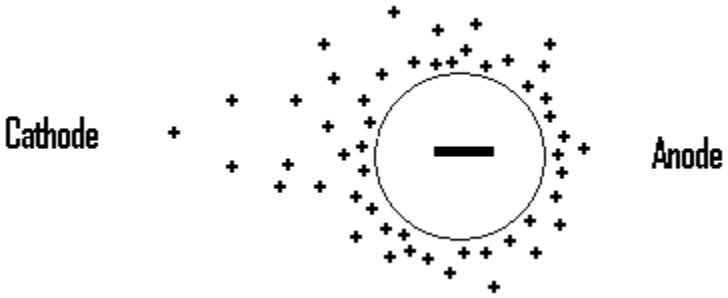


Figure 10. The diffuse layer of ions surrounding the quantum dots in solution

When a colloidal particle with a surface charge is in a solution with an applied potential, the particle will begin to attract ions of opposite charge from the solution. When this happens a potential, described through the Smoluchowski and Hückel equations (equations 6-9, page 9), is created with a depth (its effect upon the buffer

solution) extending out from the surface. Its effect will lessen with increasing distance from the particle surface, this effect is reduced exponentially with a decay constant of 1/κ. This gives rise to a third force acting on the particle (equations 6,7 and 9) Combining the equations Henry made a combined mobility equation for colloidal particles (equation 10) [27]. F(κa) within equation 10 is the expansion shown in equation

(10) $$\mu_{ep} = \varepsilon\zeta a / 6\pi\eta * f(\kappa a)$$

$\zeta$ = zeta potential
$\eta$ = viscosity
$a$ = stokes radius
$\varepsilon$ = dielectric constant
$f(\kappa a)$ = effective size

11 and is an approximation for spherical particles within solution.

Using the theory described in equation 8, the zeta potential and the Debye length were calculated at several ionic strengths (table 1). This data agrees closely with previously reported data[28].

Electrophoresis was used to separate the microspheres and to determine the zeta potential through the use of the Smoluchowski and Huckle equations. These equations can describe colloidal particles due to the affect that the particle's surface charge has on the bulk solution. Particle charge will effect the mobility of the particles in solution by attracting ions and creating the ionic double layer mentioned above. Using the combined equation (11) for the particle's mobility f(κa) was found by expanding the function

(11) $$f(\kappa a) = \frac{3}{2} - \frac{9}{2\kappa a} + \frac{75}{2\kappa^2 a^2} - \frac{330}{\kappa^3 a^3}$$

(12) $$\mu_E = (4\pi\varepsilon_0) * (\frac{D\zeta}{6\pi\eta})$$

$\eta$ = viscosity
$a$ = stokes radius
$\mu_E$ = electrophoretic mobility
$\varepsilon_0$ = permittivity of free space
$\zeta$ = zeta potential
$\kappa$ = 1/debye length
$D$ = diffusion coefficient

Table 1. $\kappa a$ values – size determined through manufacturer's specifications

| Ionic strength | 100 nm | 110 nm | 202 nm | 217 nm | 350 nm | EDL thickness (nm) |
|---|---|---|---|---|---|---|
| 0.0100 M | 11.26 | 12.33 | 35.18 | 36.66 | 55.93 | 3.04 |
| 0.0150 M | 13.79 | 15.10 | 43.09 | 44.90 | 68.69 | 2.48 |
| 0.0200 M | 15.93 | 17.44 | 49.75 | 51.85 | 79.10 | 2.15 |

equation (12). This expansion assumes that the particles are spherical which is a valid assumption when discussing microspheres, but potentially could bring about a degree of error when smaller, less characterized species such as quantum dots are discussed. The zeta potential for each sphere was found by using the mobility of the spheres in solution (table 2) and solving for the zeta potential (table 3). The small differences in the zeta potential of the spheres of the same size are due to the small differences in the ionic strength in the buffer solutions.

Table 2. Electrophoretic mobility values ($cm^2/V\ s$) x $10^{-3}$

| Ionic strength | 100 nm | 110 nm | 202 nm | 217 nm | 350 nm | EOF |
|---|---|---|---|---|---|---|
| 0.0100 | -7.5 | -7.8 | -8.6 | -8.7 | -9.7 | 11.47 |
| 0.0150 | -6.6 | -7.6 | -8.7 | -9.5 | -9.9 | 11.99 |
| 0.0200 | -6.9 | -7.1 | -7.8 | -8.3 | -8.8 | 11.10 |

Table 3. ζ-potential (mV)

| Ionic strength | 100 nm | 110 nm | 202 nm | 217 nm | 350 nm |
|---|---|---|---|---|---|
| 0.0100 | -10.15 | -10.41 | -11.34 | -11.36 | -12.54 |
| 0.0150 | -9.01 | -10.18 | -11.48 | -12.45 | -12.89 |
| 0.0200 | -9.31 | -9.48 | -10.15 | -10.80 | -11.38 |

### 1.3.1 Sphere mobility information from zeta sizer

A particle sizing instrument was used in order to gain secondary confirmation of the size and surface properties of the microspheres. Relative particle size information can be gained by observing particles diffusing in and out of a laser beam spot. The particles scatter, the laser radiation which is collected and averaged. By measuring the amount of scatter an average value for a particular concentration of particles can be found. This average will vary depending on the particles under the detection zone which will be governed by the Brownian motion of the particles. The change in the scatter can then be used to determine the relative size of the particles through statistical methods. This will determine the particle's effective size in a solution by using its mobility in a solution. This effective size is referred to as the particle's zeta size.

The goal of the experiment was to determine whether there was a significant change from the actual size of the particle and the particle's effective size in water. Polysciences offers particle size information in their literature which is measured through microscopic methods (TEM). These sizes will take into account only the physical size of the particles. In Figure 11 the zeta size was plotted against the company TEM measured

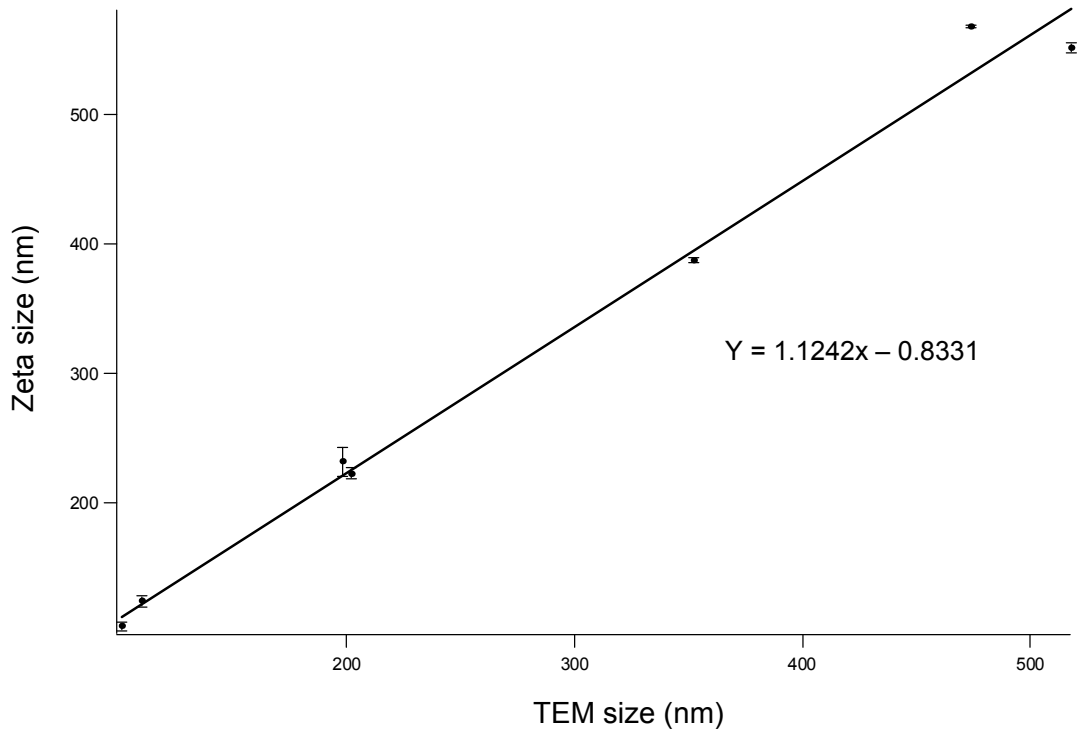


Figure 11. TEM measured size from Evident Technologies graphed against the zeta size found for each sphere. Each point represents 3 measurements

size. What is clear from this data is that the particles closely follow the manufacture's specified sizes. Only small changes are observed when the particles are added to an aqueous solution (Figure 11). It should be noted that particle zeta size will be affected by the ionic strength of the surrounding buffer. The ionic strength used in this experiment was 0.010 and a higher ionic strength would reduce the size of the spheres. The higher that the ionic strength becomes, the smaller that the hydrodynamic radii will become. This is due to a reduction of the effect that the particle surface charge has on its solution.

Zeta potential was also determined using the Zetasizer 3000 in order to give a secondary measurement of the particle surface potential in solution. In Figure 12 the zeta size is plotted against the zeta potential to determine if a trend exists in the size of the particles and its zeta potential in solution. Two trends become apparent in this data. First is the correlation between the particle size for the particle zeta potential. These two

properties should be correlated so long as we assume that the coat of the materials are identical. As the species of particles increase in size, the surface charge will be larger even if the charge density remains the same. Similar results were found when using capillary electrophoresis, observing the order of migration. The unfortunate aspect to these finding is that the 0.2c and 0.2p spheres reversed in order. A change in order is unexpected as the 0.2p spheres were found to migrate faster when injected into an electrophoresis separation.

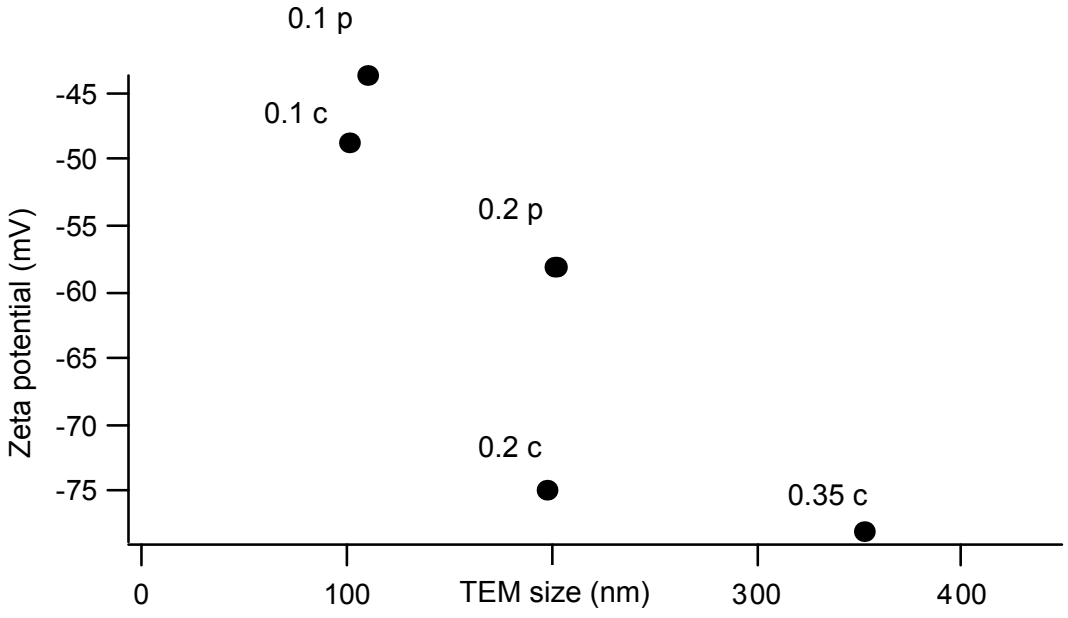


Figure 12. Zeta potential plotted against zeta size. The larger microspheres are shown to have a larger surface charge

One other interesting aspect of this data is that the particles in the carboxylate series follow closely to a linear line as the size increases in regards to the zeta potential. This trend is not nearly as obvious when the sulfonated particles are added onto the graph. This indicates that the difference in surface charge density between the two surface coatings are changing the zeta potential, and therefore particle mobility, to a high degree. This relationship is described in equation 11 and fully explained in the literature

[25]. The primary utility of the equation in this application is the relationship between the κa value, zeta potential ζ and the surface charge $\sigma_e$.

The mobility itself was also determined using the zetasizer's second function.

$$\sigma_e = \varepsilon_0 D \frac{kT}{ze} \kappa (2\sinh(\frac{z\zeta}{2}) + \frac{4}{\kappa a}\tanh(\frac{z\zeta}{4})) \quad (11)$$

This part of the instrument used a channel in a quartz crystal cuvette filled with a buffer solution that had the particles being studied (I = 0.0100). A voltage was applied across the channel and a laser was directed at the cuvette. The laser Doppler effect was observed to determine the mobility of the particles in solution. Mobility data was taken and graphed in Figure 13. The mobility data from a previous experiment was plotted along with the zeta sizing data for comparison. Differences can clearly be seen in the data sets which could be attributed to slightly different buffer conditions or temperature changes. Buffer ionic strength used in the electrophoresis experiment was set to 0.0100. The temperature of either experiment was not regulated and therefore could be a potential cause of error between the two sets of data [29]. The change observed in Figure 13 is likely the result of several factors as the change in room temperature could not account entirely for the changes observed.

### 1.3.2 Quantum dot recoating experiment

In order to utilize the lab's expertise in aqueous capillary electrophoresis and to use the model system of the microsphere separations, aqueous quantum dots were required. Trioctylphosphine oxide (TOPO) capped dots purchased from Evident

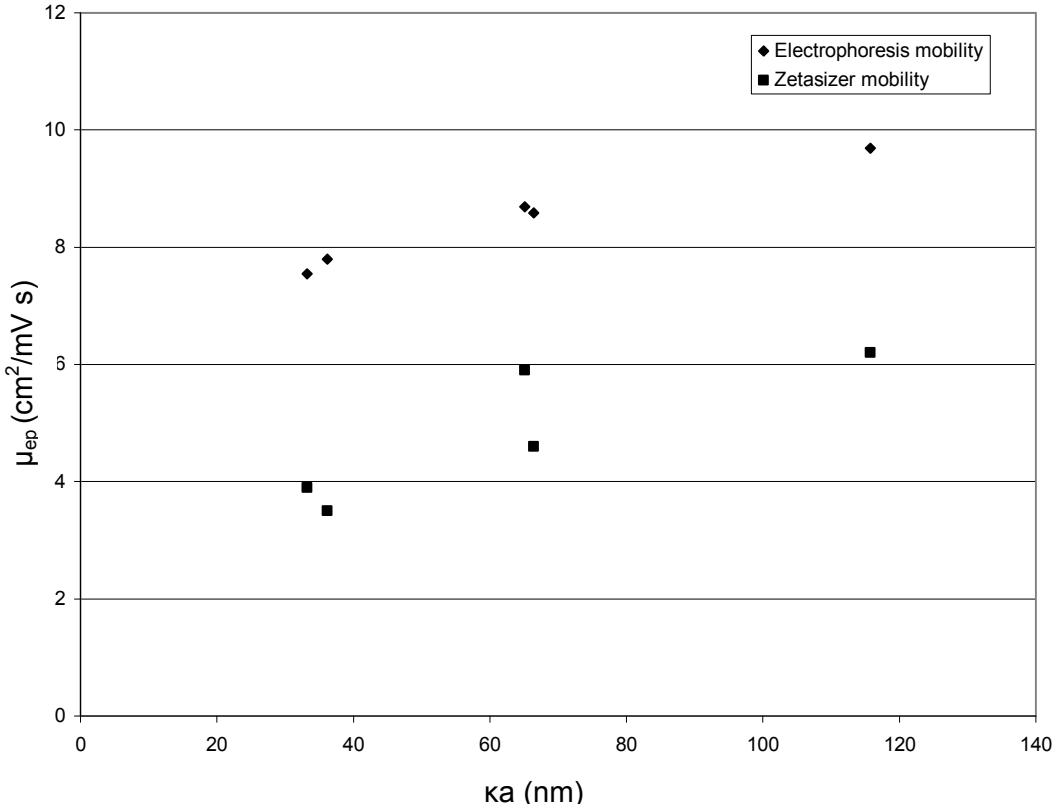


Figure 13. Comparison of mobility calculated from electrophoresis and mobility from zetasizer with respect to the particle $\kappa a$. $a$ values were derived from company specifications

Technologies were re-coated in a water soluble cap [15]. Three dot stocks were purchased, Andirondack Green (2.1 nm diameter, emission 520 nm), Catskill Green (2.4 nm diameter, 540 nm emission) and Hops Yellow (2.6 nm diameter, 560 nm emission). The size information indicates the size of the core diameter in these core-shell (CdSe/ZnS) nanocrystals. Re-coating was accomplished by replacing the TOPO coat [19]; as the dots are oxygen sensitive, this procedure was done under an argon atmosphere using a Schlenck line. The reaction solution contained 1ml MeOH, 20 µl dots (0.5 mg/ml) in toluene, and 20 µg thiosalicylic acid (4-mercapto benzoic acid,

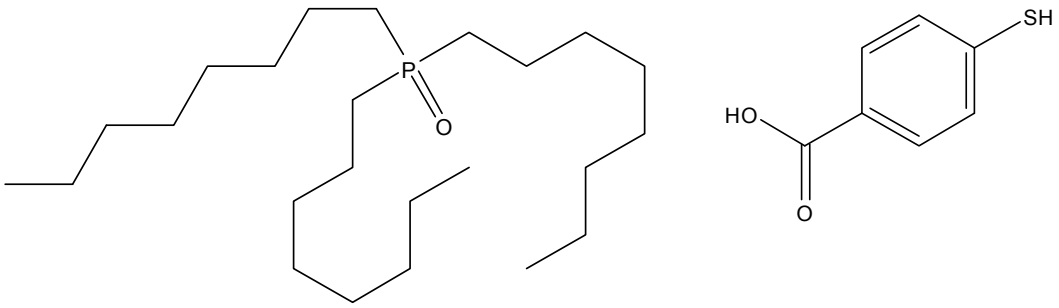


Figure 14. left, TOPO (Tri-n-octylphosphine oxide); right, 4-mercaptobenzoic acid

Aldrich) (see Figure 14 for structures). Re-coated the dots to have a free carboxylic acid group giving a rise in overall polarity.

The reactants were placed into vials and stir bars were added to each of the samples. The temperature was raised to 60˚C and the solution was allowed to stir for 3 hours. The heat was removed and the mixture was then stirred at room temperature overnight. This entire reaction was done in the absence of light to avoid any photo-effects that could potentially damage the dots or reduce the yield of the reaction.

Once the reaction procedure described above was complete, the vials were emptied into centrifuge tubes and 2 ml THF were added to each. The centrifuge was run at 10,000 RPM (15000 x g) for 8 min and a pellet was formed. The supernatant was removed and saved and the pellet was re-suspended in MeOH. This step was done three times in order to drive off aqueous soluble starting material and to ease problems likely to occur in CE separations to follow. After the final wash, the pellet was dissolved in borate buffer (I=0.0100, pH=9.2) and filtered using a 0.2 μm syringe filter. No investigation was given to the % recovery of this procedure.

### 1.3.3 Electrophoretic separation of quantum dots

Separations of the mixture of the recoated dots were attempted in an uncoated capillary and were found to be difficult. Instabilities in the separation were found. These problems were thought to be caused by analyte impurities and impurities in the buffer. Sample injection itself altered the charge on the capillary wall leading to poor resolution and the extension of peaks as the analytes would elute in a chromatographic mechanism as well as an electrophoretic one. As a result, non-reproducible results were obtained. It was determined that stabilizing the capillary wall charge could provide the stability that the separation needed.

Several wall coatings were available for surface charge stabilization for use in aqueous systems. The first attempt was reducing the surface charge by coating the capillary with a trimethylsilane (TMS) permanent coating and myristyltrimethylammonium bromide (MTAB) in the separation buffer [30, 31]. Although this reduced the charge on the inner surface of the capillary and slowed the EOF, inconsistencies were still apparent and resolution and reproducibility suffered. The second coat that was attempted was using a series of successive multiple ionic polymer layers (SMIL) coat. The procedure for the coating of each of the capillaries is described in detail in chapter 2. The SMIL coated capillary appeared to offer a great increase in both resolution and reproducibility that was not apparent in either the uncoated nor the TMS coated capillaries. Figure 15 shows a separation using a SMIL coated capillary. Nanocrystal concentrations were varied to determine peak identities.

The variation of the peak intensities shown in the separation was due to a combination of several factors. The most relevant factors included sample

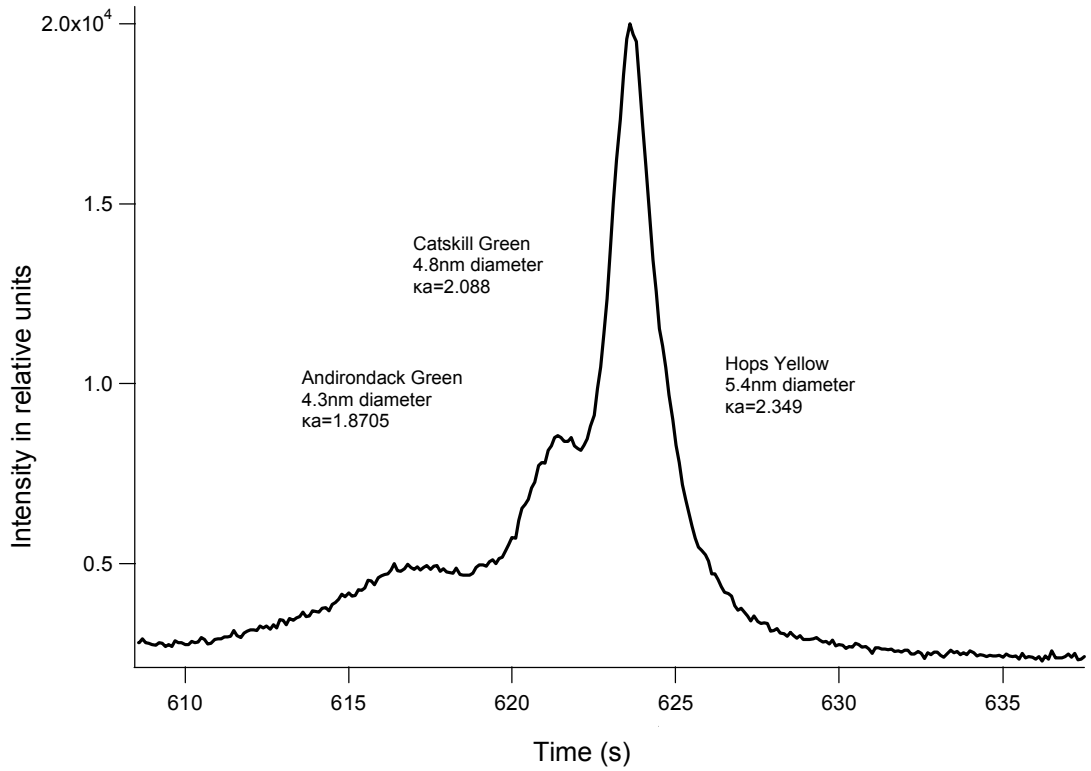


Figure 15. Electrophoretic separation of quantum dots in an aqueous buffer. Borate buffer, pH = 9.2 from NaOH addition I=0.0700; 5 s electrophoretic injection @ 10kV, 50 μm internal diameter, 368 μm outer diameter Polybrene, dextran sulfate (negatively) coated capillary. 40 microwatt laser power, excitation at 488 nm, running voltage 10kV

concentrations, emission efficiencies at an excitation wavelength of 488 nm, and the use of filters that partially block the emission wavelengths from reaching the detector. While the dot efficiencies could not be changed without altering the structure of the dots, the sample concentration and the effects of the filter could be easily altered. It became clear that there was no ideal filter that could be used for the entire series of dots. The notch filters were less than ideal as they cut a large portion of the fluorescence emitted by the dots. The long pass filter was also problematic as the scattered laser light increased background and therefore decreased the signal to noise ratio. The 525 DF40 filter was used as it decreased the background significantly while allowing much of the fluorescence of the dots to the detector. While the detection filter was one easily

remedied problem while detecting the nanocrystals, one aspect that could not be remedied was the intensity of the Andirondack Green crystals. This is thought to be due to inefficiency in the re-coating procedure and is seen throughout the re-coating experiments in the intensity of the electropherogram peaks.

In order to increase the resolution of the separation, the buffer ionic strength and

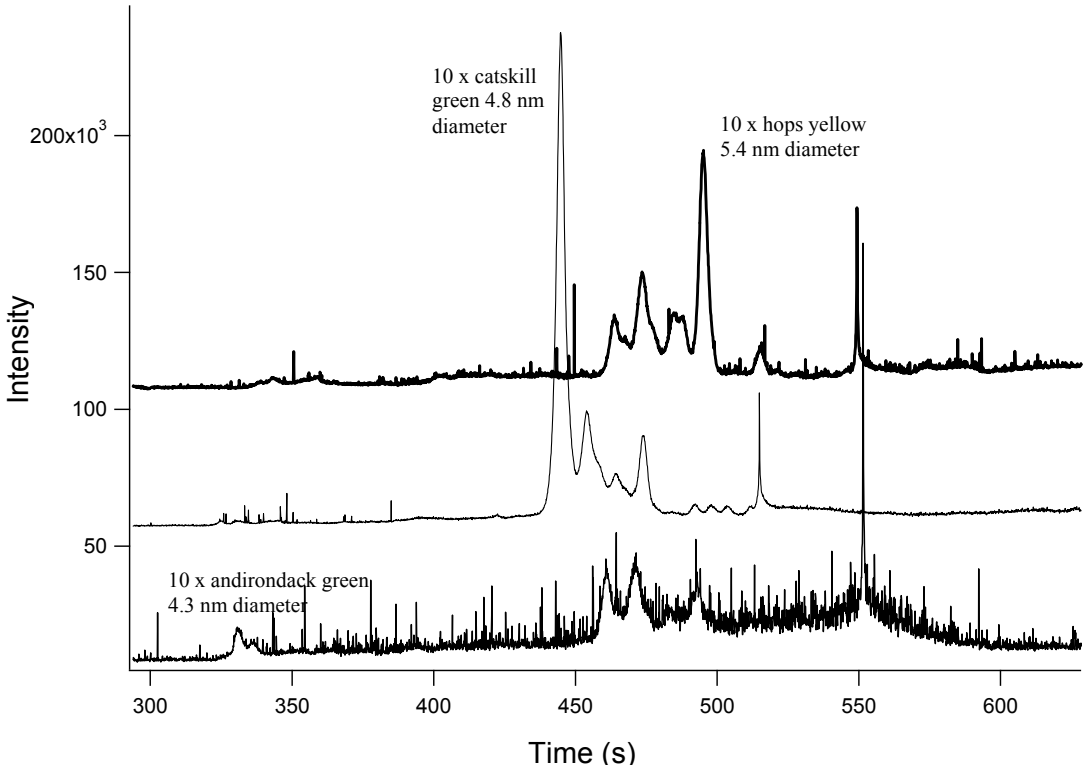


Figure 16. Sample spikes (10 times normal concentration) confirming peak position of individual series of quantum dots. Top, Hops Yellow spike; Center, Catskill Green spike; Bottom, Andirondack Green spike. pH = 10.2, I = 0.0328, capillary ID = 50 μm, OD = 368 μm, running voltage 25 kV, 5 s electrophoretic injection at 5 kV.

pH was adjusted. The pH of the buffer was raised to 10.2 to increase the EOF. This increased the resolution of the separation but the poor yield of Adirondack Green quantum dots remained a problem as they were difficult to discern above baseline without spiking the sample with a spike of a concentration order of magnitude greater. Figure 16 shows the spiked samples. The peaks could be identified through this

procedure, but several peaks that migrated through the system around 475 s did not correspond directly to any single dot series. Filtering these impurities out was attempted, but the peaks remained. A possible explanation of these peaks was that, during the re-coating experiment, the crystals were uncoated for a short period of time and some of the dots managed to form together to yield a larger dot. This seems likely, as the detector would only detect emissions and scatter coming from particles migrating through the capillary within the wavelengths not filtered out through the detection optics (described above). EOF in these experiments was determined through a neutral label, coumarin 334. One of the unexpected effects that the raising of the buffer pH was that the intensity of the individual dot fluorescence increased. This is potentially due to a strengthening of the outer coat at higher pH as was reported in [32].

In order to find the zeta potential and the κa value as described above, the buffer ionic strength was observed over a range of concentrations (0.1M to 0.0001M). At lower ionic strength reproducibility seemed to be reduced and stable separations became difficult. This was unfortunate as theory suggests that the lower the ionic strength the more the analyte will behave as a free ion in solution [25, 33]. Increasing the size of the electronic double layer surrounding the dots by decreasing the buffer ionic strength (equation 6) would be beneficial to the resolution and increasing the ionic strength can potentially cause heating effects [29]. By decreasing the ionic strength slightly the EOF was increased. This increase caused the EOF to dominate the separation and the electrophoretic mobility to have a lesser effect. As a result the resolution was decreased. This indicates that the ionic strength affects the EOF to a greater extent than the EP and is further confirmed by the observation that increasing the ionic strength has an opposite

effect (equations 3-5). A secondary effect of increasing the ionic strength was to increase the time of separation. The dispersion due to diffusion will be minor due to the size of the particle, but will have some effect as the run times become large. The cause of the dispersion was not pursued, but low concentration of the nanocrystal samples and long run times made signal to noise poor (in some cases < 2).

One interesting item taken from the change in buffer concentration experiments was that the effect of the change in the double layer of the dots was secondary to the change in the capillary double layer when discussing the separation. This means that when the ionic strength was altered the effect on the EOF was dramatic, but the effect on the peak shapes and resolution did not alter significantly. Smaller changes in the buffer

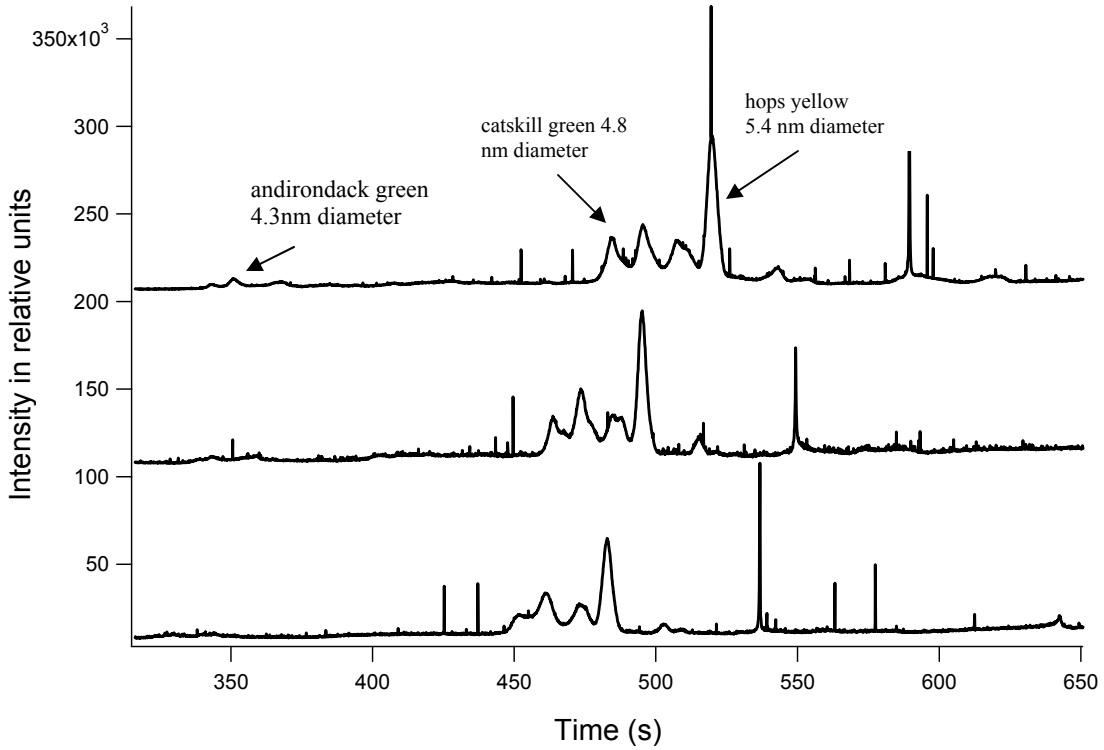


Figure 17. Altering ionic strength of a separation of a series of quantum dots. top 0.0437, middle 0.0328, bottom 0.02186, pH = 10.2, capillary ID = 50 µm, OD = 368 µm, running voltage 25 kV, 5 s electrophoretic injection at 5 kV.

ionic strength can give a better indication of the effect on the dots double layer. Figure 17 shows smaller effects of the ionic strength. Resolution and peak shapes improve slightly as the ionic strength increases and the elution time increases.

In an attempt to further increase resolution the voltage of the separation was also adjusted. An increase in the running voltage increased the EOF and made a shorter overall run time. The overall resolution between peaks appeared to be unaffected by changes made in the running voltage. It is likely that the electrophoretic inhomegeniety is the primary factor involved in determining resolution. An inhomegeniety would not increase or decrease resolution when the applied electric field was added. These findings agree with previous findings of similar particles [28].

### 1.3.4 Quantum dot mobility and zeta size

The zeta-sizer 3000 was used to determine the mobility of water soluble quantum dot samples from Evident Technologies. The series of five different sized dots were taken and placed in separate buffer solutions (I = 0.01 borate buffer). The zeta sizer was then used to determine the hydrodynamic radii of the dots as described above for microspheres. Results are graphed in Figure 18. There is a general trend in this graph in that the larger dots have larger hydrodynamic radii. A larger radii would seem reasonable in that there could easily be more surface charges on the larger dots and this would create a larger effect on an aqueous solution. In this graph it is shown that the hydrodynamic radii were significantly larger than the actual sizes of the dots. The size difference between the hydrodynamic radii and the crystal size could be accounted for by a large surface charge density. The apparent linear relationship is not expected to remain

on the same trend when smaller dots are observed. The trend line crosses the x axis around 1 nm, this would indicate that the zeta size would reduce faster than crystal size.

Mobility was also measured in the same manner as in the microsphere experiment. Buffer ionic strength remained constant (I = 0.0100) and the dot samples were pumped using a syringe into the mobility cuvette as before. The mobility data that was received from this experiment seemed to have no trends and reproducibility appeared to be less than ideal. It was suspected that the detection limit was reached for the instrument's mobility optics as the company specification of lower limit of detection was approximately the same size as the dots being studied.

The effective size of the nanocrystals from electrophoretic data was found using the calculations above (microsphere section). Table 4 and 5 show the double layer thickness and mobility of the dot series. Similar trends are in the nanocrystal data as

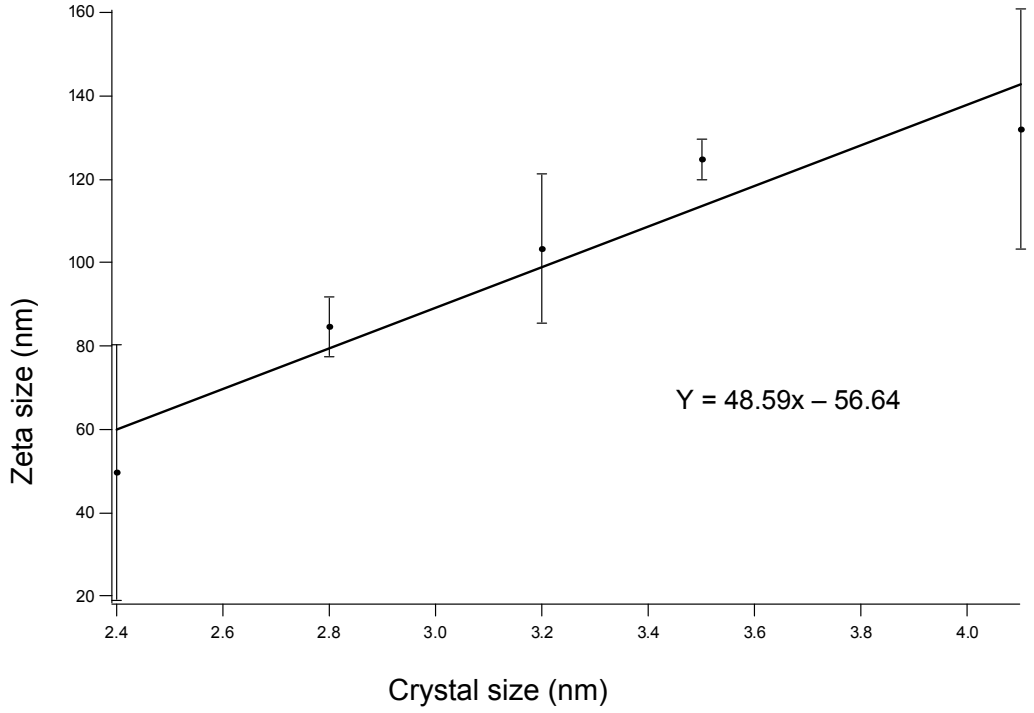


Figure 18. Comparison between nominal crystal size and effective size in solution (zeta size). Each point represents 30 measurements.

there are in the microsphere data in that the larger nanocrystals migrate slower than the smaller nanocrystals. This indicates that the surface charge of the larger crystals is more dense than that of the smaller crystals. An interesting trend developed in the zeta potential data shown in table 6. The reduction of κa due to the small size of the nanocrystals and high mobility of the crystals in the ionic strength of the solutions that were tested, the zeta potentials of the 4.8 nm nanocrystals were lower than that of the larger nanocrystals. These findings indicate that the surface charge of the particles will be reduced as the particles become smaller.

Table 4. κa values (nm) -- size determined through manufactures specifications

| Ionic strength | 4.3 nm | 4.8 nm | 5.4 nm | EDL thickness (nm) |
|---|---|---|---|---|
| 0.0219 | 2.09 | 2.33 | 2.63 | 2.06 |
| 0.0328 | 2.56 | 2.86 | 3.22 | 1.68 |
| 0.0437 | 2.96 | 3.30 | 3.71 | 1.45 |

Table 5. μep ($cm^2/V\ s$) x $10^{-3}$, size indicates dot dimeter

| Ionic strength | 4.3 nm | 4.8 nm | 5.4 nm | EOF |
|---|---|---|---|---|
| 0.0219 | -0.84 | -2.25 | -2.25 | 5.46 |
| 0.0328 | -1.06 | -2.28 | -2.49 | 5.54 |
| 0.0437 | -1.37 | -2.66 | -2.87 | 5.79 |

Table 6. ζ-potential (mV) from electrophoresis

| Ionic strength | 4.3 nm | 4.8 nm | 5.2 nm |
|---|---|---|---|
| 0.0219 | -0.767 | -1.84 | -1.93 |
| 0.0328 | -0.793 | -1.52 | -1.48 |
| 0.0437 | -0.886 | -1.54 | -1.48 |

### 1.3.5 Water soluble quantum dot separations

Water soluble core shell quantum dots were purchased from Evident Technologies. These dots had a carboxylate coat and were known to fluoresce at different wavelengths depending on their core size. As the dots in this series emit light at a larger range than the previous series discussed above, the filter in the barrel before the detector was changed to a DLP 520 long pass filter. This had the desired effect of being able to detect the entire series of dots, but also had the undesirable effect of increasing the background. This caused a change in experimental conditions as the dot concentration had to be increased in order to detect the dots eluting through the capillary.

The purchased dots had a large advantage to the re-coated dots in that they were aqueous soluble and no after market modification needed to be performed. The disadvantage was that the structural information regarding the surface of the dots and the coating on the dots were proprietary information of Evident Technologies and was not open for public use. As a result not much was known of the structure and surface properties of these dots other than the coating had carboxylate groups on its surface.

While exploring the new dots' properties, one of the items that was found was that the properties of the solution that the dots were placed in were vital. The dots only

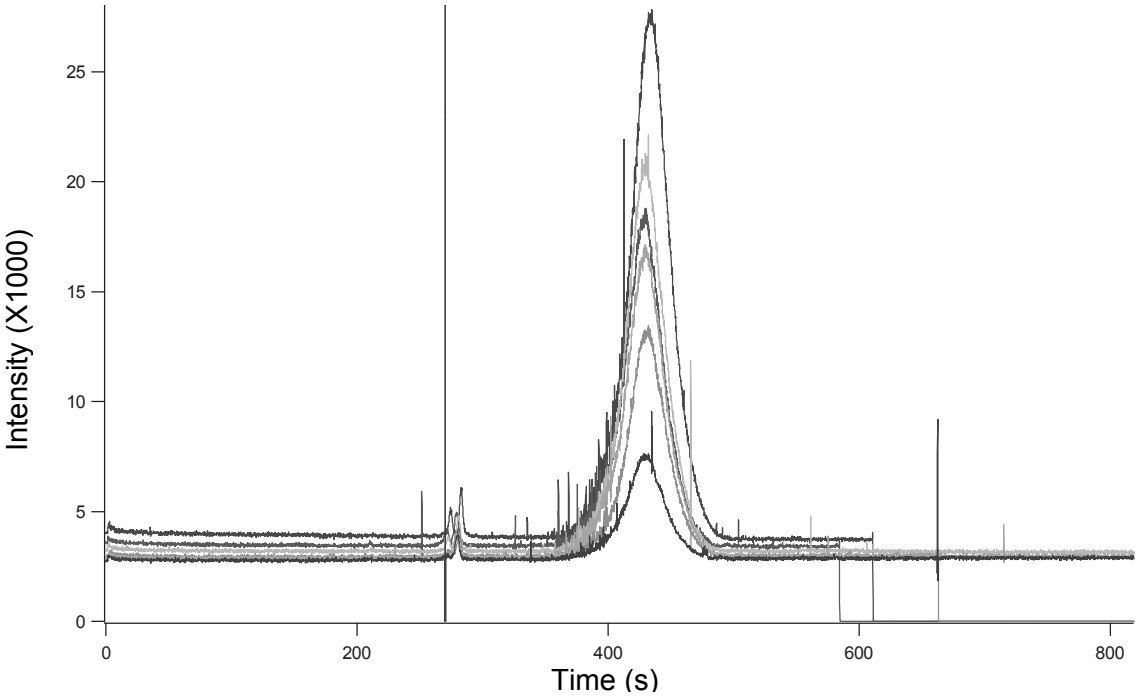


Figure 19. Replicate injections of forest orange quantum dots in phosphate buffer (I=0.0100) at identical concentrations over time. Florescence intensity is attenuated in later (bottom) traces. pH = 10.2, capillary ID = 50 μm, OD = 368 μm, running voltage 25 kV, 5 s electrophoretic injection at 5 kV.

fluoresced in basic solutions above pH 7 and increased their fluorescence intensity as the pH was raised. Buffers such as phosphate buffer tended to destroy the dots faster than other buffers. Destruction of the dots was observed in the loss of fluorescence intensity seen in the electropherograms. The primary three buffers that were tested in this research were borate, carbonate and phosphate buffer. Borate buffer tended to be the superior buffer for dot shelf life and has a buffering range which is high enough to detect the dots with adequate intensity. Storage of the nanocrystals in borate buffer gave a shelf life of about 1 week before the sample degraded to the point of significant emission loss, whereas the phosphate buffer destroyed the dots on the scale of minutes (Figure 19).

Buffer additives have been known to be used to alter the mobilities of analytes for a variety of applications. This is widely used in the study of proteins where the surfactants will denature the species and simplify the separation. Nanocrystals differ

greatly from proteins, but the effect of surfactants on the particle has been shown to alter the surface properties [34].

Nanocrystal surface properties were altered through the addition of surfactants in the separation solution. By adding surfactants under the critical micelle concentration the surfactant will alter the surface of the particles and give rise to a change in both the surface charge and the zeta potential of the particle. Several different buffers were utilized in order to improve resolution, these included sodium dodecylsulfate (SDS), cholate, myristyl trimethylammonium bromide (MTAB), and cetyltrimethylammoniumbromide (CTAB). Although possible separations were realized, the electropherograms were not reproducible. What was observed from this set of experiments was that although the surface was most certainly modified by the surfactants, the increase in ionic strength of the buffer altered the EOF. This had a secondary effect on the separation in that the run time was slowed. The increase in time was only problematic when the surfactant concentration was relatively high (equal to the concentration of the buffer and above).

Overall the addition of surfactant to the supporting buffer did not benefit the colloidal separation. Small changes in the mobilities were observed, but not to the extent that they could not be accounted for purely though the additional ionic strength added to the buffer. Further investigation into the surfactants effect on the nanocrystals was not sought.

### 1.3.6 Buffer ionic strength

A set of experiments was designed to determine whether the separation could be improved by increasing the capillary length and altering the buffer concentration to a significantly higher concentration. Coupled together these two parameters provided for excessively long run times where diffusion was a problem for even the largest dot samples. The run times also became prohibitively long (4+ hours). Separation reproducibility proved to be impossible as the longer run times. It was not established what the source of the irreproducibility was but a decrease in current across the capillary indicated that the ionic strength of the buffer was decreasing.

The separation of nanoscale crystalline lattices at different hydrodynamic radii proved in this work to be possible. The utility of such a separation is limited in that the fluorescence emission wavelength can be altered, not only by crystalline size, but also be the addition of impurities into the lattice. The separation of the TOPO series of dots indicates that these dots were synthesized by adjusting the size of the core crystal and the shell of the dot corresponded to the core size. The shell of the crystalline lattices was expected to be relatively close for each species of dot as the stability of the quantum dot will be affected by the shell thickness [18, 22, 35]. It was not observed that one species of nanocrystal was more or less stable than the other crystals.

## 1.4 Conclusions

Through the use of free zone capillary electrophoresis the surface properties of microspheres and nanocrystals was observed. The electrophoretic mobility of the particles that were analyzed was determined to be affected by relaxation forces that are

not apparent in ion separations. The difference is due to the effect of surface charge in the colloidal systems. Small molecules and ions do not have surface charges and can be thought of as point charges [23]. The simple equations for electrophoretic mobility that are derived with the assumption of point charges have been found to be inadequate for describing larger analytes such as microspheres [28].

Quantum dots were separated based on charge and size and it was observed that the surfaces were highly charged. Similar findings for colloidal gold, which is of a similar scale, have been reported [20]. The primary utility of this finding is the observation of coating material properties. An understanding of the properties of coating materials and the effect of the surrounding buffer on those properties is vital to the development of secondary structures, linking quantum dots [10].

# REFERENCES


1. Bruchez, M.; Gin, P.; Weiss, S.; Alivisatos, P., *semiconductor nanocrystals as fluorescent biological lables.* Science, 1998. **281**: p. 2013-2016.

2. Rosenthal, S., *Bar-coding biomolecules with fluorescent nanocrystals.* Nature biotechnology, 2001. **19**: p. 621.

3. Jaiswal, H.; Mauro, M.; Simon, S., *Long-term multiple color imaging of live cells using quantum dot bioconjugates.* Nature biotechnology, 2003. **21**: p. 47.

4. Mitchell, P., *Turning the spotlight on cellular imaging.* Nature biotechnology, 2001. **19**: p. 1013.

5. Mattoussi, M.; Goldman, E.; Anderson, G.; Sundar, V.; Mikulec, F.; Bawendi, M., *Self-assembly of CdSe-ZnS quantum dot bioconjugates using an engineered recombinant protein.* J. Am. Chem. Soc., 2000. **122**: p. 12142-12150.

6. Gerion, F.; Williams, S.; Parak, W.; Zanchet, D.; Weiss, S.; Alizisatos, P., *Synthesis and properties of biocompatible water-soluble Silica-coated CdSe/ZnS Semiconductor quantum dots.* Journal of Physical Chemistry, 2001. **105**: p. 8861-8871.

7. Dameron, C.; Dennis R., *Characterization of Peptide-Coated Cadmium-Sulfide Crystallites.* Inorganic Chemistry, 1990. **29**: p. 1343-1348.

8. Dameron, C., Brooke R.; Winge, D., *Glutathione-coated Cadmium Sulfide crystallites in candida glabrata.* Journal of biological chemistry, 1989. **264**(29): p. 17355-17360.

9. Castagnola, D.; Misiti, F.; Cassiano, L.; Giardina, D.; Messana, I., *Modification of capillary electrophoresis selectivity in hydro-organic solutions Dissociation constants and Stokes radius measurements of peptides in water-2,2,2-trifluoroethanol mixtures.* Journal of Chromatography A, 1997. **792**: p. 57-65.

10. Murphy, C., *Quantum dots: A primer.* Applied spectroscopy, 2002. **56**(number 1): p. 16A-27A.

11. Koberlin, A.; Basche, T., *Single-dot spectroscopy of CdS nanocrystals and CdS/HgS heterostructures.* Physical Review B, 1999. **60**(3): p. 1921-1927.

12. Empedocles, D.; Bawendi, M., *Photoluminescence spectroscopy of single CdSe nanocrystallite quantum dots.* Physical Review Letters, 1996. **77**(18): p. 3873.

13. Michalet, F.; Lacoste, T.; Dahan, M.; Bruchez, M.; Alivisatos, P.; Weiss, S., *Properties of fluorescent semiconductor nanocrystals and their application to biological labeling.* Single Molecules, 2001. **2**(4): p. 261.

14. Arnim, H., *Small-Particle research: Physicochemical properties of extremely small colloidal metal and semiconductor particles.* Chem. Rev., 1989. **89**: p. 1861-1873.

15. Pathak, S.; Arnheim, N.; Thompson, M., *Hydroxylated quantum dots as luminescent probes for in situ hybridization.* J. Am. Chem. Soc., 2001. **123**: p. 4103-4104.

16. Cohen, L.; Shanzer, A.; Cahen, D.; Liu, A.; Rosenwaks, Y.; Lorenz, J.; Ellis, A., *Molecular Control over semiconductor surface electronic properties: Dicarboxylic acids on CdTe, CdSe, GaAs, and InP.* Journal of American Chemical Society, 1999. **121**: p. 10545-10553.

17. Rabani, B.; Berne, B. , *Electronic properties of CdSe nanocrystals in the absence and presence of a dielectric medium.* J. Chem. Phys., 1999. **110**(11): p. 5355-5369.

18. Bingham, J., *Deactivation of Q-CdS photoluminescence through polynucleotide surface binding.* The Journal of Physical Chemistry, 1992. **96**(26): p. 10581-10586.

19. Rosenthal, S.; Adkins, E.; Schroeter, S.; Adams, S.; Swafford, L.; McBride, J.; Wang, Y.; DeFelice, L.; Blakely, R., *Targeting cell surface receptors with ligand-conjugated nanocrystals.* J. Am. Chem. Soc., 2002. **124**: p. 4586.

20. Wei, G.-., Churng-Ren C.; Liu, F.; Chang, S., *Separation of Nanostructured Gold Particles by Capillary Zone Electrophoresis.* Journal of the Chinese Chemical Society, 1998. **45**(1): p. 47-52.

21. Wiersema, P.; Overbeek, J., *Calculation of the electrophoretic mobility of a spherical colloid particle.* Journal of Colloidal and interface Science, 1966. **22**: p. 78-99.

22. Alivisatos, A., *Electrical Studies of semiconductor-nanocrystal colloids.* MRS Bulletin, 1998: p. 1-53.

23. *Handbook of Capillary Electrophoresis*. 2 ed, ed. J.P. Landers. 1997, New York: CRC Press.

24. Huang, Q.; Moorefield, C.; Newkome, G., *Counterion binding of charged spheres: Effect of pH and ionic strength on the mobility of carboxyl-terminated dendrimers.* J. Phys. Chem B, 2000. **104**: p. 898-904.

25. Radko, M.; Chrambach, A., *Capillary zone electrophoresis of sub-micrometer-sized particles in electrolyte solutions of various ionic strengths: Size-dependent electrophoretic migration and separation efficiency.* Electrophoresis, 2000. **21**: p. 3583-3592.

26. Charambach, A.; Sergey P., *Size-dependent retardation and resolution by electrophoresis of rigid, submicron-sized particles, using buffered solutions in presence of polymers: A review of recent work from the authors laboratory.* Electrophoresis, 2000. **21**: p. 259-265.

27. Radko, A., *Separation and characterization of sub-um and um-sized particles by capillary zone electrophoresis.* Electrophoresis, 2002. **23**(13): p. 1957-1972.

28. Stokes, J.; Johnson, M., *Resolution in sub-micrometer particle separations by capillary electrophoresis.* Microchemical Journal, 2004. **76**: p. 121-129.

29. Balcom, N., *Solvent dependence of carboxylic acid condensation with dicyclohexylcarbodiimide.* Journal of Organic Chemistry, 1988. **54**: p. 1922-1927.

30. Gallaher, D.; Johnson, M., *Development of near-infrared fluorophoric labels for the determination of fatty acids separated by capillary electrophoresis with diode laser induced fluorescence detection.* The Analyst, 1999. **124**: p. 1541-1546.

31. Gallaher, D.; Johnson, M., *Nonaqueous capillary Electrophoresis of Fatty Acids Derivatized with a Near-Infrared Fluorophore.* Analytical Chemistry, 2000. **72**(9): p. 2080.

32. Porras, S.; Susanne, K.; Strandman, Satu; Tenhu, Heikki; Riekkola, Marja-Liisa, *Novel dynamic polymer coating for capillary electrophoresis in nonaqueous methanolic background electrolytes.* Electrophoresis, 2001. **22**: p. 3805-3812.

33. Tiselius, A., *The influence of electrolyte concentration on the electrophoretic mobility of egg albumin.* Trans. Faraday Soc., 1940. **36**: p. 16-22.

34. Spanhel, L.; Weller, H.; Henglein, A., *Photochemistry of colloidal semiconductors. 20. Surface modification and stability of strong luminescing CdS particles.* J. Am. Chem. Soc., 1987. **109**: p. 5649-5655.

35. Nirmal, M.; Louis, N, *Luminescence photophysics in semiconductor nanocrystals.* Accounts of Chemical Reasearch, 1999. **32**: p. 407-414.

# Chapter 2

## Determination of the Effects of Capillary Surface Coatings on Fatty Acid Separations

### 2.1 Introduction

Capillary electrophoresis (CE) is a powerful separation technique which is able to separate a wide variety of analytes with high efficiency [1-4]. Historically CE is an technique that is primarily used with aqueous buffers and has seen much growth in the last twenty years [5, 6]. This growth has been driven by the vast knowledge base of aqueous buffer properties found throughout literature. While aqueous applications of capillary electrophoresis grow in number every year, non-aqueous applications have been slower to appear [7, 8]. Primarily this is due to the properties of the solvents that are available. The growth of aqueous capillary electrophoresis has expanded the fundamental understanding of the basic properties of water under electrophoretic conditions. For many other solvents the bulk of research detailing electrophoretic effects is not found. Lack of understanding deters the use of solvents that could potentially be used in a non-aqueous CE application. Further complications are found due to the vast quantity of solvents that are available, making choice of solvent difficult.

An understanding of the effect of the solvent on electrophoretic properties such as electroosmotic flow (EOF) and electrophoretic mobility (EP) appeared in the literature soon after the emergence of CE as a viable separation technique [9]. The introduction of non-aqueous capillary electrophoresis began in 1984 when a series of quinoline compounds were separated in acetonitrile. While this project opened the door for other applications into the field, growth was slow due to difficulties discussed above and the general lack of reproducibility that was not well understood. In the mid 1990's interest grew in non-aqueous separations with the development of capillary wall coatings [10, 11] and the interest in non-polar separations. The addition of capillary wall coatings was a vital addition to ensuring stable EOF in non-aqueous CE as discussed later in this work.

### 2.1.1 Non-aqueous capillary electrophoresis

Non-aqueous capillary electrophoresis (NACE) is necessary for certain analytes and can have great advantages over its aqueous analog when the analyte is nonpolar and solubility becomes problematic. When nonpolar, hydrophobic molecules such as those that are found in many biological systems are studied, aqueous buffers are not an option for supporting solvent due to low solubility. Much of the research developed for chromatographic (HPLC) separations utilizes the polarity of a wide variety of solvents. The effect of an applied electric potential on non-aqueous solvents and the properties of analytes under these conditions is necessary in order to parallel the vast body of chromatographic research.

Aqueous CE and non-aqueous CE share many similarities. The basic equations that describe the electrophoretic effect (discussed earlier in this text) remain unchanged.

Careful control over the ionic strength and the solvent pH* (discussed later) is required, similar to aqueous applications.

The primary differences between non-aqueous and aqueous CE are the properties of the solvent. The two properties that have the largest effect on the EOF are the viscosity and the dielectric constant (equation 1). These two properties directly influence the mobility of the solvent molecules under an electric field and can greatly influence the speed of the bulk flow of the solvent under an electric field (equation 1) and the electrophoretic mobility (equation 2). Solvents have a variety of dielectric constants (ε) that can be between 20 and 200 depending on the individual solvent [7, 12]. This constant cannot be changed without changing the solvent; water for instance, has an ε of 80 which would give rise to far different $\mu_{eo}$ values than methanol, which has an ε value of 32.7.

### 2.1.2 Electroosmotic flow

The EOF inherent to a particular solvent will be greatly effected by the solvent's viscosity (equation 1). The higher the viscosity of a solvent the lower the velocity of the solvent under an electric field. A higher solvent viscosity will also reduce the electrophoretic mobility of analytes that are in the solution (equation 2). This can be an

(1) $$\mu_{eo} = \frac{\zeta \varepsilon_r \varepsilon_0 E}{\eta}$$

$\mu_{eo}$ - electroosmotic mobility
$\zeta$ – zeta potential
$\varepsilon_r$ – dielectric constant
$\varepsilon_0$ – permittivity of vacuum
$\eta$ - viscosity

(2) $$\mu_{ep} = \frac{q}{6\pi\eta r}$$

$\mu_{ep}$ - electrophoretic mobility
q – analyte charge
$\eta$ – viscosity
r –radius

advantage when a separation based on size (radius (r) in equation 2 assumes a spherical analyte) is desired. Common methods of increasing solvent viscosity can also be used such as buffer additives (surfactants and thickening agents) [13, 14], but these can greatly affect ionic strength and zeta potential of both the capillary wall and the analyte in solution. A limited amount of research is available in the literature, but adjustment of solvent viscosity in this way has not been fully developed.

Due to the applied electrical current found in electrophoretic separations, choice of a solvent is complicated by other factors. One common problem in all electrophoretic separations is what is referred to as Joule heating. Joule heating is defined as the rise in kinetic energy brought about by the movement of ions within solution. If the heat capacity of a solvent cannot compensate for the additional kinetic energy within the capillary then problems could occur. Small amounts of Joule heating will cause the viscosity of the solvent to decrease, while large amounts could potentially cause the solvent to vaporize. Thermal and electrical conductivity will change depending on the solvent and a wide range of these two properties exist for the many buffers that have been used for CE. For biological molecule separations in nonaqueous systems, the common solvents are methanol and acetonitrile due to their low electrical conductivity and relatively high thermal conductivity compared to water [8, 15, 16]. When the thermal conductivity is high and electrical conductivity is low, there is a low amount of Joule heating.

Riekkola et al. have classified solvents into several convenient classes for use in CE [8]. These classes include protic solvents which can act as Brönstead acids or bases (alcohols and water), protic solvents that act primarily as Brönstead acids (organic acids),

protic solvents which act primarily as Brönstead bases (amides), aprotic solvents that are not subject to autoproteolysis yet can accept protons (acetonitrile), and inert solvents (hexane) which are not generally useable in CE due to insolubility of ionic species.

The choice of a solvent class, and individual solvent, to be used as media in a CE separation is based on the factors above and the solubility of the analyte within the buffer. Careful attention must be given to develop a separation in which the analyte of interest can be detected at a concentration that is readily soluble in the solvent. Polarity of the solvent therefore plays a significant role in the choice of solvent along with the solvents optical or electrochemical properties, which can interfere with detection.

### 2.1.3 Detection

The choice of detection techniques will occasionally become problematic depending on the solvent that has been chosen as the properties of the solvent (e.g. absorbance, electrochemical, fluorescence) can vary widely. Careful attention to these issues when choosing a detection technique is required as this can potentially be a great advantage, but can potentially cause problems. The choice of detection is a complex question that is analyte dependant, but can be broken up into three primary techniques.

Electrochemical detection is a method of detection that will detect a change in oxidation state of an ion of interest. An electrochemical tag such as $Cu^{2+}$ is generally used in biomolecular applications. Shen et al. have reported detection of peptides in the 60 pM range using electrochemical detection [17].

Optical methods of detection include the use of absorption and emission techniques. Absorption is the simplest and is a method of detecting the amount of light that is absorbed at a particular wavelength. While absorbance detection in CE can give

detection limits of $10^{-7}$ M [18], generally concentrations are reported in the micromolar range [19]. Due to the availability of much of the biologically relevant material, absorbance is not generally an ideal detection technique. Emission techniques will detect the light emitting from the analyte of interest and is a far more selective technique. Fluorescence techniques are limited in that the analyte of interest must emit. In biomolecules, this is a relatively rare phenomenon that is occasionally found in proteins due to tryptophan residues, but is rare in smaller molecules except tryptophan derivatives. In order to detect small biomolecules with fluorescence detection, a molecule that will emit at a desired wavelength when excited is bound to the biomolecule. This is known as labeling or tagging a molecule and will not only allow detection of the desired molecule, but the choice of emission wavelength can eliminate unwanted biological contaminants from the electropherogram as they will not fluoresce. When an analyte is tagged for detection careful attention must be given to the optical properties of the solvent and the additives to avoid unwanted interferences to detection. Detection limits will range depending on the fluorescent label used and the application of the label, but detection has been reported below the zeptomole level ($10^{-21}$ moles) [20].

In electrophoretic separations, the EOF is driven by the ionic strength of the supporting buffer. This ionic strength is provided by three primary sources. First is the contribution of the analyte to the overall ionic strength. The addition of a charged analyte into the capillary causes an increased electric field within the sample plug. This effect can potentially cause sample stacking as the electric field is not uniform across the sample plug, but the effect of the sample plug is typically small compared to the bulk of the capillary. If the analyte is adhering to the capillary internal wall then there will be a

small increase in the overall ionic strength with every injection and will be a cause of irreproducibility, yet in most applications this effect will be minor. The second source of ion concentration is the buffer's protolytic cleavage. A major difference between solvents, including water, is the solvent's protolytic cleavage; which is unique for each buffer chosen. The effect of pH on aqueous buffer systems is well established in the literature and it is necessary in any electrophoretic separation to have tight control over the pH. Each protic solvent has a concentration of ions inherent to itself that is caused by the release of protons from the solvent molecules themselves. Releasing protons will cause an increase in ionic strength; with aqueous systems this contribution to ionic strength is governed by pH. By changing the buffer, there is a change in the reference points when pH is measured as each new solvent will have its own concentration of ions. The reference point is the quantity of ions the solvent will release at a particular temperature when no additives are present. Changing the ambient ion concentration in this way for each solvent used complicates matters as a simple pH meter is no longer sufficient to determine the hydrogen ion concentration without changing the reference points of the solvent. $pK_a$ values can be found in the literature for many solvents and must be determined to find the true ionic strength of the buffer solution. The pH that is found in this method is referred to in the literature as the pH*, indicating that the reference has changed.

The third primary source of ionic concentration is the supporting analyte within the buffer. Additives are introduced into the buffer in order to gain control over the ionic strength and increase it over the ambient level of the solvent (the ion concentration due to hydrolysis). The choice of additive can be potentially challenging as the additive should

not interfere with the analytes and also not adhere to the surface of the capillary (or any coat on the surface). Solvent additives will function differently for different solvents. The ideal additive in one solvent can potentially be unusable in a different solvent due to simple solubility of the additive within that solvent. Briefly, when choosing an additive for the increase of ionic strength of a solvent conjugate acids and bases are desirable as a buffer will be made. When salt additives that increase ionic strength are placed in a supporting buffer they will dissociate. Increase in the background electrolyte will govern the ionic strength of the solvent and therefore will affect the EOF of the separation.

### 2.1.4 Additives

Other additives can be used to change mobilities within the separation. Outside of changing the ionic strength, additives have been used to increase viscosity, change the surface properties of analytes, alter the surface properties of the capillary, and to create micelles for addition of a chromatographic component to the separation. The subject of solvent and buffer additives is complex and can greatly influence the utility of a non-aqueous system but careful attention is needed to ensure problems do not arise.

The utility of NACE, and any electrophoretic system, is tempered by analyte adsorption on the capillary walls and the small dynamic variances in electroosmotic flow (EOF) that can arise from it. In order to alleviate these problems, a large variety of capillary wall coatings have been developed and have become widely used [11, 21-24]. The challenge in finding a coating when observing a NACE system is that the coating must be able to withstand the harsh effects of the solvent being used. Degradation of the wall coating will dramatically decrease run-to-run reproducibility.

### 2.1.5 Capillary coatings

Although capillary wall coatings have become common for aqueous applications, their use in nonaqueous CE has been rare [7]. Nonaqueous capillary coatings act in a similar way to aqueous applications in that they will lessen the effect of analyte adsorption, but there are also several characteristics unique to nonaqueous media [12, 25]. Having a stable, uniform surface charge on the capillary is the primary goal in both aqueous and nonaqueous CE. Under nonaqueous conditions stable capillary surface charge can prove challenging depending on the stability of the coating material in the media being studied[16]. The wall coating must be ionized by the solvent conditions in order to provide a stable surface charge on the capillary when EOF is desired. If no charge is present on the surface of the capillary then there will be no EOF to drive an electrophoretic separation.

Two primary types of wall coatings are used in nonaqueous capillary electrophoresis: either permanent wall coatings that irreversibly change the properties of the capillary wall or dynamic coatings, which can be modified relatively easily. Dynamic coatings use reagents that adhere to the capillary surface without covalent bonds or polymeric crosslinking. The coat is generally generated through the use of buffer additives [23]. Dynamic coating procedures can be as simple as adding a small amount of the coating material to the separation buffer. Dynamic coating procedures have a second advantage in that they can be easily regenerated by simple reconditioning reactions when the coating degrades [26]. The method of construction of dynamic coatings generally falls to the manipulation of hydrophobicity or the manipulation of the properties of analytes to form complexes that do not interact with the surface of the capillary.

### 2.1.6 Dynamic capillary coatings

Dynamic capillary coatings fall into two categories, surfactants and analyte modifiers. Analyte modifiers are not universally used as they are greatly dependant on the substance being studied. A significant body of work has been developed for the study of amino acids and substances that will modify the amine groups [27-29]. Additives successful in the reduction of analyte interaction with the capillary surface are primarily additives with amine functional groups that will preferentially bind to the surface of the capillary, reducing the adsorption of the amino acid of interest to the surface. A review of these buffer additives was written by Righetti et al. [13].

The use of surfactants can be further divided into two categories: below the critical micelle concentration (CMC) and above the CMC. In the latter case a chromatographic component is added to the separation and CE separations are referred to as micellular electrokinetic chromatography (MEKC) which will not be discussed as micelle formation is rare in nonaqueous solvents due to the lack of aggregation usually brought about through hydrophobic interactions. When the concentration is below the CMC, surfactants have several properties that will affect the separation. Viscosity and ionic strength are two properties that will dramatically be altered by the addition of surfactant to the separation buffer [30]. While these properties must be accounted for, the primary use of surfactants in non-aqueous separations is to suppress or modify the EOF. Polyvinyl alcohol (PVA) and polyethylene glycol (PEG) have both been used to suppress EOF [31]. Hanson et al. observed the reversal of EOF in a methanolic separation when hexadimethrine bromide (HDB) was added to the separation buffer [32]. Sodium cholate

has also been utilized in the non-aqueous separation of urine samples and it was found that the modification due to sodium cholate increased the utility of the separation [33].

There are several different approaches that have been developed to solve the problem of biomolecules adhering to the surface of capillaries. Among these methods are the PEM coating method described above; another is the addition of additives such as surfactants in order to create a dynamic coat, blocking the amino functional group responsible for the attraction of the analyte to the surface of the capillary. This dynamic coating has proven effective in reducing analyte adhering to the capillary wall, but has some disadvantages. Primarily, by introducing a surfactant into the running buffer the ionic strength will be altered. Surfactant will also be coupled to the outer layers of the coat migrating with the bulk solvent flow. When the coating material migrates like this it causes small changes to the coat creates problems when run-to-run reproducibility is observed.

The capabilities of the mobile coat are similar to those of a permanent coat. The reversal of EOF was found to be dependent on the concentration of the surfactant cetyltrimethylammonium bromide (CTAB) or didodecyldimethyl ammonium bromide (DDAB) in a study on inorganic anions [34]. The surfactants used in this experiment were kept under the critical micelle concentration (CMC) to avoid a chromatographic component to the separation. The authors of this study determined that the EOF became steady after 10% of the CMC is added to the mixture and observe this in several solutions of increasing methanol concentrations. The reversal in this study is attributed to aggregates that build up on the capillary surface, creating a change in capillary surface charge. The increase in methanol concentration is shown to lessen this effect, which

shows the necessity of a second source of binding when application of surfactants to non-aqueous systems are observed.

### 2.1.7 Permanent capillary coatings

There are two approaches to a permanent capillary coating. First is to covalently bond the coating material to the surface of the capillary. Found primarily in aqueous applications, covalent bonding is generally used to create a permanent modification to the surface of the capillary and will typically reduce EOF and analyte-wall interactions greatly depending on the application [11]. Covalently bonded coats are rare in non-aqueous capillary electrophoresis, but have been found to stabilize and even reverse EOF in methanolic systems [35]. The primary drawback to the use of covalently bonded, permanent coatings is that the methods used to create these coatings can be time consuming and experimentally complex (requiring anhydrous conditions and complicated reagent transfer procedures). It has also been reported that many of these procedures do not allow for uniform and reproducible wall coatings from capillary to capillary [35]. The second common method for the creation of a permanent capillary coat is through the use of multilayers of polymers and polyelectrolytes. Non-covalent coatings typically have the advantage of having relatively simple coating procedures [36].

One of the common methods of coating capillaries is through the use of multiple ionic polymer layers (PEM coats). In this method of surface modification, thin polymer layers carrying a charged group are placed on the inner surface of a capillary. Once established, the layer will alter the surface charge of the capillary. It has been found that several layers of oppositely charged polymers will provide a more stable capillary surface [37]. This modification in the capillary charge can potentially be quite large and has been

observed to eliminate or even change the direction of the EOF of a given capillary. Several attempts to determine the nature of these polymer layers in order to further manipulate the surface charge that is provided by them [37, 38]. Application of PEM layers is generally done through the use of the polymer in a supporting buffer being pumped through the capillary at a given rate. The polymer will adhere to the surface of the capillary and become interwoven. Although the application of these coatings is relatively simple compared to other coating systems, the coating itself has been found to be a complex interwoven mixture of the polymer layers [39]. Atomic force microscopy images have shown that the polymeric layers are not well behaved layers, but the polymers are an interwoven system [40]. The method of application has also been found to be important in regards to the properties of the final PEM system [37]. Ionic strength in the polymer solution has been found to affect the polymer layers but are highly dependent on the ions that are used [38, 41]. The effect of the molecular weight of the coating materials has also been studied, and it was found that polymers of higher molecular weight would dominate the surface coating over smaller molecular weight species [42].

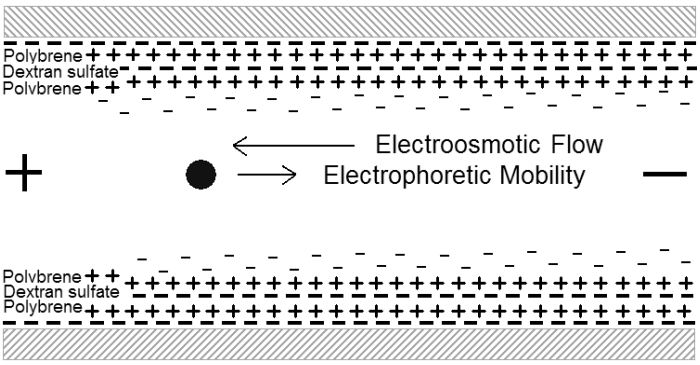


Figure 1. PEM coat of Polybrene™ and dextran sulfate

Primary uses of PEM coats have been found in aqueous media. These studies revolve around the prevention of analyte adsorption to the surface of the capillary. In aqueous media the free silanols on the surface of the

glass capillary will provide a partial negative charge above a pH of 5. A negative surface charge on the capillary will draw the positive ions from the buffer and build up a relatively higher concentration of ions as compared to the bulk solvent. This buildup of ions will extend into the buffer and will progressively weaken the farther away from the surface of the capillary. Ionic buildup such as this is referred to as the charged double layer and has been discussed previously in this work. Charge on the capillary is a major cause of analytes adhering to the surface, causing deformations in peak shape and poor resolution in separations. PEM multilayers give a level of control over the capillary charge that is unattainable in bare fused silica capillaries.

The primary development of PEM capillary coats came about due to difficulties involving the separation of proteins and peptides. The separation of biological macromolecules is notoriously difficult due to the multiple charges that can be found on them at biological pH. Raising the pH to eliminate this effect will denature the protein and render the use of the separation more limited. Katayama et al. separated a series of acidic proteins at a pH of 7.4 by showing that a PEM coating, called successive multiple ionic layers or SMIL, could provide pH independent EOF within a wide range of pH 2 to 11 [10]. Similar results were found with a different PEM coat when Schlenoff et al. alternated layers of poly(diallyldimethylammonium chloride) (PDADMAC) and polystyrene sulfonate (PSS) to separate a series of proteins [43]. While the aqueous applications of PEM coats continue to grow from this early work, the non-aqueous applications have received significantly less notice.

Assuncao et al. have observed the effect of a capillary coated with poly-N,N-dimethylacrylamide (PDMA) in a non-aqueous system [1]. The primary goal of their

study was the reduction of protein adsorption on the capillary surface. They found that there was a 'reduction' of the EOF although they did not quantify this reduction. The buffer used in their separation was a mixture of acetonitrile, methanol and acetic acid.

While the primary attention to capillary coatings have involved aqueous applications, coatings have been applied to non-aqueous studies for several applications. The choice of solvent/buffer has varied from partially aqueous to neat solvent. Due to the wide variety of properties associated to the buffers, their effect on coating materials varies widely. Because of this, a direct comparison of different buffer systems is not a worthwhile endeavor. One coating that controls EOF in one solvent system could potentially break down rapidly after a change in solvent. While this property is known, a full study is not available. Zou et al. compiled lifetimes of different coatings and found that they range in time from a single run to over a month of use [44].

### 2.1.8 Capillary coatings in non-aqueous capillary electrophoresis

Several capillary coatings have been applied to methanol solvent systems. Polyvinyl alcohol (PVA) and polyethylene glycol (PEG) were the first to be developed for methanolic applications. When these two coatings were compared [11], it was found that the PVA coating provided a high efficiency (N=400,000) for the separation of acidic drugs in a methanol solvent using ammonium acetate as a charge carrier. This study also observed that no loss of resolution was found after 100 injections. This capillary was directly compared to a polyethylene glycol (PEG) coated capillary. In that capillary, resolution was similar, but the coating would show significant deterioration after only 40 injections. The difficulty in these types of coatings is the lengthy process of immobilizing the coat on the capillary.

Polytetrafluoroethylene (PTFE) capillaries have been used in a non-aqueous separation of fatty acids in fish oils [45]. In this study it was found that PTFE capillaries suffer from poor baseline stability and a long stabilizing period was required before injections. The separation of saturated, even chain length acids from $C_{16}$ to $C_{26}$ resulted in almost baseline resolution. Limits of detection at a signal to noise ratio of 1 to 3 were found to be 0.025mM when applying indirect UV detection.

Belder et al. determined that the EOF in a PEG coated capillary was dependent on the cation. In their study, the direction of EOF was reversed when comparing potassium ion to lithium ion [46]. The concentration of water found in the separation was also determined to be of vital importance as it reduced the EOF of an acetonitrile system [47].

One of the primary difficulties in determining the extent of analyte absorption onto a capillary wall is that there is no direct measurement for this phenomenon. The extent is inferred by secondary effects of the phenomenon such as peak shape and homogeneity. General traits that will indicate that absorption is a problem include peak tailing, where an electrophoretic peak is asymmetrical, and the raising of the background. Only one method has been developed for direct analysis of absorption and it is time and resource prohibitive [48].

In this study, capillaries were modified with two different types of capillary coats. Tri-methylsilane (TMS) was bonded to a capillary and myristyltrimethylammonium (MTAB) bromide was added to the running buffer to create a positive dynamic coat [49]. As discussed above, the surfactant MTAB can potentially be used for modification of EOF, yet problems will arise in a methanolic solvent. In order to strengthen the interaction of the surfactant to the capillary wall a polarity interaction is utilized. TMS is

covalently bound to the capillary wall to create an area of low polarity that will interact with the long non-polar tails of the MTAB. The coating's effect on the resolution of a separation of a homologous series of fatty acids labeled with a NIR fluorescent probe was compared to a permanent polymer coat which was comprised of a series of alternating layers of positively charged Polybrene® and negatively charged dextran sulfate discussed above. The pH* range of this PEM coat made it an ideal system for use in non-aqueous separations in which deterioration of a coat is a concern. Resolution between separated peaks was monitored in order to determine the effect of the coats and develop an understanding of the coat properties.

## 2.2 Reagents and materials

Linear saturated fatty acids C6 (caproic acid), C8 (caprylic acid), C10 (capric acid), C12 (lauric acid), C14 (myristic acid), C16 (palmitic acid) as well as N,N-dicyclohexylcarbodiimide (DCC) and myristyltrimethylammonium bromide (MTAB) were all purchased from Acros Organics. Tetraethylammonium chloride (TEAC) originally from Eastman Kodak (Rochester, NY) was obtained from house stores. Polybrene® (hexadimethrine bromide) and dextran sulfate (avg. mol. Wt. = 5000 D) were purchased from Aldrich Chemical Corporation (Milwaukee, WI, USA). Methanol and chloroform used as solvents were HPLC grade and purchased from Fisher Scientific (Fair Lawn, NJ).

### 2.2.1 Apparatus

Capillary electrophoresis was performed on fused silica capillaries with 50 μm internal diameter and 360 μm outer diameter, purchased from Polymicro Technologies (Phoenix, AZ, USA). A detection window of 1 cm was created by pyrolysis of the polyimide coating using a low intensity butane flame. The capillary was then fixed to a microscope slide using epoxy.

Voltage was applied during electrophoretic separations using a CZE 1000R (Spellman High Voltage Electronics Corporation, Plainview, NY). Injections for Trimethylsilane/Successive multiple ionic layer (TMS/SMIL) comparison experiments were performed electrokinetically (15 kV for 5 s) at the cathode. Injections for the SMIL coating experiments were performed electrokinetically (5 kV for 5 s) at the anode.

Detection was achieved by laser-induced fluorescence using a laboratory-constructed epifluorescence microscope. Excitation was with a near-infrared laser operating at 785 nm (Sanyo DL7140-201 S, purchased from Thorlabs). The beam was passed through a mica half-wave plate (Melles Griot) and a calcite Glan-Thompson polarizer (Karl Lambrecht, Chicago, IL) for control of light intensity and polarization. The collimated beam was reflected by a dichroic reflector (Omega Optical, Brattleboro, VT, 810 DRLP) and focused into the capillary by a 40 X, 0.85 NA microscope objective (Nikon Fluor 40, Nikon Corp, Tokyo). Fluorescence was collected by the same objective, passed through the dichroic, spatially filtered with a 600 μm pinhole (National Aperture), and spectrally filtered with an Omega 810EFLP long pass filter. The remaining fluorescence was focused with a pair of 24 mm EFL achromats (Rolyn Optics, Covina, AC) onto the active area of a single photon counting avalanche photodiode

(SPCM module, EG&G Canada, now PE Instruments). Data collection was performed with an MCS plug-in card (MCSII, Tennelec/Nucleus, Oak Ridge, TN), usually at a rate of 250 ms/MCS bin, residing in an AT bus PC.

Peak analysis was done with Igor Pro 4.02A (Wavemetrics, Eugene, OR) using multipeak fit package version 1.30. Electropherogram peaks were fit to the Gaussian shape.

### 2.2.2 Fatty Acid Derivatization Protocol

The procedures for labeling the fatty acids with the near-infrared fluorescent probe, and for synthesizing the probe have been previously reported [50]. Briefly, stock solutions of various fatty acids and DCC were prepared in chloroform (1 M). A stock solution of the NIR fluorescent probe was prepared in anhydrous dimethylformamide (1 M). To perform a derivatization, a 100 μL aliquot of fatty acid solution was pipetted into a 2 mL glass reaction vial and stirred with a magnetic stirrer. A 100 μL aliquot of DCC stock was added and the mixture was allowed to stir for 30 seconds. A 100 μL aliquot of the labeling reagent was added and the reaction vessel was capped and allowed to react for 8 hours, while shielded from ambient light.

At the end of the reaction period, precipitated dicyclohexylurea was filtered off using a 0.2 μm nylon syringe filter and aliquots of the reaction mixture were diluted in methanolic run buffer for CE analysis. To create a mixture of fatty acids, aliquots of the various individual reactions were combined and subjected to an identical work up procedure.

### 2.2.3 Coating procedure

TMS capillary coatings were prepared by washing capillaries were with methanol, anhydrous acetone, anhydrous chloroform for 10 min each at a flow rate of 6.9 μL/min, then neat chlorotrimethylsilane was flushed through the capillary overnight. The chlorotrimethylsilane was pulled from the capillary via vacuum, then the capillary was washed with anhydrous chloroform, anhydrous acetone, methanol for 10 min each at a flow rate of 6.9 μL/min. After this procedure the capillary was then flushed and stabilized in background electrolyte. The SMIL capillary used in the comparison study was an adaptation of the procedure developed by Katayama, et al.[10]. Bare fused silica capillaries (50 μm ID, 360 μm OD) were washed with ultrapurified (18 MΩ•cm) water for 30 minutes followed by 0.1 M NaOH for 15 min followed by a 15 min wash of ultrapurified (18 MΩ•cm) water. The capillaries were then evacuated by suction and a solution of 10% w/v Polybrene® was flushed through the capillary at a rate of 6.9 μL/min for 30 min. The capillary was then evacuated and 10% w/v dextran sulfate was flushed at the same rate for 30 min. Finally, the capillary was evacuated a third time and the final coat of Polybrene® was flushed as described above for 30 min. The capillary was again evacuated and allowed to stand for 8 hours. Procedures for capillary modification in the timed SMIL coat experiment are identical to the SMIL coating procedure described above with the exception of the coating time. The first 2 layers, Polybrene® and dextran sulfate, were flushed through the capillary for 4 hours. The final layer of Polybrene® was pumped for a variable amount of time to determine the effect of the final layer on the overall separation.

### 2.2.4 Electroosmotic flow determination

EOF was determined through the method described in [51]. In short, the running buffer was pumped into the capillary and a voltage was applied to the capillary to equilibrate the charge. The current across the capillary was monitored by placing a resistor (100.0 kΩ) between the buffer vial and the ground and recording the voltage across this resistor using Logger Pro® software (Vernier Software & Technology). The ionic strength of the buffer at the anode (cathode in the SMIL experiments) was changed to a concentration 0.9 x the original ionic strength. As the buffer at the lower ionic strength migrated across the capillary the total resistance across the capillary would change accordingly. When the new, lower ionic strength reached the cathode (anode in SMIL experiments) a new current would stabilize. The time to reach the new current was taken over the length of the capillary, this was the velocity of the EOF and when the electric current component was added the $\mu_{eof}$ was determined.

## 2.3 Results and discussion

In order to determine how robust the separation in each treated capillary is and to develop an understanding of separation properties resulting from specific coating procedures, the separation efficiency and resolution in both the TMS and SMIL coated capillaries was calculated from sets of back-to-back injections. The resolution was found by using the same set of labeled acids in both capillaries. Resolution is defined by equation 3 where resolution of 1.5 corresponds to a baseline separation of the two components. The peak shapes were fit using Igor Pro software's multi-peak fit macro

and were found to fit well with the Gaussian profile expected in CE separations. From the values obtained with the fits, analyte mobility, peak width, plate height (HETP), and resolution were calculated (equation 3) for each labeled fatty acid. Averages from this data are shown in Table 1 and 2.

(3) $$\text{resolution} = \frac{|p_1 - p_2|}{2(w_1 + w_2)}$$

$p_1$ = position of peak 1
$p_2$ = position of peak 2
$w_1$ = width of peak 1 at baseline
$w_2$ = width of peak 2 at baseline

Table 1. TMS/MTAB capillary average EOF = 6.825 x $10^4$ ($cm^2$/V s), average injection volume 7.41 nl

| Chain length | average electrophoretic mobility *$10^4$($cm^2$/V s) | Average number of plates | Average plate height (μm) | Average resolution |
|---|---|---|---|---|
| 6 | 1.148 | 46843 | 7.47 | |
| 8 | 1.126 | 44834 | 7.81 | 1.80 |
| 10 | 1.109 | 48628 | 7.20 | 1.71 |
| 12 | 1.091 | 49658 | 7.05 | 1.71 |
| 14 | 1.073 | 45432 | 7.70 | 1.67 |
| 16 | 1.058 | 44582 | 7.85 | 1.42 |

Table 2. SMIL capillary average EOF = 1. 872 x $10^3$ ($cm^2$/V s) average injection volume 19.68 nl

| Chain length | average electrophoretic mobility *$10^{-4}$($cm^2$/V s) | Average number of plates | Average plate height (μm) | Average resolution |
|---|---|---|---|---|
| 6 | 3.071 | 30280 | 11.56 | |
| 8 | 3.004 | 34017 | 10.29 | 1.53 |
| 10 | 2.940 | 35317 | 9.91 | 1.49 |
| 12 | 2.878 | 36807 | 9.51 | 1.49 |
| 14 | 2.818 | 34276 | 10.21 | 1.50 |
| 16 | 2.762 | 77089 | 4.54 | 1.43 |

Values were compiled to find the reproducibility and the stability of the experiment. In Figures 3 and 5, the resolution between the two coatings is compared. Multiple, back-to-back runs on each of the capillary coatings can be observed, shown in

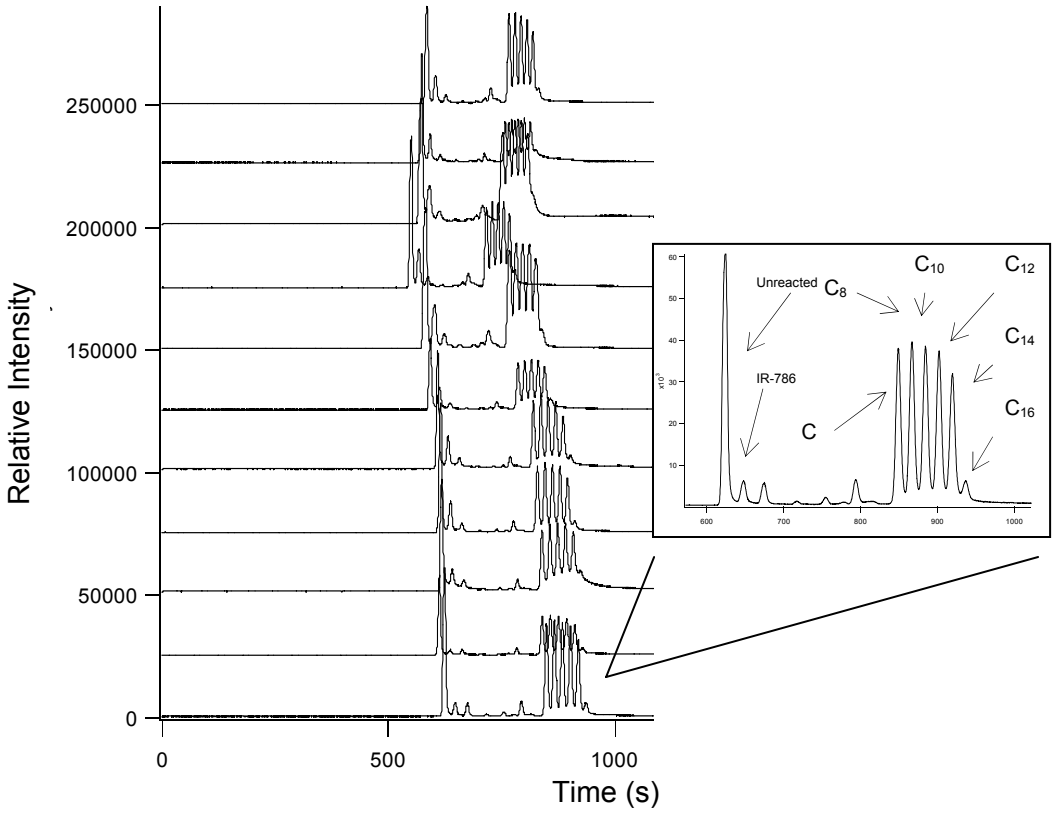


Figure 2: The series of saturated fatty acids separated in the TMS/MTAB coated capillary. The first injection is the bottom trace. Resolution between the peaks can be observed to decrease slightly through subsequent injections. Capillary ID 50 µm total length 65 cm, 5 sec 15 kV injection, running voltage 25 kV. Subsequent traces are offset

Figures 2 and 4. While the resolution is deteriorating throughout both of the series, there are two trends that predominate. The first trend that seems apparent when comparing the resolution of the two coating systems is that the TMS/MTAB capillary has higher overall resolution. This appears to be primarily due to the lower TMS/MTAB capillary EOF that will dictate the injection plug length along with the amount of diffusion that will affect the sample plug as it travels through the capillary. Plugs were introduced into the capillary by electrokinetic injection (5 s, at 15 kV) for both experiments. Injection

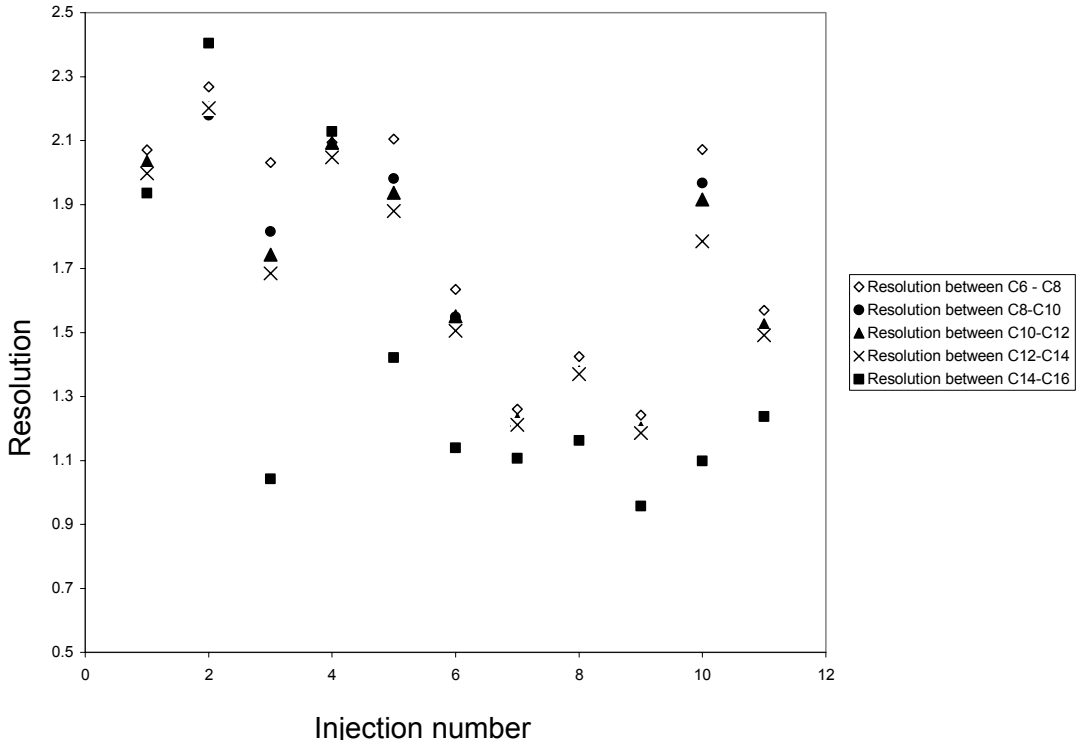


Figure 3. TMS/MTAB resolution broken down by acid pair. MTAB concentration 20 mM, capillary length 65 cm, length to detection 35 cm, running voltage 25kV, 50µm ID

background electrolyte consisted of 0.0125 M TEAC solution in methanol for both the TMS/MTAB and the SMIL capillaries. In the TMS/MTAB experiments, addition of MTAB into the solution caused the ionic strength to increase from 0.0125 M to 0.0325 M. This change in ionic strength along with the difference in the capillary internal surface charge effects the electroosmotic flow of both the injection and the separation. The injection plug length differed in volume between the two systems; 7.41 nl for TMS capillaries and 19.68 nl for SMIL used in comparison study. The affect of the plug length on the average variance in each series of separations was minimal (Table 3). The SMIL capillary having a slightly larger sample plug caused a small increase in the percentage of

(4) $$\sigma^2_{total} = \sigma^2_{\text{diffusion}} + \sigma^2_{temprature} + \sigma^2_{injection} + \sigma^2_{wall}$$ σ = variance

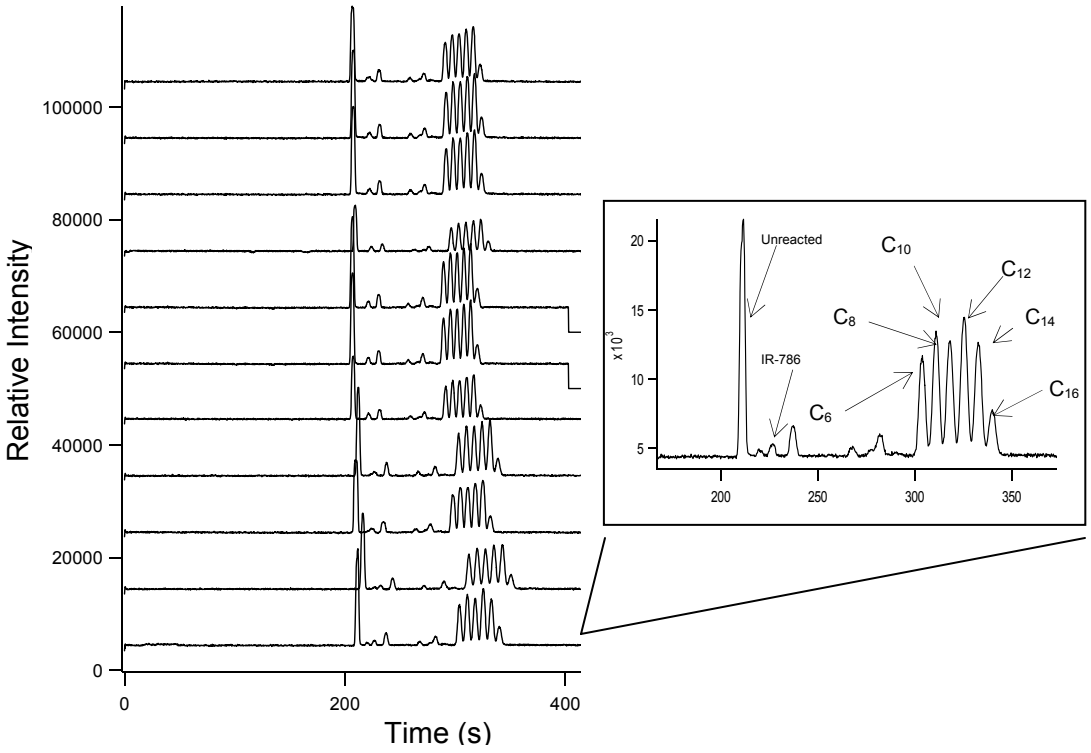


Figure 4: The series of saturated fatty acids separated in the SMIL 30/30/30 coated capillary. The first injection is the bottom trace. Resolution between the peaks can be observed to decrease slightly through subsequent injections. Capillary ID 50 μm total length 65 cm, 5 sec 15 kV injection, running voltage 25 kV. Subsequent traces are offset.

the variance due to the plug length (see equation 4). The slightly larger plug length will adversely affect the resolution.

Table 3. Average variance from SMIL and TMS/MTAB separations shown in figures 2 and 4. Variance broken down into its components

| | Total variance | Injection | Diffusion | 'Other' | % injection | % Other |
|---|---|---|---|---|---|---|
| TMS/MTAB | 9.62 $\mu m^2$ | 1.42 $\mu m^2$ | 0.0038 $\mu m^2$ | 8.38 $\mu m^2$ | 12.87 | 87.09 |
| SMIL | 42.26 $\mu m^2$ | 9.98 $\mu m^2$ | 0.0038 $\mu m^2$ | 32.28 $\mu m^2$ | 23.61 | 76.38 |

Analyte – coat interaction appears to be minimal as this would cause peak tailing which would reduce the symmetry of the peaks and create a problem in fitting the peaks to the Gaussian profile. A chromatographic effect was observed with the TMS capillary with longer acid chain lengths, but the effect appeared only with longer chain lengths

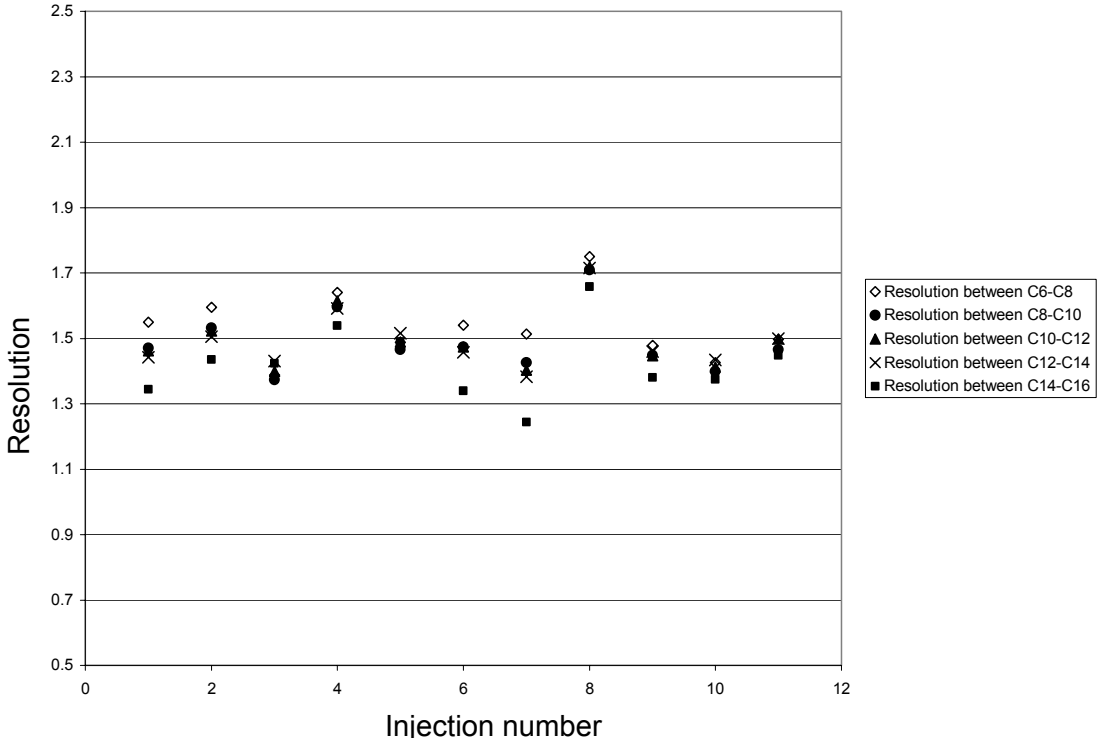


Figure 5. SMIL resolution broken down by acid pair. Capillary length 65 cm, length to detection 35 cm, running voltage 25kV, 50µm ID

(discussed below). Temperature was not controlled in these experiments and no attempt was made to determine the effect of temperature on the variance. It was assumed that the effect of temperature was negligible for determination of the effect of analyte-wall interactions.

The zeta potential and the surface charge of the capillary due to the coat will cause the primary change in EOF. A larger surface charge density will cause EOF to increase although there will be components of the EOF that are caused by smaller interactions. One small component to the EOF is due to the decrease to the buffer ionic strength caused by the absence of buffer additives in the SMIL capillary (Tables 1 and 2).

The increase in EOF observed in the SMIL capillary had the effect of decreasing the total amount of time that the acids took to reach the detection system. By decreasing

the total migration time, the effects of diffusion will be lessened slightly. The ideal separation will occur where the EOF will minimizes the time an analyte migrates to the detector therefore the effects of diffusion and analyte-wall interactions would be lessened but does not negate the electrophoretic mobility inherent to the analyte, which would cause a loss of separation.

The second trend seen in the analysis of the resolution data is that the separations in the SMIL-coated capillary seem to be more stable than in the TMS-coated system. Presumably, the stability is due to having a coating that is permanently adhered to the capillary wall making it less prone to small changes that arise from slight differences in buffer concentrations and the slight differences of coating material that could greatly affect the resolution of the TMS/MTAB capillary separations.

Both coats had similar long-term stability and could be used without further modification for at minimum 50 injections (where our experiment ended) without a large decrease in the overall resolution. The capillaries were not tested beyond this point to determine the point at which the coats deteriorated.

When the resolution between individual acid pairs is examined (Figures 2 and 4) an interesting artifact was observed. The longer chain lengths in the TMS capillary had significantly worse resolution when compared to their counterparts in the SMIL capillary. This decrease in resolution was probably caused by the longer, more hydrophobic acid chains being drawn to the hydrophobic TMS coating, or the hydrophobic tail of the MTAB, causing a slight chromatographic effect on the separation that was not observed in the SMIL coating. Due to this effect, the TMS coating has a limitation to smaller chain lengths and more hydrophilic analytes when compared to the SMIL coat.

### 2.3.1 Developing greater EOF control through modulation of SMIL coats

In order to gain a greater degree of control over the surface properties of SMIL capillaries and control their EOF to a greater degree, the coating procedure was modified. The surface charge density of the capillary surface is the primary factor affecting the EOF and greater control over this property will improve separations. These capillaries primarily differed from the capillaries discussed earlier in this chapter in that the coating procedure of these capillaries was altered to change the surface coat.

Increasing the length of time the final coat is deposited increases the effect of that coat. In the electropherograms shown in Figure 6, the final layer was deposited for 1-4

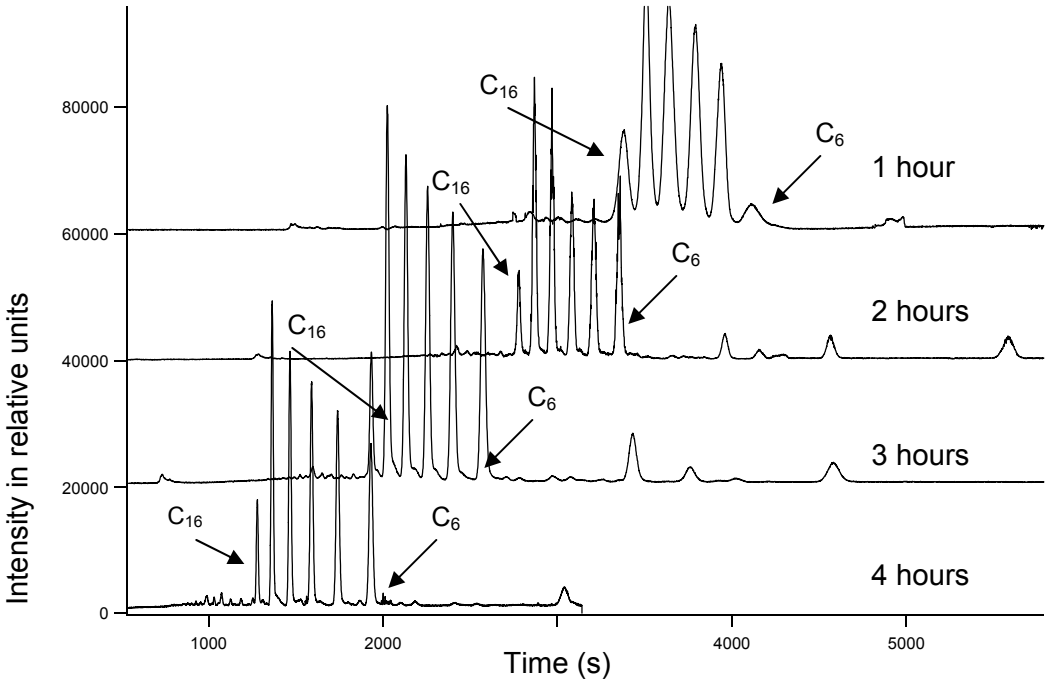


Figure 6. Separations of straight chain fatty acids with different coating times. SMIL coating time for initial layers 4 hours Polybrene® followed by 4 hours dextran sulfate. Final application time of Polybrene® on graph. Capillary length 65cm, length to detection 35cm, running voltage 25kV, 50µm ID. Subsequent traces are offset.

hours and has a dramatic effect on the separations. The effect of the coating on theoretical plate height and resolution is shown in Table 4. While the velocity of delivery of the coating material was steady for the extent of the procedure, the flow rate and mass used was not monitored. This information was not easily attained as there was no way of determining the extent, or thickness of the coating during the procedure.

Table 4. Number of theoretical plates, theoretical plate height and resolution of the separation shown in Figure 6

| | 1 hour | 2 hour | 3 hour | 4 hour |
|---|---|---|---|---|
| Chain length | N | | | |
| 16 | 18192.65 | 96807.74 | 63889.35 | 58045.74 |
| 14 | 44848.43 | 67409.54 | 51513.52 | 45876.74 |
| 12 | 24238.73 | 62289.39 | 47602.36 | 46604.3 |
| 10 | 26320.37 | 72185.09 | 41710.1 | 36879.15 |
| 8 | 26429.62 | 59401.37 | 35456 | 37990.09 |
| 6 | 12671.57 | 64811.71 | 38165.06 | 39009.35 |

| | 1 hour | 2 hour | 3 hour | 4 hour |
|---|---|---|---|---|
| Chain length | H (μm) | | | |
| 16 | 19.23853 | 3.615413 | 5.478221 | 6.029728 |
| 14 | 7.804063 | 5.192143 | 6.794333 | 7.629138 |
| 12 | 14.4397 | 5.618934 | 7.352576 | 7.510036 |
| 10 | 13.29769 | 4.848647 | 8.391252 | 9.490457 |
| 8 | 13.24272 | 5.89212 | 9.87139 | 9.212929 |
| 6 | 27.6209 | 5.400259 | 9.170692 | 8.972208 |

| | 1 hour | 2 hour | 3 hour | 4 hour |
|---|---|---|---|---|
| Chain lengths | Resolution | | | |
| 16-14 | 1.117904 | 1.896907 | 1.735849 | 2.178344 |
| 14-12 | 1.102564 | 1.92381 | 1.927928 | 2.369942 |
| 12-10 | 1.214286 | 2.11215 | 2.137931 | 2.520408 |
| 10-8 | 1.226891 | 2.306306 | 2.267717 | 2.60793 |
| 8-6 | 1.230769 | 2.217054 | 2.386207 | 3.019763 |

Permanent coatings such as this SMIL coat will not affect the inherent mobilities of the analytes being analyzed. The direction of the apparent mobility (cathode to anode) coupled to the order of elution reversing itself, as compared to the capillaries described above, indicates that the EOF in this set of capillaries is flowing in the opposite direction

of the electrophoretic mobility of the labeled acids. Labeled acids with smaller chain lengths have a higher electrophoretic mobility [49].

By determining the electrophoretic mobility of the individual acids throughout the series of capillaries, the effect of various band broadening mechanisms can be evaluated. Table 5 shows the EOF and electrophoretic mobility for this series of capillary coatings. The mobility of the acids remains stable throughout the series and therefore indicates that the secondary effects have a minimal effect.

Table 5. EOF, apparent mobility, and electrophoretic mobility of labeled acids with chain lengths of 4, 6, 8 and 10. (note: all EOF and mobility numbers $*10^3$)

| Time of final coat application (min) | 2 | 10 | 15 | 30 | 45 |
|---|---|---|---|---|---|
| EOF ($cm^2V^{-1}s^{-1}$) | 2.01 | 2.06 | 2.14 | 2.16 | 2.30 |
| Capillary ζ-potential (mV) | 36.0 | 36.9 | 38.3 | 38.7 | 41.2 |
| Apparent mobility $*10^4$ ($cm^2V^{-1}s^{-1}$) | | | | | |
| c6 | 0.58 | 0.62 | 0.65 | 0.69 | 0.79 |
| c8 | 0.52 | 0.57 | 0.61 | 0.66 | 0.74 |
| c10 | 0.47 | 0.53 | 0.56 | 0.62 | 0.69 |
| c12 | 0.42 | 0.49 | 0.52 | 0.57 | 0.63 |
| Electrophoretic mobility $*10^4$ ($cm^2V^{-1}s^{-1}$) | | | | | |
| c6 | 1.43 | 1.45 | 1.49 | 1.47 | 1.51 |
| c8 | 1.49 | 1.49 | 1.53 | 1.51 | 1.56 |
| c10 | 1.54 | 1.53 | 1.58 | 1.55 | 1.61 |
| c12 | 1.60 | 1.58 | 1.62 | 1.59 | 1.67 |

Figure 6 shows a sample of one electropherogram from each of the capillaries. It is apparent that there is a dramatic increase in resolution as the final coat increases its effect. This observation seems logical in that the final coat, polybrene, increases the overall charge of the capillary making it more and more positive. Creation of a deeper charged double layer at the inner surface of the capillary will increase the EOF in the capillary. When the EOF is increased, then the electrophoretic mobilities of the labeled acids will have a less dominant effect on the separation.

Maintaining control over the capillary EOF and reducing the time of elution can be accomplished by using the SMIL procedure and reducing the total length of the capillaries. This effect could be seen in a new series of capillaries as net effect of these shorter capillaries was an increase in the field strength and a decrease in the time of separation. Figure 7 shows the peak position of 4 acids when the capillary surface was changed using the method described above. The migration times show that there is an inverse relationship with coating time. There appears to be an asymptote where EOF no longer takes part in the separation around t=0, when the final layer of coating material first starts being pumped. Logically the EOF will reverse when the capillary has a net negative charge from the dextran sulfate polymer layer. The lower the EOF becomes the

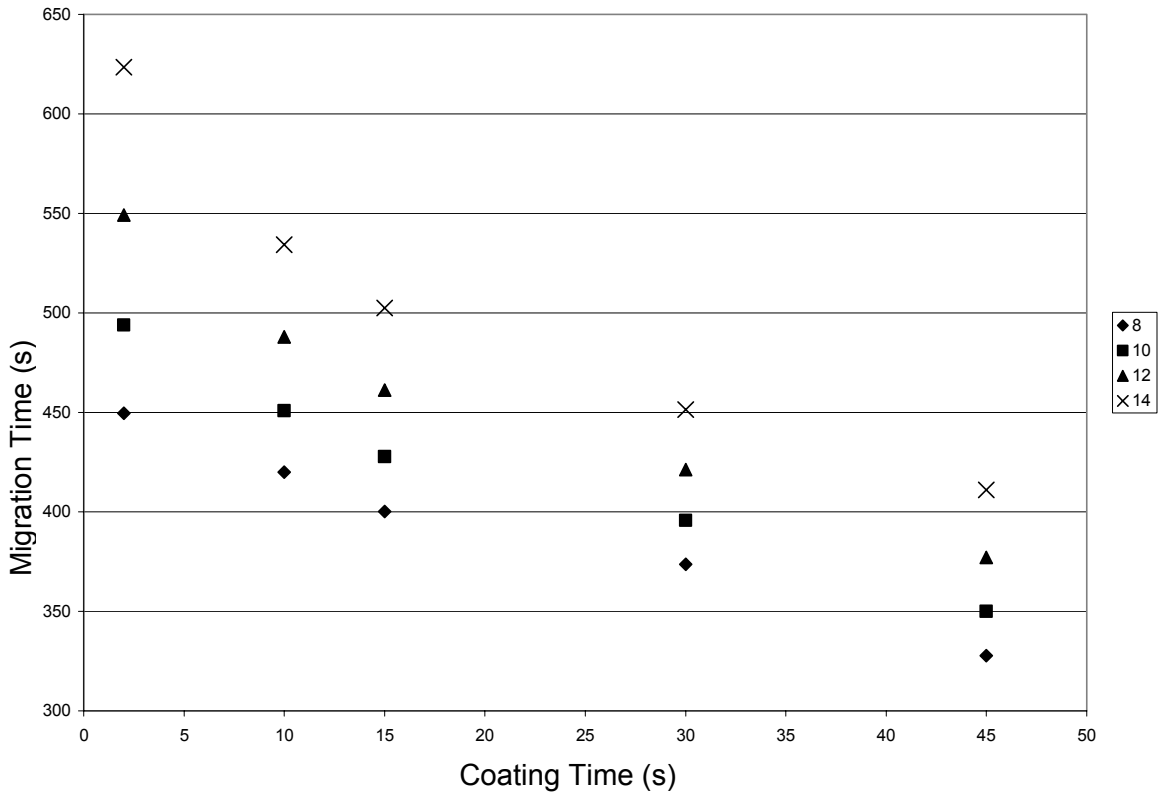


Figure 7: The inverse relationship between the final polymeric layer coating time and elution time. SMIL coating time for initial layers 4 hours Polybrene® followed by 4 hours dextran sulfate. Final application time of Polybrene® on graph. Capillary length 36cm, length to detection 18cm, running voltage 25kV, 50µm ID

more the electrophoretic mobility will dominate the separation.

Peak separation will increase as the EOF is decreased but it may not have an overall positive effect on the resolution of the analytes being separated. Although electrophoretic mobility of the individual analytes dominates the separation and the effect of the EOF decreases, several sources contribute to the overall band broadening. These sources primarily include diffusion of analytes, and analyte-wall interactions. The band broadening due to diffusion is more of a problem in separations with longer the migration time. Analyte-wall interactions can also become increasingly problematic, depending on the charge of the analyte being studied, as the overall charge of the surface of the capillary wall is changed. Highly charged ions of charge opposite to that of the final layer of the capillary coating and smaller ions that have a high diffusion coefficient will likely have inferior resolution in an electrophoretic separation, where as more neutral ions and larger ions will have less band broadening due to diffusion or wall interactions.

## 2.4 Conclusions

The modification of capillaries through the use of coats has been used to reduce analyte-wall interactions [28]. In previous work with non-aqueous capillary electrophoresis it was shown that wall coatings could alter EOF and improve the separation of a series of fatty acids [49]. Through a comparison of the TMS/MTAB capillary and the SMIL capillary it was found that stability in the resolution between peaks was significantly higher with the permanent SMIL coat.

Through careful control over EOF in non-aqueous capillary electrophoresis the EP will dominate the separation. The use of capillary coats such as the SMIL coat used

in this study provided EOF control without altering the EP of the analytes. It was found that through altering the deposition time of the capillary coating material the EOF of the capillary could be modified. An increase in peak to peak resolution was shown when observing a separation of saturated fatty acids when capillaries with slightly different capillary coats were used.

# REFERENCES


1. Assuncao, N.; Leandro G.; Paulino, L.; Lupetti, K.; Carrilho, E., *Nonaqueous capillary electrophroesis in coated capillaries: An interesting alternative for protomic applications.* Electrophoresis, 2005. **26**: p. 3292-3299.

2. Du, G.; Shuzhen, G; Xie, J.; Zhong, B.; Liu, K., *Chiral separation of anticholinergic drug enantiomers in nonaqueous capillary electrophoresis.* Journal of Chromatography A, 2005. **1074**: p. 195-200.

3. Li, Y.; Xiaojun,X; Qi, S.; Gao, W.; Chen, X.; Hu, Z., *Separation and determination of strychnine and brucine in Strychonos nux-vomica L. and its preparation by nonaqueous capillary electrophroesis.* Journal of Pharmaceutical and biomedical analysis, 2006. **41**: p. 400-407.

4. Qi, S.; Lan, D; Tian, K.; Chen, X.; Hu, Z., *Novel and simple nonaqueous capillary electrophoresis separation and determination bioactive triterpenes in Chinese herbs.* Journal of Pharmaceutical and biomedical analysis, 2006. **40**: p. 35-41.

5. Kuhn, R., *Capillary Electrophoresis: Principles and Practice*. 1993, New York: Springer-Verlag.

6. *Handbook of Capillary Electrophoresis*. 2 ed, ed. J.P. Landers. 1997, New York: CRC Press.

7. Riekkola, M., *Recent advances in nonaqueous capillary electrophoresis.* Electrophoresis, 2002. **23**: p. 3865-3883.

8. Riekkola, M.; Matti, J; Porras, S.; Valko, I., *Non-aqueous capillary electrophoresis.* Journal of Chromatography A, 2000. **892**: p. 155-170.

9. Balcom, B.; Niles O., *Solvent dependence of carboxylic acid condensation with dicyclohexylcarbodiimide.* Journal of Organic Chemistry, 1988. **54**: p. 1922-1927.

10. Katayama, H.; Yasushi, I.; Asakawa, N., *Development of novel capillary coating based on physical adsorption for capillary electrophoresis.* Analytical Sciences, 1998. **14**: p. 407-408.

11. Belder, D.; Husmann, H., *Use of coated capillaries for nonaqueous capillary electrophoresis.* Journal of Microcolumn Separations, 1999. **11**(3): p. 209-213.

12. Fillet, M.; Anne-Catherine, S.; Crommen, J., *Effects of background electrolyte composition and addition of selectors on separation selectivity in nonaqueous capillary electrophoresis.* Electrophoresis, 2003. **24**: p. 1499-1507.

13. Righetti, P.; Cecilia, G.; Verzola, B.; Castelletti, L., *The state of the art of dynamic coatings.* Electrophoresis, 2001. **22**: p. 603-611.

14. Maelanson, J.; Lucy, C., *Dynamic capillary coatings for electroosmotic flow control in capillary electrophoresis.* Trends in Analytical Chemistry, 2001. **20**(6): p. 365-374.

15. Porras, S.; Ernst, K., *Capillary zone electrophoresis in non-aqueous solutions: pH of the background electrolyte.* Journal of Chromatography A, 2004. **1037**: p. 455-465.

16. Steiner, M., *Nonaqueous capillary electrophoresis: A versatile completion of electrophoretic separation techniques.* Electrophoresis, 2000. **21**: p. 3994-4016.

17. Shen, H.; Steven R.; Boyd, B.; Kennedy, R., *Detection of peptides by precolumn derivatization with burette reagent and preconcentration on capillary liquid chromatography columns with electrochemical detection.* Analytical Chemistry, 1999. **71**: p. 987-994.

18. Xue, E., *Characterization of band broadening in capillary electrophoresis due to nonuniform capillary geometries.* Analytical Chemistry, 1994. **66**: p. 3575-3580.

19. Culbertson, C., *Lowering the UV absorbance detection limit in capillary zone electrophoresis using a single linear photodiode array detector.* Analytical Chemistry, 1998. **70**: p. 2629-2638.

20. Arriaga, E.; Yanni, Z.; Dovichi, N., *Use of 3-(p-carboxybenzoyl) quinoline-2-carboxaldehyde to label amino acids for high-sensitivity fluorescence detection in capillary electrophoresis.* Analytica Chimica Acta, 1995. **299**: p. 319-326.

21. Dolnik, V., *Wall coating for capillary electrophoresis on microchips.* Electrophoresis, 2004. **25**: p. 3589-3601.

22. Horvath, J.; Vladislav D., *Polymer wall coatings for capillary electrophoresis.* Electrophoresis, 2001. **22**: p. 644-655.

23. Vayaboury, W.; Daniel K.; Giani, O.; Cottet, H., *Noncovalent coatings for the separation of synthetic polypeptides by nonaqueous capillary electrophoresis.* Electrophoresis, 2005. **26**: p. 2187-2197.

24. Xu, L.; Yu-Qi, F.; Shi, Z.; Da, S.; Gu, J., *Nonaqueous capillary electrophoresis using a zirconia-coated capillary.* Analytica Chimica Acta, 2004. **514**: p. 179-184.

25. Matysik, F., *Non-aqueous capillary electrophoresis with electrochemical detection.* Journal of Chromatography A, 1998. **802**: p. 349-354.

26. Porras, S.; Susanne K.; Strandman, S.; Tenhu, H.; Riekkola, M., *Novel dynamic polymer coating for capillary electrophoresis in nonaqueous methanolic background electrolytes.* Electrophoresis, 2001. **22**: p. 3805-3812.

27. Issaq, H.; King C.; Muschik, G.; Janini, G., *Applications of capillary zone electrophoresis and micellar electrokinetic chromatography in cancer research.* Journal of Liquid Chromatography, 1995. **18**(7): p. 1273-1288.

28. Castelletti, L.; Barbra V.; Gelfi, C.; Stroyanov, A.; Reghetti, P., *Quantitative studies on the adsorption of proteins to the bare silica wall in capillary electrophoresis III: Effects of adsorbed surfactants on quenching the interaction.* Journal of Chromatography A, 2000. **894**: p. 281-289.

29. VandeGoor T.; Janssen, P.; Van Zeeland, M.; Everaerts, F., *Capillary electrophoresis of peptides. Analysis of adrenocorticotropic hormone-related fragments.* Journal of Chromatography, 1991. **545**(2): p. 379-389.

30. McLaughlin, G.; Lindahl, J.; Palmieri, R.; Anderson, K.; Morris, S..; Morrison, J.; Bronzert, T., *Pharmaceutical drug separations by HPCE: practical guidelines.* Journal of Liquid Chromatography, 1992. **15**: p. 961-1021.

31. Heinig, K.; Carla, V.; Werner, G., *Determination of cationic surfactants by capillary electrophoresis.* Fresenius' Journal of Analytical Chemistry, 1997. **358**(4): p. 500-505.

32. Hansen, S.; Bjornsdottir, I., *Assay of acetylsalicylic acid and three of its metabolites in human plasma and urine using non-aqueous capillary electrophoresis with reversed electroosmotic flow.* Journal of Pharmaceutical and biomedical analysis, 1998. **17**: p. 1155-1160.

33. Chung, Y.; Lin, C., *On-line identification of 3,4-methylenedioxymethamphetamine in human urine by non-aqueous capillary electrophoresis-fluorescence spectroscopy at 77 k.* Journal of Chromatography B, 2001. **795**: p. 219-226.

34. Diress, A.; Charles A., *Electroosmotic flow reversal for the determination of inorganic anions by capillary electrophoresis with methanol-water buffers.* Journal of Chromatography A, 2004. **1027**: p. 185-191.

35. Steiner, F.; Marc A., *Control of electroosmotic flow in nonaqueous capillary electrophoresis by polymer capillary coatings* Electrophoresis, 2003. **24**: p. 399-407.

36. Cretich, M.; Marcella C.; Pirri, G.; Crippa, A., *Electroosmotic flow suppression in capillary electrophoresis: Chemisorption of trimethoxy silane-modified polydimethylacrylamide.* Electrophoresis, 2005. **26**: p. 1913-1919.

37. Kamande, M., Kristin A.; Lowry, M.; Warner, I., *Capillary electrochromatography using polyelectrolyte multilayer coatings.* J. Sep. Sci., 2005. **28**: p. 710-718.

38. Mermut, O., *Effects of the charge density and counterions on the assembly of polyelectrolyte multilayers.* J. Phys. Chem. B, 2003. **107**: p. 2525-2530.

39. McCormick, N.; Graf, R.; Barrett, C.; Reven, L.; Spiess, H., *NMR studies of the effect of adsorbed water on polyelectrolyte multilayer films in the solid state.* Macromolecules, 2003. **36**: p. 3616-3625.

40. McAloney, M.; Dudnik, V.; Goh, C. *Atomic force microscopy studies of salt effects on polyelectrolyte multilayer film morphology.* Langmuir, 2001. **17**: p. 6655-6663.

41. Graul, J., *Capillaries modified by polyelectrolyte multilayers for electrophoretic separations.* Analytical Chemistry, 1999. **71**: p. 4007-4013.

42. Sui, D.; Schlenoff, J., *Effect of molecular weight on the construction of polyelectrolyte multilayers: Stripping versus sticking.* Langmuir, 2003. **19**: p. 2491-2495.

43. Sui, J., *Controlling electroosmotic flow in microchannels with pH-responsive polyelectrolyte multilayers.* Langmuir, 2003. **19**: p. 7829-7831.

44. Liu, Z.; Ren'an, Z. ; Hanfa, T., *Recent progress in adsorbed stationary phases for capillary electrochromatography.* Electrophoresis, 2002. **23**: p. 3954-3972.

45. Drange, E., *Determination of long-chained fatty acids using non-aqueous capillary electrophoresis and indirect UV detection.* Journal of Chromatography A, 1997. **771**: p. 301-309.

46. Belder, J, *Electrokinetic effects in poly(ethylene glycol)-coated capillaries induced by specific adsorption of cations.* Langmuir, 2001. **17**(16): p. 4962-4966.

47. Belder, J; Warnke, J., *Directed control of electroosmotic flow in nonaqueous electrolytes using poly(ethylene glycol) coated capillaries.* Electrophoresis, 2001. **22**(4): p. 666-672.

48. Regnier, S., *High Performance Capillary Electrophoresis, Theory, Techniques and Applications*, ed. M.G. Khaledi. 1998, New York: Wiley.

49. Gallaher, D.; Johnson, M., *Nonaqueous capillary electrophoresis of fatty acids derivatized with a near-infrared fluorophore.* Analytical Chemistry, 2000. **72**: p. 2080-2086.

50. Gallaher, D.; Johnson, M., *Development of near-infrared fluorophoric labels for the determination of fatty acids separated by capillary electrophoresis with diode laser induced fluorescence detection.* The Analyst, 1999. **124**: p. 1541-1546.

51. Huang, M.; Zare, R., *Current-Monitoring method for measuring the electroosmotic flow rate in capillary zone electrophoresis.* Analytical Chemistry, 1988. **60**: p. 1837-1838.

# Chapter 3

## Detection Limit of Fluorescently Labeled Fatty Acids

### 3.1 Introduction

Detection of molecules relevant to biological systems is vital to the growth of the biomedical field. Many diseases and conditions are diagnosed through the existence or a change in concentration of a particular biomolecule. The primary issues in using a particular biomolecule within a biological system for the diagnosis of a disease is the separation of the molecule of interest from the bulk tissue or fluid and the detection of the molecule. Laser induced fluorescence and electrochemical detection techniques have limits of detection low enough to give molecular detection. Low volumes and sometimes picomolar and lower concentrations of the analyte of interest will severely limit the options available for separation and detection. Due to these problems, a highly efficient separation technique needs to be coupled with an extremely sensitive detection technique for these applications.

### 3.1.1 Electrophoretic separations

Electrophoretic separation of biomolecules has been a source of rapid growth in research in the last 20 years [1]. This trend stems from the inherent resolution capable with electrophoresis. Many studies focus on aqueous separations but, due to the solubility of some biomolecules, development of nonaqueous capillary electrophoresis (NACE) is desirable. NACE is a growing field of research due to the wide range of solvents possessing properties (polarity, viscosity, dielectric constant) that vary greatly compared to water. These solvents present several potential problems including the choice of ideal charge carriers in a variety of solvents [2], effect of capillary coatings on EOF [3] and problems with detection of analytes within solvents [4, 5].

### 3.1.2 Detection

One potential challenge when separating with capillary electrophoresis is method of detection [6]. In HPLC and GC analysis structural information can be obtained through the use of mass spectrometry detection [7]. The ionic strengths of the charge carriers that are required in NACE can cause problems when coupled to mass spectrometry [8]. As a result, technology is being developed, but mass spectrometric detection is not readily available with capillary electrophoretic separation. Alternative detection methods easily coupled to capillary electrophoresis include detection of changes in electrochemical conductivity, light absorption and fluorescence properties. These three detection techniques have the potential to be sensitive, ($10^{-9}$ mol/L, $10^{-10}$ mol/L, $10^{-13}$ mol/L respectively [5, 6, 9, 10]) but both absorption and electrochemical

detection tend to be nondiscriminatory when several different components are separated. In order to increase sensitivity, laser induced fluorescence can be used.

Laser induced fluorescence can give detection limits on the molecular level when combined with capillary electrophoresis. Selectivity can be achieved through the use of an excitation wavelength that specifically excites an analyte of interest. Most biomolecules are not fluorescent which is useful for low backgrounds, but a hindrance to analyte detection. Fluorescent tags must be used in order to detect most biomolecules [11]. These tags can be chosen to excite or emit at a wavelength that other biomolecules found in the separation will not. This makes fluorescence detection an attractive method due to the selectivity coupled to the sensitivity. Sensitivity is achieved by designing tags to bind specifically to functional groups found in the analyte of interest. The most significant deterrent is the labeling process, as it can complicate the determination of concentrations of analyte by involving complicated and time consuming reactions [12].

The fundamental limit for detection in capillary electrophoresis using laser induced fluorescence has been determined to be at the molecular level for selective dye molecules. While exceptionally low concentrations have been shown to be detectable in several publications, these projects involved pure analytes, such as molecular dyes. It is not reasonable to say that molecular detection is possible for every application in a CE-LIF instrument. The utility of fluorescent dyes is to detect a desired analyte through linking the dye to an analyte of interest. Adding this aspect to the problem of detection limit creates a far more complex problem. A biomolecule of interest could potentially be found at extremely small concentrations in a very small portion of a system. This

generates the necessity for a labeling reaction to be attempted at exceptionally small concentrations.

### 3.1.3 Biomolecular labeling

Due to the low concentrations and minute volumes often present within biological systems, highly sensitive and efficient techniques are required for analysis. Several methods have been developed for separation and detection of biological molecules at concentrations available in relevant systems. Unfortunately, many of these methods are only in the developmental stage and the detection limits that are reported are dilutions of analytes that were labeled at much higher concentrations than are readily available in a typical system. Labeling reactions at concentrations that are reasonably available have been known to have several problems that are not relevant at higher concentrations. The most significant problem found in labeling and detecting at these small concentrations is that side reactions of the labeling reaction and impurities in the dye itself. Craig and Dovichi report a complex analysis of labeled proteins due to multiple peaks forming a single broad peak [13]. This was attributed to side reactions involving the dye 3-(2-furoyl)quinoline-2-carboxaldehyde (FQ) and the proteins in the sample. Pinto et al. report the analysis of proteins at concentrations under $10^{-10}$ M but due to the low concentration, side products and impurities from FQ dye caused detection problems [14]. These two problems can cause significant problems in detection as multiple peaks can result. As the concentration of the analytes of interest are reduced, these impurities create problems due to the relative intensities of the impurities and side reactions being at similar concentrations as the analytes of interest. Analysis of the resulting data is

problematic due to peak overlap and, in the case of side reactions involving the analyte and impurities within the dye, secondary analyte peaks. Other problems such as hydrolysis of dye in aqueous media was also reported as significant in very low concentrations of dye where it can be overlooked in high concentrations [15]. These types of problems are very individual to the dye and the linking group attached to the dye.

Shen et al. described an analysis of neuropeptides in which the peptides of interest are found at 1nM concentrations [16]. Impurities in the sample complicated the analysis significantly when using electrochemical and UV absorbance detection methods. Although they were able to detect vasopressin (a neuropeptide) at 100 pM concentrations, the *in vivo* measurements were exceptionally complex and resolution suffered due to a lack of selectivity.

More complex dyes such as 2-(2,3-anthracenedicarboximido)ethyl ester have been reported to give detection limits of 0.8 fmol when a separation of 18 fatty acids were observed [17]. This chromatographic separation was completed in under 30 minutes. 3-bromomethyl-6,7-dimetoxy-1-methyl-2(1H)-quinoxalinone was used by Masatoshi et al to separate a series of fatty acids using HPLC [18]. While this separation yielded detection limits of 0.3 - 1 fmol and a small injection volume of 5 μl (concentration of 60 - 200 pM) the labeling reaction was complex with the addition of 18-crown-6 to produce fluorescent esters.

Brando et al. report attomol detection limits in the detection of fatty acids using aminofluorescein (AF) [19]. In this study, baseline resolutions were observed using CE in an acetonitrile solvent but this was only observed in the standard solutions. The other

problem the authors report is that the reactivity of the AF dye used necessitated the use of highly concentrated analytes in order for the reaction to complete.

### 3.1.4 Biological samples, problems

Analysis of biomolecules is a source of interest for use in the diagnosis and treatment of many diseases. The relative and absolute levels of individual biomolecules can determine the existence and extent of many diseases. Concentrations of many biomolecules, relative to an individual across time, are generally more useful due to the differences in individual organisms. Difficulties arise when attempting to determine this information due to the complexity of the samples taken from tissue or fluid. Biological mixtures are mixtures of many components with a variety of properties and functionalities. The basic analytical difficulties present in almost any separation are found, and even amplified in biological separations. This creates a challenging analytical problem for determination of the concentrations of these components. Multi-step processes have been developed and are widely used for this type of determination [20-22]. These processes include methods of homogenation, centrifugation, solid phase extraction, liquid phase extraction, and chromatographic methods. Many components need to be removed from a biological sample before analysis is possible. The target of the analysis, that is, the biomolecule concentration that is desired, must be separated from the mixture. This is the primary goal of these pre-separation procedures.

Purity of the sample is vital to the separation and analysis of the biomolecule; unfortunately, pure samples are rarely found. There is a loss of analyte, the biomolecule of interest, in any separation. A loss of analyte can range from insignificant trace

amounts, to entire populations. Properties of the analyte of interest are important to the choice of these methods as well as the properties of the contaminants. This subject is very individual for the sample of interest and goes far beyond the scope of this work. Briefly, for separations of fatty acids, the acid group at higher pH will provide a negative charge in solution. Negatively charged molecules can be separated from neutral and positively charged molecules through the use of chromatographic techniques and SPE. The relatively non-polar nature of the long tails found in fatty acids can be separated from more polar molecules by solvent based polarity techniques. The choice of pre-separation techniques is key in the determination of the extent of the analyte loss. These techniques are well established in textbooks [23] and loss of analyte can be determined through the use of a standard (discussed later).

Loss of analyte through these techniques is needs to be accounted for, but is far from the only source of difficulty. The choice of detection of an analyte becomes a subject of interest. There are a variety of detection techniques that are available for detection and numerous techniques developed for the detection of biological materials. The choice depends on the analyte of interest and the contaminants, other material in the separation matrix, that are found in the sample.

### 3.1.5 NIR detection

Optical detection techniques such as absorbance and fluorescence detection have been developed for the detection of biomolecules. Many biomolecules, including fatty acids, do not fluoresce. This both limits the use, and increases the utility, of fluorescence techniques. In order to detect the analytes of interest, a fluorescent label is required.

These labels are fluorescently active dyes that can be attached or adsorbed to the molecule of interest.

By attaching a label that will emit in a region where autofluorescence is rare, selectivity can be increased dramatically. The near infrared region of the electromagnetic spectrum is ideal for these applications. Autofluorescence is low for biological molecules at wavelengths above 700 nm and below 1000 nm. Scatter associated with Raman and Rayleigh effects are related by $1/\nu^4$ and therefore are much reduced in this region. The choice of NIR active labels for binding and detection is also attractive as the instrumentation cost is relatively low. Diode lasers that emit in the near IR are readily available at low cost, high beam quality and long lifetimes.

### 3.1.6 Fluorescent labeling

Detection of biomolecules through the use of a label is a well established field. Labels have been used to determine both quantititative and qualitative information throughout the last 50 years. There are two different types of labeling technique available for determination of biological molecules. First is through the use of a dye which is non-covalently bound to the biomolecule of interest. The primary advantages of non-covalent binding are the speed of the labeling technique and not altering the molecule of interest dramatically. This type of technique has been developed for the use of cyanine dyes labeling larger molecules such as proteins. Non-covalent techniques are also known to be selective due to the unique nature of binding sites that larger biomolecules exhibit. The primary disadvantage is the stability of the complex of interest. Stability of non-covalent complexes is inferior to covalent techniques, which

severely limits the utility of these types of techniques. Covalently bonded techniques bond a dye molecule to the biomolecule of interest. The properties of the biomolecule change dramatically due to the addition of the attached dye. Difficulties may occur when larger molecules will bond to several dye molecules and will therefore emit significantly more than if one dye molecule. While multiple binding will permit the detection limit to be reduced, the possibility of multiple binding must be accounted for. The presence of different species of the same molecule could give rise to multiple peaks within a separation of analytes. Multiple peaks will make quantitation and peak identification problematic.

The extent and speed of the labeling reaction is of significant interest. A lengthy reaction required for labeling could potentially cause the loss of the analyte of interest. Loss of analyte is a problem primarily when the analyte of interest is unstable under labeling reaction conditions [12]. The extent of the reaction is important if quantitative data is sought or if the extent of the reaction is dependant on the concentrations of the analyte to the label. The utility of the reaction is limited if the reaction cannot be accomplished quickly and without differences in labeling.

### 3.1.7 Fatty acids

Fatty acids are biologically relevant molecules found throughout the body with a variety of different functions. Separation of fatty acids through chromatographic (GC, HPLC) methods is common but complex labeling reactions and difficulties is separating 'critical pairs' [24] can be problematic (discussed further in chapter 4). In a previous study we have reported the CE separation of fatty acids labeled with a near IR fluorescent

dye [25]. This separation was carried out in nonaqueous media in order to provide the necessary solubility for the longer chain fatty acids. Resolution was better than baseline with a detection limit in the nanomolar range [26]. Reproducibility was found to be stable over multiple injections (chapter 2). These two factors indicate a potential use in biological samples, but the concentrations necessary and the time in which the labeling reaction took place was not investigated and could potentially present difficulties in biological testing.

Separations of biologically relevant fatty acids have been reported primarily with gas chromatography and HPLC. The concentration range of free fatty acids found in normal human serum is in the range between 0.3 μmol/L and 31 μmol/L [27]. In this study it is shown that the reaction between biologically relevant fatty acids and a fluorescent dye (Patonay 3) [28] can be utilized to label samples of acids at a concentration small enough that the reaction itself will not be the limiting step in the detection of fatty acids at biological concentrations. The time of the reaction is also shown to be of a useable interval of minutes and not several hours as was previously reported.

## 3.2 Experimental reagents and materials

Linear saturated fatty acids C6 (caproic), C8 (caprylic), C10 (capric), C12 (lauric), C14 (myristic), C16 (palmitic) as well as N,N-dicyclohexylcarbodiimide (DCC) and myristyltrimethylammonium bromide (MTAB) were all purchased from Acros Organics. Tetraethylammonium chloride (TEAC) originally from Eastman Kodak (Rochester, NY) was obtained from house stores. Polybrene® (hexadimethrine bromide)

and dextran sulfate (avg. mol. Wt. = 5000 D) were purchased from Aldrich Chemical Corporation (Milwaukee, WI, USA). Methanol and chloroform used as solvents were HPLC grade and purchased from Fisher Scientific (Fair Lawn, NJ).

### 3.2.1 Apparatus

Capillary electrophoresis was performed on fused silica capillaries 50 μm internal diameter, 360 μm outer diameter, purchased from Polymicro Technologies (Phoenix, AZ, USA). A detection window of 1 cm was created by burning off the polyimide coating using a low intensity butane flame. The capillary was then fixed to a microscope slide using epoxy.

Voltage was applied during electrophoretic separations using a CZE 1000R (Spellman High Voltage Electronics Corporation, Plainview, NY). Injections were gravimetric injections at the cathode by raising the capillary 10 cm for 5 seconds.

Detection was achieved using laser induced fluorescence using a laboratory-constructed epifluorescence microscope. Excitation was with a near-infrared laser operating at 785 nm (Sanyo DL7140-201 S). The beam was passed through a mica half-wave plate (Melles Griot) and a calcite Glan-Thompson polarizer (Karl Lambrecht, Chicago, IL) for control of light intensity and polarization state. The collimated beam was reflected by a dichroic reflector (Omega, 810 DRLP) and focused into the capillary by a 40X, 0.85 NA microscope objective (Nikon Fluor 40, Nikon Corp, Tokyo). Fluorescence was collected by the same objective, passed through the dichroic, spatially filtered with an 600 μm pinhole, and spectrally filtered with an 810EFLP (Omega) long pass filter. The remaining fluorescence was focused with a pair of 24 mm EFL

achromats (Rolyn Optics, Covina, AC) onto the active area of a single photon counting avalanche photodiode (SPCM module, EG&G Canada, now PE Instruments). Data collection was performed with an MCS plug-in card (MCSII, Tennelec/Nucleus, Oak Ridge, TN), usually at a rate of 250 ms/MCS bin, residing in an AT bus PC.

Peak analysis was done with Igor Pro 4.02A (Wavemetrics, Eugene, OR) using multipeak fit package version 1.30. Electropherograms were fit to the Gaussian peak shape.

### 3.2.2 Fatty Acid Derivatization Protocol

The procedures for labeling the fatty acids with the near-infrared fluorescent probe, and for synthesizing the probe have been modified from the procedure previously reported [25]. Stock solutions of various fatty acids and DCC were prepared in chloroform. A stock solution of the NIR fluorescent probe (Patonay 3) was prepared in anhydrous dimethylformamide.(for structures see Figures 1 and 2) Stock solutions were altered in order to maintain reaction conditions necessary to retrieve kinetic data from the reactions. To perform a derivatization, a 100 μL aliquot of fatty acid solution was pipetted into a 2 mL glass reaction vial and stirred with a magnetic stirrer. A 100 μL aliquot of DCC stock was added and the mixture was allowed to stir for 30 seconds. A 100 μL aliquot of the labeling reagent was added and the reaction vessel was capped and allowed to react for several hours, while shielded from ambient light.

At the end of the reaction period, precipitated dicyclohexylurea was filtered off using a 0.2 μm nylon syringe filter and aliquots of the reaction mixture were diluted in methanol for CE analysis. To create a mixture of fatty acids, aliquots of the various

individual reactions were combined and subjected to an identical work up procedure. To ensure separation conditions were reproducible, IR 786 dye was added to the stock buffer and used as an internal marker.

### 3.2.3 Coating procedure

SMIL capillary coatings were utilized in the separations and have been described earlier in this volume. Briefly, the coating utilized in the separations was made by flushing a 10% Polybrene® solution through the capillary at a rate of 6.9 μL/min for 4 hr. The capillary was then evacuated and 10% dextran sulfate was flushed at the same rate for 4 hr. Finally, the capillary was evacuated a third time and the final coat of Polybrene® was flushed as described above for 4 hr. The capillary was then evacuated and allowed to sit overnight.

## 3.3 Results and discussion

In order to detect the relative concentrations of labeled dye, a separation of unreacted dye from the dye labeling acids needed to be achieved. Patomy 3 dye has no change in excitation wavelength or any other distinguishing property that will easily set the unreacted dye apart from the dye that has been linked to an acid. The electrophoretic technique described earlier in this volume was used as it was proven to be stable and separations were reproducible over many injections under non-aqueous conditions. With migration times on the order of 10 minutes, high sensitivity, and minimal pre-injection preparation, the technique was ideal.

The necessity of a separation technique in the determination of kinetic data complicates the procedure considerably. Much of the kinetic data in the literature is based on procedures involving a spectrophotometric technique where only a product or a reactant is observed. One of the potential sources of error is the injection method that is used. The electrophoretic system utilized in these experiments lacks an autosampler and there will be variation in injection volumes regardless of the injection method. A lack of reproducible injection will translate into variations in the peak height and width that could be detrimental to the determination of reaction coefficients and constants as these quantities are based on concentrations of reactants and products. In order to be certain that data could be compared between injections the use of IR-786 laser dye was utilized as a neutral marker. Dye was added to the injection buffer at a constant concentration and data was normalized to this peak. As the IR-786 dye was at a constant concentration, variations in peak areas arising from injection volume could be eliminated by normalization to the marker peak area.

Labeling the fatty acids was made possible by the activation of the acids by the

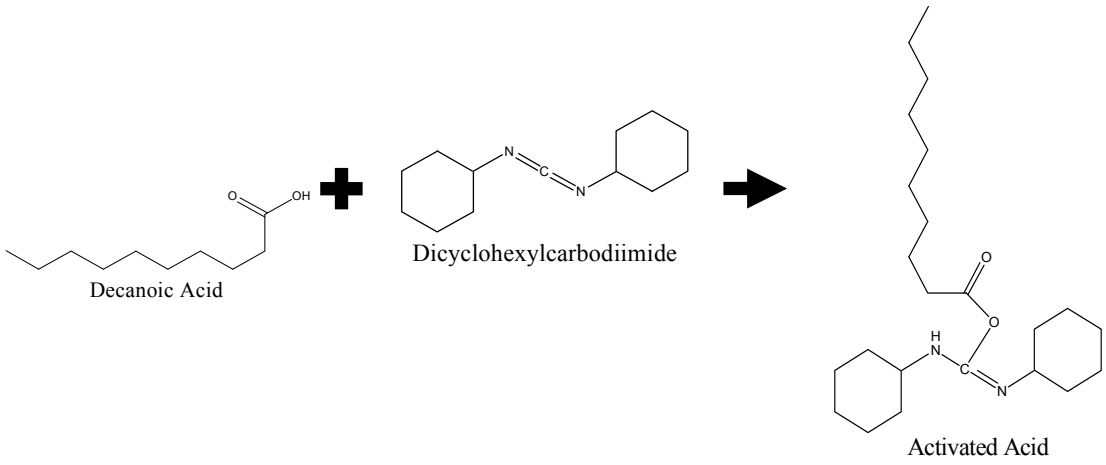


Figure 1. Structural diagrams of acid and dicyclohexylcarbodiimide (DCC). Activation of the acid allows the attachment of the dye to the acid

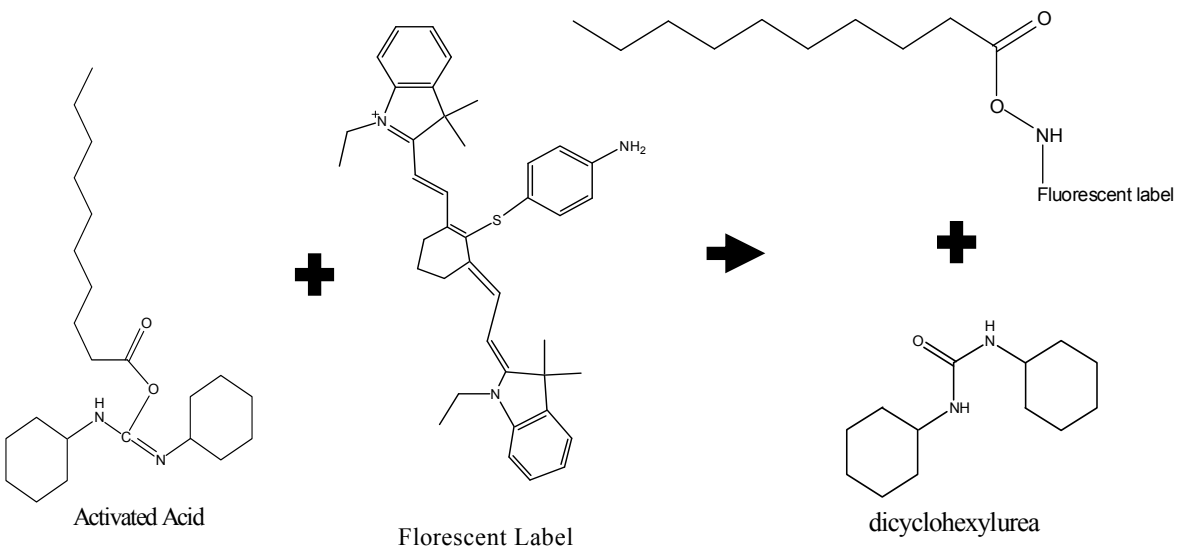


Figure 2. Structural diagrams of activated acid, Patony 3 fluorescent label and the reaction products.

addition of DCC. Figure 1 shows the reaction scheme with structures of each component. By attaching DCC to the acid of interest, the reaction in Figure 2 is able to occur. Final products include the labeled acid and dicyclohexylurea which will precipitate out of solution and can be removed by filtration with a 0.2 μm membrane filter.

Labeling reaction conditions were optimized using a series of fatty acids. C6 (hexanoic), C8 (octanoic), C10 (decanoic), C12 (lauric), C14 (myristic), and C16 (palmitic) acids were added with constant concentrations of 151.0 mM while label was added to the reactions in a range of (1.509 mM) to (0.0472 mM). While the reaction proceeded, aliquots were taken at intervals of time and the reactions in these samples were stopped by dilution to injection concentrations. 10 μl of the reaction mixture was taken from the reaction vessel and diluted 1:10,000 in running buffer. Temperature was not controlled for these experiments and was therefore at room temperature. These concentrations were chosen in order to determine the reaction order with respect to the dye (see appendix 1).

From each injection, the area of each of the three peaks corresponding to the labeled acids was determined. This was accomplished by fitting individual peaks through the use of Igor Pro peak fitting package and determining the area under the fit peak. The peak corresponding to the IR-786 laser dye was also integrated in this way and the peaks were normalized to this peak. This procedure was done in triplicate, using different vials

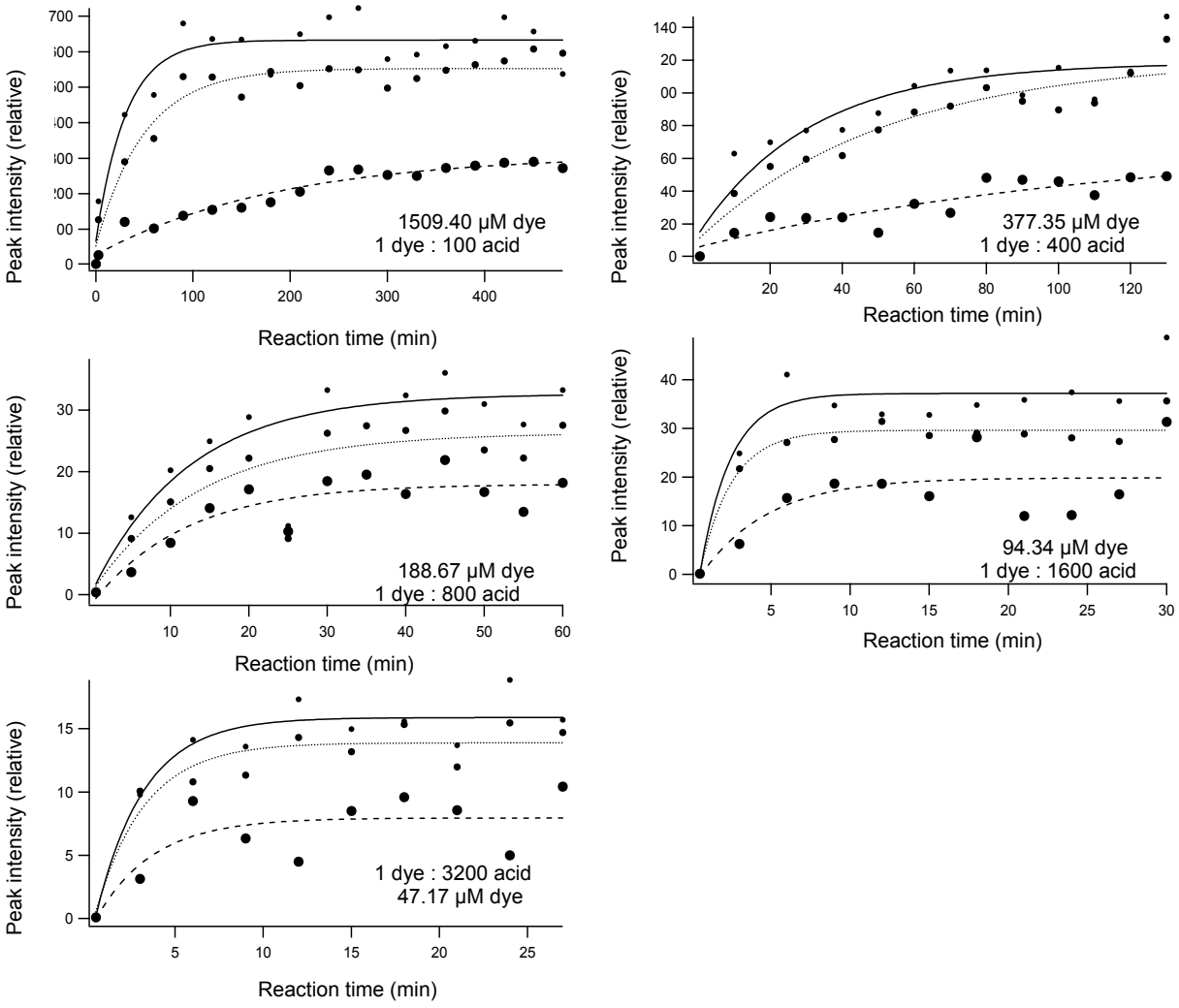


Figure 3. Peak area of product diluted to running concentration graphed against time. Concentration of starting acid remained constant at 151 mM. Concentration of dye given for each graph. Solid line and smaller points indicate C6, dotted line indicates C12; dashed line and larger points indicate C16

but at identical concentrations, to ensure reliability of the data.

Figure 3 shows the data collected from these separations for 3 acids (C6, C12 and C16) separated from each other and from unreacted label after the reaction was allowed to continue for an amount of time (x-axis of graphs). Each plot is at a different concentration of dye. The ratio of dye to acid is vital to the determination of the reaction order.

Two different methods were utilized in order to determine the reaction order with respect to the label. First was to observe the relationship of the change in label concentration with respect to the time given for the reaction. The equations found in appendix 1 indicate that a logarithmic relationship will exist between these two variables in a first order reaction. Assuming that the reaction will go to completion, the linear relationship shown in Figure 4 indicates that the reaction is pseudo first order with respect to the label and with an rate constant found to be -0.00184 (see appendix 1 for equations).

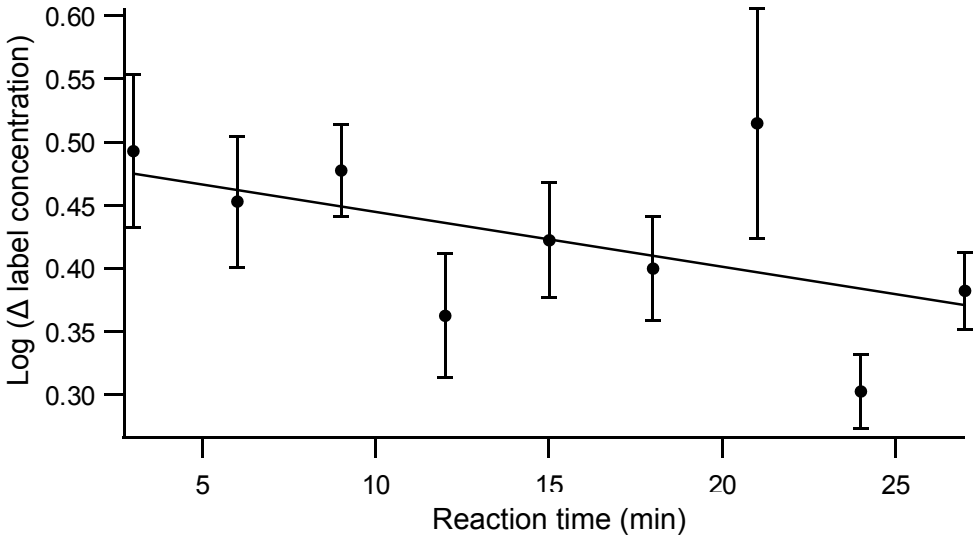


Figure 4. log of Δ label concentration against time. A linear slope indicates a pseudo first order reaction with respect to the label.

In order to find the relationship between acid and label in the reaction a second method was used on the collected data. With this method the tau values retrieved from the data shown in Figure 3 was used. These tau values are the inverse of the time of half change ($t_{1/2}$) in the reaction being observed. With this known, the log of the $t_{1/2}$ values were graphed against the log of the reaction concentration of the acid. When graphed

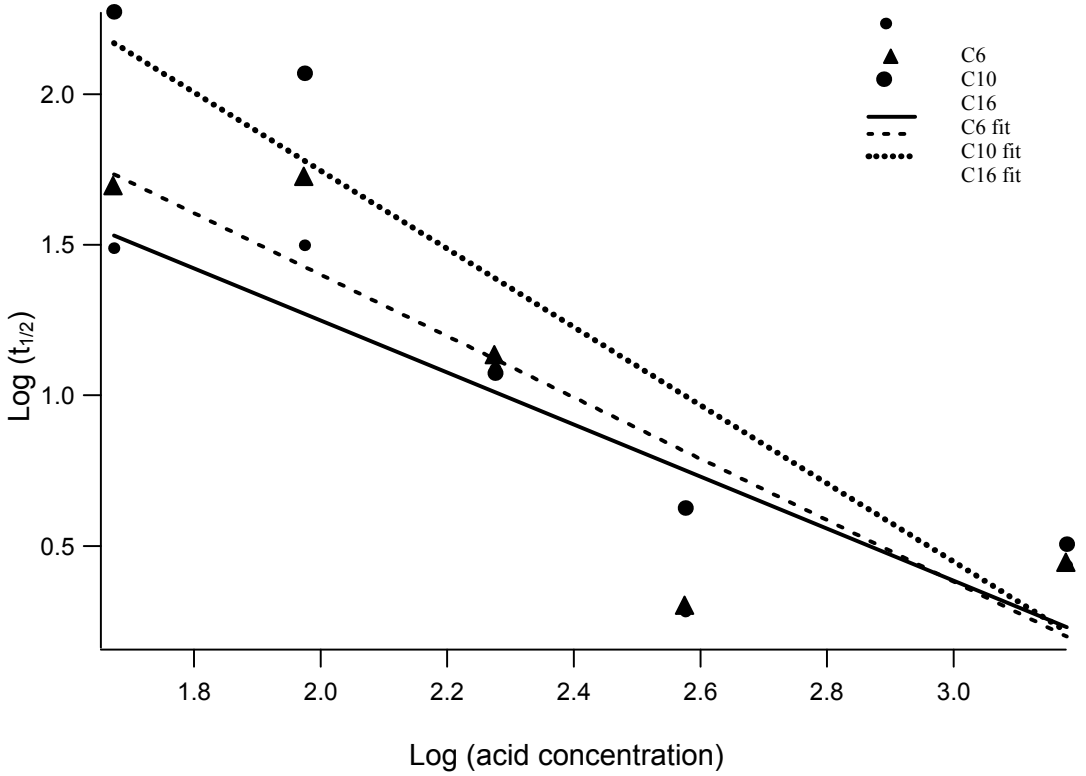


Figure 5. log of $t_{1/2}$ plotted against log of the acid concentration. Slope indicates a dependence on the concentration of acid

(Figure 5), the slope of each function was found to be -0.813 for C6, -0.965 for C12, and -1.28 for C16 which shows a dependence of the reaction on acid chain length.

The concentration of the products were graphed against the time of the reaction and these values were fit to a curve similar Figure 3. These graphs are identical to Figure 3 in that they are graphs of ratios and the adjustment to concentration units will not change the relevant data as it pertains to the tau value. Determination of the reaction

order with respect to the dye concentration was done through the use of the equations in appendix 1. Equilibrium constant values are constant over the time of the reaction so a constant slope (linear line) will appear when the correct order equation is used. The graph shown in Figures 4 show that the reaction is first order with respect to the dye concentration.

Reaction order with respect to label concentration was difficult to determine. Side reaction products were apparent in the CE separations when acid concentrations were lower than a 1:100 ratio of acid to label. This was determined through a series of experiments which the range on concentrations in the acid was from 200.00 μM to 0.01

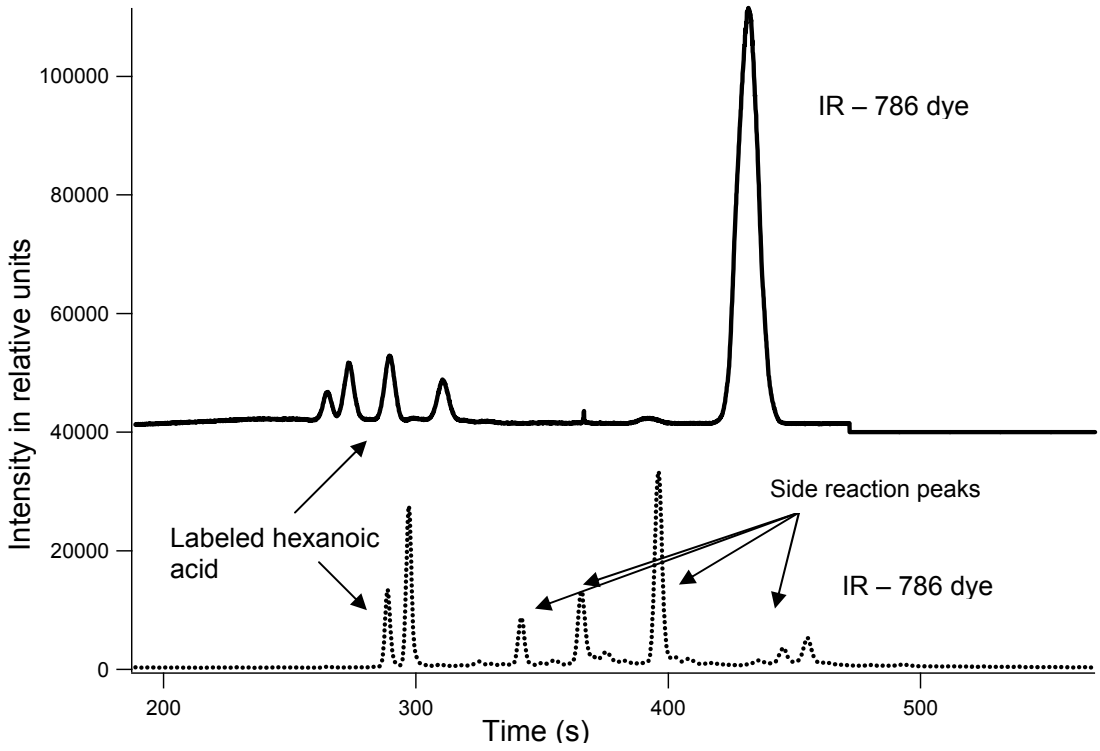


Figure 6. Top: 1:100; 151 mM acid : 1.509 mM label; Bottom: 1:1; 1.509 mM label to 1.509 mM acid concentration ratio. The emergence of side reactions can be seen when the dye concentration becomes high with respect to the acid concentration. SMIL 4,4,4 capillary (pos charge) 50 μm ID, 36 cm length, 18 cm detection length. Upper trace 20 kV, 15 kV 5 s injection; lower running voltage 25 kV, 5 kV 5 s injection.

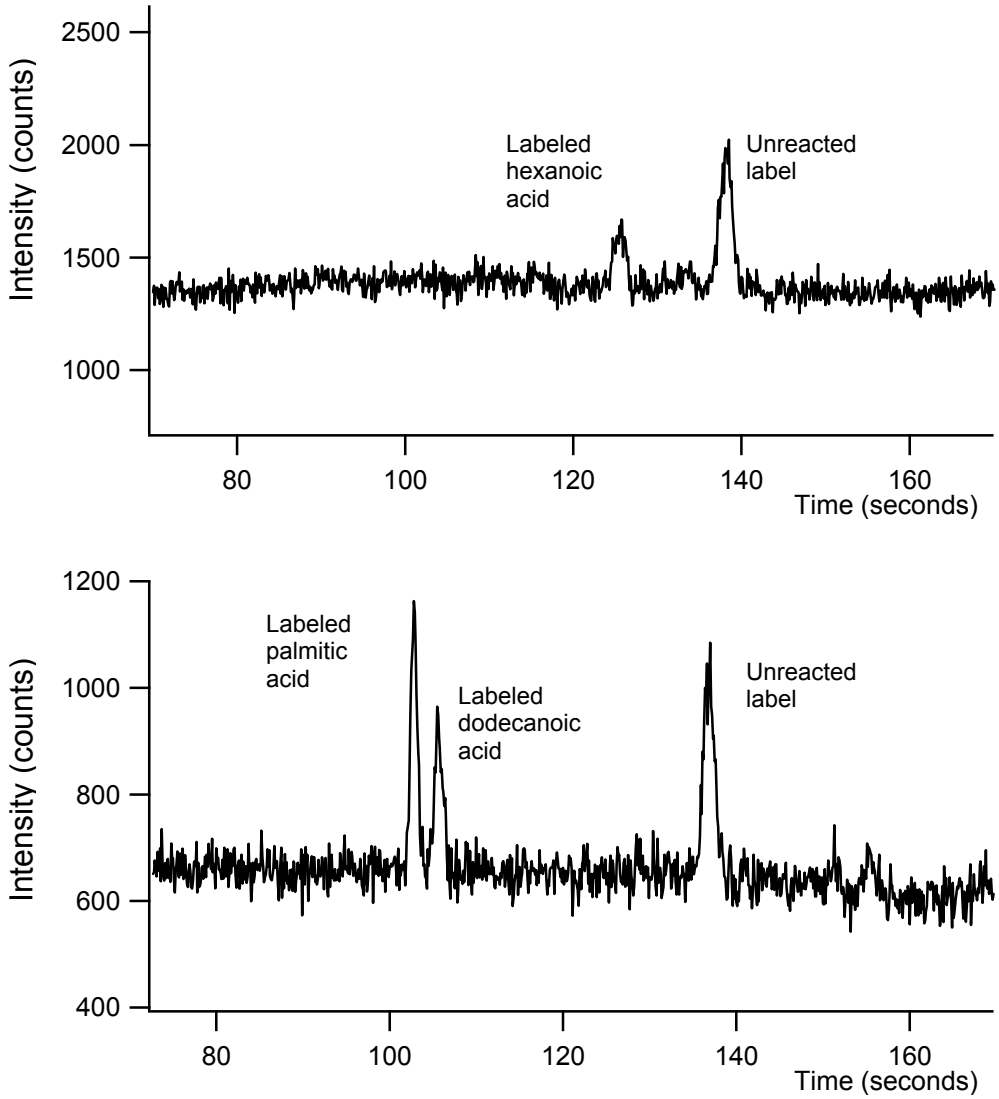


Figure 7. Top: 5 s, 15 kV injection of labeled hexanoic acid (5 nM). Bottom: 5 second 15 kV injection of mixed labeled dodecanoic and palmitic acids (10 nM). Capillary conditions ID 50 μm, length 36 cm, length to detection 18 cm, running voltage 25 kV, and excitation wavelength 785 nm.

μM. The label concentration remained stable throughout the reaction series at 1.50 μM.

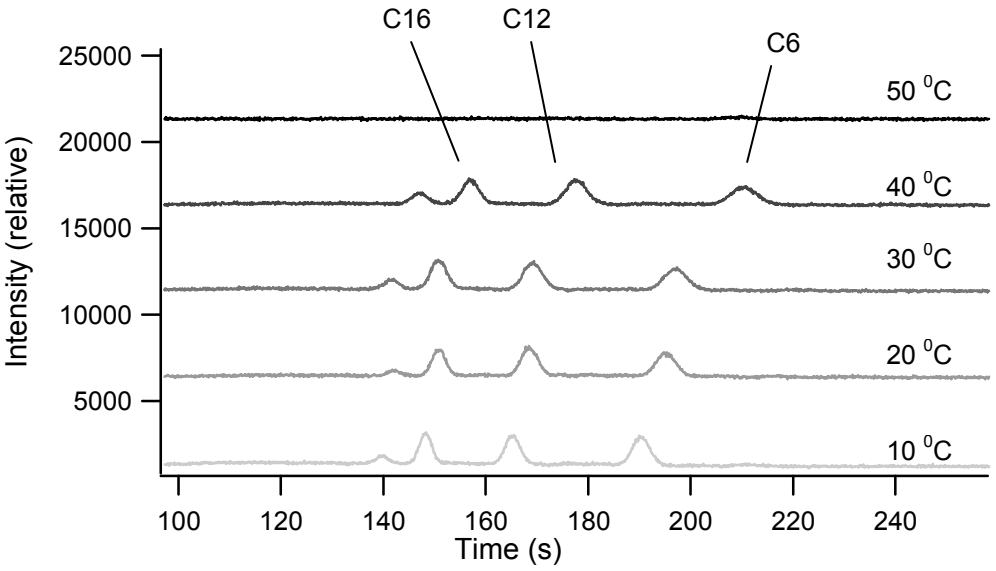


Figure 8. Temperature effect on labeled acid separation. 151 mM acid : 1.509 mM label Capillary conditions ID 50 µm, length 36 cm, length to detection 18 cm, running voltage 25 kV, and excitation wavelength 785 nm. Subsequent injections offset for clarity.

The side reactions were not a problem when the acid concentration was high with respect to the label concentration, (above a 1 to 1 ratio) but became apparent when the acid concentration was lowered. Figure 6 shows two electropherograms in which the concentration of the acid is lowered. It can be seen in this data that side products could potentially become a problem if these side products are abundant enough to overwhelm the separation. Small differences in the elution time and peak shape when comparing this data can be attributed to the differences in the injection, running voltage and capillary stability.

With these constraints, the peaks were monitored as the concentrations of the acid and dye were lowered in order to determine the lowest concentration that the reactions could occur and be detected over baseline (s/n > 3). It was found (Figure 7) that the lowest concentration of labeled hexanoic acid detectable was 5 nM (5 sec 15 kV injection) and slightly higher for the larger chain length acids palmitic and lauric acids 10

nM (5 sec 15 KV injection) (Figure 7). Throughout these experiments, injections were made directly from the reaction vessel. Three factors (concentration, time of reaction and temperature) were observed when determining a viable reaction. Low detection limits are vital in a biological sample large amounts of tissue may not be readily available. The time and temperature of the labeling reaction is important as some acids are known to break down over time. It was reported that the reaction takes place 'overnight' but no further investigation took place [26]. A long time frame was used to ensure a full reaction took place. The time of reaction was observed and it was found that the reaction can easily reach completion in under 10 minutes when conditions are desirable (table 1). At concentrations of acids that are closer to what is available in biological organisms (1-100 nM), the reaction requires a longer time frame in order to reach completion (60 minutes).

It was found that the reaction rate would speed up when the temperature was raised to 30 degrees but the label would break down when the temperature exceeded 40 degrees. While the breakdown products could not be directly observed, the absence of analyte peaks was apparent (Figure 8). The downfield peak that is attributed to excess label was also found to migrate farther downfield as the temperature increased. Further investigation of the peak movement and the loss of analyte signal was not sought. The effect of temperature on the reaction time found can be seen in Table 2.

Table 1. Effect of concentration on reaction time

| | Dye concentration (μM) | Acid concentration(mM) | Time to completion |
|---|---|---|---|
| 1 | 1509 | 151.0 | 110 minutes |
| 2 | 377 | 151.0 | 80 minutes |
| 3 | 188 | 151.0 | 25 minutes |
| 4 | 94.3 | 151.0 | 9 minutes |
| 5 | 47.2 | 151.0 | 6 minutes |

Table 2. Effect of temperature on reaction time. 188 μM dye, 151.0 μM acid

| | Temperature of reaction | Time to completion |
|---|---|---|
| 1 | 10$^{o}$C | 40 minutes |
| 2 | 20$^{o}$C | 25 minutes |
| 3 | 30$^{o}$C | 7.5 minutes |
| 4 | 40$^{o}$C | 3 minutes |

## 3.4 Conclusions

Labeling reaction conditions were determined in the labeling of biologically relevant fatty acids. It was found that the dye Patonay 3 could be attached through the DCC pathway at concentrations low enough to be used to detect biological concentrations of fatty acids. Investigations into temperature of reactions found that the reaction rate could be increased by raising the temperature but is limited to 40$^{o}$C when the label began to break down. Problems such as reaction side products were found when label concentration exceeded the concentration of the acid being analyzed.

Hexanoic acid at 5 nM was separated from unreacted label and detected above baseline using the electrophoretic system. With injection volumes under 10 nl, detection limits found for hexanoic acid were 50 fmol. Dodecanoic and palmitic acid's detection limits were slightly higher at 100 fmol. Detection limits have been found to be lower in the analysis of some biological analytes with more complex labeling procedures, such as Criag et al's chromatographic separation of labeled proteins with a 1 fmol detection limit [13]. While the method described in this work has a detection limit 2 orders of magnitude higher than methods such as Criag's method, free fatty acids have been determined to be found in human serum at a concentration range of 0.3 μmol/L and 31 μmol/L [27]. In this concentration range, a 10 μl injection (30 pmol) would be well within the detection limit of the labeling and separation system.

# REFERENCES


1. Assuncao, N.; Leandro G.; Paulino, L.; Lupetti, K.; Carrilho, E., *Nonaqueous capillary electrophroesis in coated capillaries: An interesting alternative for protomic applications.* Electrophoresis, 2005. **26**: p. 3292-3299.

2. Fillet, M.; Anne-Catherine, S.; Crommen, J., *Effects of background electrolyte composition and addition of selectors on separation selectivity in nonaqueous capillary electrophoresis.* Electrophoresis, 2003. **24**: p. 1499-1507.

3. Belder, K.; Husmann, H., *Use of coated capillaries for nonaqueous capillary electrophoresis.* Journal of Microcolumn Separations, 1999. **11**(3): p. 209-213.

4. Matysik, F., *Non-aqueous capillary electrophoresis with electrochemical detection.* Journal of Chromatography A, 1998. **802**: p. 349-354.

5. Matysik, F., *Special aspects of detection methodology in nonaqueous capillary electrophoresis.* Electrophoresis, 2002. **23**: p. 400-407.

6. Steiner, M., *Nonaqueous capillary electrophoresis: A versatile completion of electrophoretic separation techniques.* Electrophoresis, 2000. **21**: p. 3994-4016.

7. Hall, N.; Geoffrey W.; Hjelm, M., *Ratios for very long chain fatty acids in plasma of subjects with peroxisomal disorders, as determined by HPLC and validated by gas chromatography-mass spectrometry.* Clinical Chemistry, 1988. **34**(6): p. 1041-1045.

8. Sturm, S.; Eva-Maria, S.; Stuppner, H., *Quantification of Fumaria officinalis isoquinoline alkaloids by nonaqueous capillary electrophoresis-electrospray ion trap mass spectrometry.* Journal of Chromatography A, 2006. **1112**: p. 331-338.

9. Johnson, M.; Landers, J., *Fundamentals and practice for ultrasensitive laser-induced fluorescence detection in microanalytical systems.* Electrophoresis, 2004. **25**: p. 3513-3527.

10. Kraly, J.; Schoenherr, R.; Bonn, R.; Harwood, M.; Turner, E.; Jones, M.; Dovichi, N., *Bioanalytical applications of capillary electrophoresis.* Analytical Chemistry, 2006. **78**: p. 4097.

11. Bardelmeijer, H.; Ruiter, C.; Underberg, W.J.M., *Derivatization in capillary electrophoresis.* Journal of Chromatography A, 1998. **807**: p. 3-26.

12. Jong, J.; Lucy, C., *Noncovalent labeling of myoglobin for capillary electrophoresis with laser-induced fluorescence detection by reconstitution with a fluorescent porphyrin.* Electrophoresis, 2004. **25**: p. 3153-3162.

13. Craig, N., *Multiple labeling of proteins.* Analytical Chemistry, 1998. **70**(13): p. 2493-2494.

14. Pinto, E.; Craig, D.; Angelova, J.; Sharma, N.; Ahmadzadeh, H.; Dovichi, N.; Boulet, C., *Picomolar assay of native proteins by capillary electrophoresis precolumn labeling, submicellar separation, and laser-induced fluorescence detection.* Analytical Chemistry, 1997. **69**: p. 3015-3021.

15. Arriaga, Z.; Yanni, J.; Dovichi, N., *Use of 3-(p-carboxybenzoyl) quinoline-2-carboxaldehyde to label amino acids for high-sensitivity fluorescence detection in capillary electrophoresis.* Analytica Chimica Acta, 1995. **299**: p. 319-326.

16. Shen, W., Steven R.; Boyd, B.; Kennedy, R., *Detection of peptides by precolumn derivatization with burette reagent and preconcentration on capillary liquid chromatography columns with electrochemical detection.* Analytical Chemistry, 1999. **71**: p. 987-994.

17. Kazuaki, O.; Hiroshi, M., *Determination of carboxylic acids by high-performance liquid chromatography with 2-(2,3-anthracenedicarboximido)ethyl trifluoromethanesulfonate as a highly sensitive fluorescent labeling reagent.* Analyst, 1993. **118**(7): p. 765-768.

18. Yamaguchi, S.; Matsunaga, R.; Nakamura, M.; Yosuke, O., *3-bromomethyl-6,7-dimethoxy-1-methyl-2(1H)-quinoxalinone as a new fluorescence derivatization reagent for carboxylic acids in high-performance liquid chromatography.* Journal of Chromatography, 1985. **346**: p. 227-236.

19. Brando, C.; Prandi, J.; Puzo, G., *Analysis of aminofluorescein-fatty acid derivatives by capillary electrophoresis with laser-induced fluorescence detection at the attomole level: application to mycobacterial fatty acids.* Journal of Chromatography A, 2002. **973**: p. 203-210.

20. Rezenka, M, *Chromatography of very long-chain fatty acids from animal and plant kingdoms.* Analytica Chimica Acta, 2002. **465**: p. 273-297.

21. Lima, P., *High-performance liquid chromatography of fatty acids in biological samples.* Analytica Chimica Acta, 2002. **246**: p. 81-91.

22. Gutnikov, G., *Fatty acid profiles of lipid samples.* Journal of Chromatography B, 1995. **671**: p. 71-89.

23. Fritz, J., *Analytical Solid-Phase Extraction*. 1999, New York, NY: Wiley & Sons.

24. Oezcimder, E. , *Fractionation of fish oil fatty acid methyl esters by argentation and reversed-phase liquid chromatography, and its utility in total fatty acid analysis.* journal of Chromatography, 1980. **187**(2): p. 307-317.

25. Gallaher, D.; Johnson, M., *Development of near-infrared fluorophoric labels for the determination of fatty acids separated by capillary electrophoresis with diode laser induced fluorescence detection.* The Analyst, 1999. **124**: p. 1541-1546.

26. Gallaher, D.; Johnson, M., *Nonaqueous capillary electrophoresis of fatty acids derivatized with a near-infrared fluorophore.* Analytical Chemistry, 2000. **72**: p. 2080-2086.

27. Puttmann, M.; Harld, E; Ochsenstein, E; Kattermann, R., *Fast HPLC determination of serum free fatty acids in the picomole range.* Clinical Chemistry, 1993. **39**(5): p. 825-832.

28. Patonay, G.A., Miquel D., *Near-infrared fluorogenic labels: New approach to an old problem.* Analytical Chemistry, 1991. **63**(6): p. 321-326.

# Chapter 4

# Development of an Electrophoretic Method for Fatty acid Analysis from Biological Extracts

## 4.1 Introduction

All living things are comprised of a complex mixture of many compounds both hydrophilic and hydrophobic that are necessary for proper function. A major component of hydrophobic biomaterial is comprised of fatty acids. A fatty acid is a long chain aliphatic group with a carboxylic acid head group. Fatty acids have many functions within living systems that range from membrane layers to fuel sources. Medical research has shown that a patient that has an overabundance or a deficiency of fatty acids is known to have major health problems that can include hypertension, coronary artery disease, and higher probability of death due to heart disease [1].

### 4.1.1 Fatty acids

When accounting for the quantities of these biomolecules two sources are known. The first source of fatty acids is through dietary intake. Ingestion of fatty acids from the

organism's diet has been found to be a significant source of fatty acids within the system. When an organism does not introduce an adequate quantity of fatty acids from intake through its diet, the need for a second source of fatty acids exists. Synthesis of fatty acids is possible within biological systems which will generate the acids not found through dietary sources.

Traditionally, fatty acid concentrations have been studied in bulk with no differentiation between individual acid species. It has been found that due to the different functions of individual acids and the inability of mammalian systems to synthesize the so called 'essential' fatty acids, linoleic and α-linolenic acid, a bulk determination of an organism's fatty acid concentrations falls short. Diagnosis of some conditions, such as disorders effecting mitochondrial fatty acid β-oxidation, can be accomplished through the quantitation of certain fatty acids. Mitochondrial fatty acid β-oxidation is a source for cellular energy and changes in its effect can have a wide variety of symptoms ranging from mild to life threatening [2]. Costa et al. developed a method of analysis of plasma fatty acids which utilizes a lengthy liquid phase extraction followed by derivitization and gas chromatographic analysis [3]. While patient plasma fatty acid concentrations were found, the method was lengthy due to the labeling and extraction techniques.

Synthesis of fatty acids within an organism is known to occur through the use of enzymes known as fatty acid synthetase. This is a general term that, in mammalian systems, consists of several different compounds that will catalyze a short chain acyl-CoA primer and extend the chain. Acetyl-CoA itself will convert to malonyl-CoA and add 2-carbon units to the growing fatty acid chain. The fatty acid chain will continue to expand by 2-carbon units in this way until the chain reaches 16 carbons in length or

palmitic acid. Palmitic acid is the generally accepted product of isolated fatty acid synthesis within mammalian systems. In order for synthesis of longer, shorter and branched chain fatty acids to occur, palmitic acid will further react with several enzymes that will compete for available substrates. These enzymes will dictate the end product of fatty acid synthesis and will include a combination of elongation, desaturation, incorporation into complex lipids and β-oxidation [4]. Enzyme concentrations and reactivities will dictate the final products of the modification and are individual to both the organisms studied and also the tissues within the organisms.

Alteration of enzyme concentrations has been found to be affected by several factors. Regulation of fatty acids within an organism is a complex subject that has been a focus of many research groups for the last 40 years and much is known about the subject. Conditions such as diabetes will greatly influence the relative quantities of fatty acids by reducing the effect of the enzymes. By causing test animals to become diabetic it was found that the enzyme responsible for the creation of fatty acid was less active. Reduction in the enzymatic activity can be reversed with the addition of insulin to the organism. Other factors that have been found to influence the regulation of fatty acids is the quantity of these biomolecules provided by diet. Several studies have researched the effect of fatty acid starvation and the effect of a diet rich in fatty acids. The latter has been found to decrease the production of fatty acids by increasing the down regulation of the enzymes discussed above. The former increases synthesis of enzymes and thus increases the synthesis of fatty acids.

The balance of an individual acid concentrations is different for many areas of an organism. A slight alteration of the concentrations of a single acid has been known to be

the cause of problems in an organism's health [4]. Therefore it is of great importance to know not only what acids are present but the concentrations of each individual acid. It is known that fatty acids of even chain length can be formed with fatty acid synthase, but some acids such as linoleic and α-linolenic acid are not and must be ingested through a diet. Saturated and unsaturated forms of acids are also known to be utilized within biological systems, although the concentrations and presence of individual acids will vary greatly from one system to the next [5, 6].

### 4.1.2 Quantitation of fatty acids

Several problems can occur when attempting to quantitate biomolecules. These problems consist, but are not limited to, the abundance and variety of bio-molecules present which can overwhelm separation and detection systems, the lack of adequate detection, the lack of separation resolution to reasonably distinguish individual species and finally the lack of sensitivity within a detection method to quantitate low concentrations of small volume samples. These problems have generated much of the interest in low concentration and low volume separation and detection techniques that have recently appeared within the literature.

Separation of fatty acids includes a combination of all of the problems discussed above. Within a mammalian system, many compounds of a wide variety of properties are present. The problems described previously arise when information on a single species is desired [7]. Pre-treatment of tissue sample is the first step in any bio-molecule separation. In order to extract the desired analyte from the bulk tissue, the tissue must be homogenized. Extraction from the homogenate can take the form of solid phase

extraction (SPE) or liquid phase extraction depending on the analyte of interest. A significant amount of interest has been taken in these methods and many techniques have been developed for the purposes of extracting particular bio-molecules. The ideal extraction technique will have a low loss of analyte within the extraction, a low quantity of tissue homogenate needed, and a fast throughput as biological molecules are not always stable for long periods of time in non-aqueous buffers. Careful attention must be taken to avoid the destruction of samples through the use of harsh conditions when pre-treatment is necessary.

In an ideal separation scheme, the pre-treatment techniques would be done on the micro scale or removed altogether. No technique is efficient enough to avoid loss of a small amount of analyte. Unfortunately, the removal of pre-treatment is not reasonable due to the limits of detection inherent to any analytical system. Within an organism, or component of interest, there exists a particular concentration of analytes of interest. When the amount of tissue available is severely limited, or the concentration of analyte is significantly dilute, the instrumental detection limit becomes a major factor. Pre-treatment of a sample through the use of SPE is a powerful technique as it performs two functions. First it will remove a portion of the unwanted material that could adversely affect the final separation technique as discussed above. Second, SPE can concentrate the molecule of interest by purification of a single class of molecule followed by solvent removal. Concentration in this way is limited in some applications as it can only be accomplished when a large quantity of homogenate is available. Even given these limitations, the purity of sample and the inherent pre-concentration make SPE ideal for the pre-treatment of fatty acids.

Several methods have been developed for the separation and quantitation of fatty acids in biological systems [8, 9]. These techniques primarily utilize gas chromatography (GC) and/or high performance liquid chromatography (HPLC) to separate the desired acids [7, 10-12].

### 4.1.3 Gas chromatography

The use of gas chromatography to separate fatty acids is the primary method of separation in the analysis of fatty acids in biological systems. This is due to the speed of separation and the high resolution. A significant amount of research has been devoted to the optimization of the pre-treatment method necessary prior to GC analysis. Modifications to fatty acids are necessary in order to lower the boiling point of the biomolecules. Boiling point is lowered by converting the acids of interest into methyl or ethyl esters[13]. Esterification is accomplished through the use of one of two classifications, acid or base catalyzed esterification.

Acid esterification is a reaction that converts fatty acids to esters through the use of an acid, generally, boron trifluoride in methanol. Other acids that are utilized include methanolic hydrochloric and sulfuric acids. Reaction rates are the primary factor in determining the acid used in the reaction. Miwa has shown that boron trifluoride will esterify all acid species within a sample in under 90 minutes [14]. The disadvantages of using acid esterification is the necessity of temperatures that are higher than 100 $^{o}$C. This is a significant disadvantage when quantification of short chain acids is desired as their methyl esters have very low boiling points and analyte can be lost at these temperatures.

Base catalyzed esterification has been developed to eliminate the loss of analyte when using high temperatures. When using potassium hydroxide or sodium methoxide, esterification can be accomplished at ambient temperatures. When GC analysis of short chain fatty acids is desired, such as in milk, base catalyzed esterification is the primary choice of modification. Primary disadvantages to this method of modification include the inability to modify free fatty acids or sphingolipids. Modification through a pre-reaction step is necessary in order to use base catalysis for these biomolecules.

In either method there are common problems. These problems include, but are not limited to, the incomplete conversion of fatty acids to methyl esters, alteration of fatty acid concentrations with esterification, side reactions that will complicate analysis with multiple peaks, damage to GC columns due to reaction components, and finally loss of short chain fatty acid methyl esters due to volatility.

### 4.1.4 High performance liquid chromatography

HPLC has also been shown by various different research groups to be an effective method of separation of fatty acids. Separations based on HPLC differ greatly from GC analysis of methyl esters of fatty acids. The GC methods described above will separate the methyl esters that correspond to the acids of interest on the basis of their volatility and polarity. It is generally shown that longer chain lengths will always have a longer retention time. In HPLC separations, the polarity of the analyte of interest is the primary factor in elution order. The degree of unsaturation and the position of unsaturation and branch chains will influence the time of elution to a much greater extent.

The advantage of using liquid chromatography over GC methods described above is that separation within an LC method can be accomplished without the high temperature that can potentially alter the chemical structure of the acids of interest. Analytes in analysis by HPLC do not have to go into the gas phase, which reduces the potential loss of smaller volatile acids.

The mechanism of separation in HPLC is based primarily on polarity. The longer the aliphatic chain in fatty acids, the more hydrophobic the molecule becomes. Long chain fatty acids, $C_{18}$ and higher, will be significantly hydrophobic and elute slower than shorter chain fatty acids. The non-polar character of these acids will create longer run times in C8 or C18 reversed phase chromatographic columns. More polar columns are rarely used in the analysis of non-polar organic acids as the reduction of the retention time causes a reduction in resolution [15]. Many solvents are used in fatty acid analysis, but primarily analysis is done in methanol and acetonitrile systems [11].

The primary concern for analysis of fatty acids by HPLC is in the method of detection. Most fatty acids have no chromophore group inherent to their structures. Lack of chromophores complicate the study of fatty acids as labeling is necessary in order to detect individual species. Direct fatty acid separation and detection by HPLC has been reported by several different groups using UV absorbance detection [11] on a specific series of fatty acids with aromatic rings inherent to their structures. The more common saturated and unsaturated, straight chain acids cannot be detected in this way.

For rapid analysis of the acids of interest several groups have used absorption and fluorescence labels. Mehta et al. successfully separated a series of saturated and unsaturated fatty acids at the nmol range in a short total run time of under 40 minutes. In

this study, the acids were derivitized with p-bromophenacyl bromide in order to improve detection using a UV detector set to 242 and 254 nm. This method was also used to label free fatty acids found in human plasma after sample preparation through liquid phase extraction. Similar methods were used to analyze fatty acids found in cottonseed oil where derivitization of cyclopropenoid fatty acids were derivitized for UV absorbance analysis [16].

UV absorbance detection coupled to HPLC separation has the advantage of being a simple and inexpensive method of analysis. Miwa et al. report detection limits of 200 fmol for the extraction and HPLC analysis of serum fatty acids labeled with 2-nitrophenylhydrazine and detected through UV absorbance at 230 nm [14]. Typically, picomole detection is reported for extraction followed by HPLC separation and UV absorbance detection [9, 17].

While effective in detection, UV absorbance suffers from a moderate detection limit. Fluorescence detection techniques have been developed and coupled to HPLC separation to reduce the detection limit significantly. Akasaka et al. report detection of 0.8 fmol in a 10 μl injection when a series of fatty acid standards were labeled with 2-(2,3-anthracenedicarboximido)ethyl trifluoromethanesulfonate [18]. Typically, fluorescent labeling with HPLC separation techniques report an order of magnitude higher detection limits [14, 19-21].

### 4.1.5 Mass spectrometry

A third common method of detection is the use of mass spectrometry (MS). MS detection is utilized as a detection method in both GC and HPLC separations, although GC-MS is a far more established technique [22]. Commonly, in GC-MS analysis of fatty acids, fatty acid methyl esters (FAMEs) are separated based on volatility and polarity (as described above) then analyzed through the use of electron impact ionization mass spectrometry [23]. This method of ionization will break the analyte of interest into fragment ions which will then be detected based on their charge to mass ratio. It has been reported that using this method of detection, positive identification of individual fatty acids can be determined, although low molecular weight fragments are far more common than their high molecular weight parent ions [23-25].

Further identification of FAMEs has been accomplished through the use of tandem mass spectrometry. With tandem MS ions are formed through the use of either electrospray (ES) or fast atom bombardment (FAB) ionization. An ion is selected by a mass analyzer and induced to enter a second collision region. This can be done through the use of a several chamber instrument, or through the use of a trapping instrument. By using a second mass analyzer, the fragments can be identified and positive identification can be give to the parent ions. Griffiths' review of these techniques as they relate to biologically relevant molecules can be found for an in depth review of these techniques [26].

HPLC coupled with mass spectrometry (LCMS) has more recently been developed. Unlike its GC counterpart, analytes eluting from a HPLC column are not in the gas phase and will have buffer salts and additives that could potentially disrupt

analysis coeluting from the column. 'Softer' ionization techniques, techniques which do not fragment ions to a high extent, are generally used for analysis in LCMS [22]. Electrospray ionization (ESI) and atmospheric pressure chemical ionization (APCI) are common methods of ionization in LCMS techniques involving biologically relevant molecules such as fatty acids. The advantage of MS detection is the addition of structural information, most notably atomic mass [27]. A review of the development of these techniques with regard to long-chain fatty acids was written by Rezanka and Votruba [28].

While the separation methods described above are powerful tools, there are inherent weaknesses to each. GC suffers from the need of the analytes to enter the gas phase which requires complex derivation procedures. HPLC methods are known to have 'critical pairs', two analytes found to co-elute. Due to the presence of unsaturation points within the chain, the polarity of the acid is altered. This creates a difference in elution time equivalent to the presence of 2 carbons less. One of the largest problems with HPLC analysis is the separation of C16:0 and C18:1, both of which are major fatty acids found in animal lipids [7]. While problems such as this will likely to occur in any separation technique, secondary and even tertiary tests are needed to determine if coelution of two or more analytes exist.

### 4.1.6 Capillary electrophoresis

Capillary electrophoresis of fatty acids has many advantages over its chromatography counterparts. The primary interest in electrophoretic separations is in the mechanism of the separation itself. Chromatography utilizes differences in polarity

(and volatility in the case of GC) to cause analytes to enter a stationary phase and increase their retention time. In CE separation is based on an analyte's charge to size ratio. The difference in separation mechanism gives CE an advantage over LC as chromatographic critical pairs could be better resolved from each other. CE has the same advantage over GC as LC in that high temperatures, which could cause sample degradation or loss, are not needed.

CE analysis of fatty acids is a developing field and has some challenges to overcome. Long chain fatty acids are non-polar and hydrophobic molecules. Solubility becomes problematic when higher chain length are being studied.

Two primary techniques have been developed for the electrophoretic analysis of fatty acids. One technique that has had a significant amount of attention is the use of micelles to aid solubility of the acids [29-32]. The addition of micelles to the running solvent will increase the solubility of the acids being analyzed, but will also cause a new, chromatographic component to be added to the separation [33]. Jussila et al. report the separation of linoleic acid oxidation products through the use of micellular electrokinetic chromatography (MEKC). By alteration of the surfactant used to create micelles the effect of on fatty acid solubility was observed. It was reported that in a phosphate buffer, sodium cholate micelles were superior to sodium dodecylsulfate (SDS) for the purposes of solubility and resolution. A separation of the fatty acids was also attempted using methanol and ethanol buffer systems, but the authors report that they were unable to separate the species using this method [34]. Isomeric epoxy fatty acids were reported to be separated using SDS MEKC in a mixed buffer of acetonitrile and aqueous borate buffer. Baseline resolution was not observed until the capillary was temperature

controlled and set to 10°C. This indicates Joule heating effects were the probable cause of poor resolution. The authors used UV detection in this study, and could have benefited from the use of a more sensitive form of detection and smaller injection volumes [35]. SDS MEKC was reported used to separate fatty acid hydroperoxides with $1x10^6$ theoretical plates by Melchior and Gab [36]. Although baseline increases due to impurities were present, the authors report an effective separation, and identification of oleic, linoleic and arachidonic acids from egg lecithin using SDS micelles in a buffer mix of acetonitrile and aqueous borate buffer.

Collet and Gareil developed a method for the optimization of selectivity and resolution in MEKC of long chain fatty acids [37]. In their work aqueous and non-aqueous buffer portions were altered and SDS concentrations were adjusted in order to improve peak efficiency. Although the baseline of their separation was far from ideal, average peak efficiency of N=90,000 was reported.

### 4.1.7 Non-aqueous capillary electrophoresis

Non-aqueous capillary electrophoresis (NACE) is the alternative method for solving the solubility problem involved with the separation of fatty acids. Separation of shorter chain acids, which is problematic in GC methods discussed above, can be accomplished with an aqueous buffer [38, 39]. Longer chain acids are problematic as they are not sufficiently soluble in aqueous systems to be analyzed. Several groups have successfully separated fatty acids by NACE and partially non-aqueous systems [29, 34, 40-42]. These reports range from completely non-aqueous systems, to primarily aqueous with small amounts of more non-polar solvents added to aqueous buffers [43-45].

Zuriguel et al. developed a separation technique using a mixture of ethanol and aqueous borate buffer that was reported to have baseline separation of acids up to $C_{11}$ [43]. Detection limits in this study were as low as 2 x $10^{-9}$ M when testing standards, and $10^{-8}$ M when serum samples were studied. The fluorescent tag 5-bromomethylfluorescein was applied to the acids in this study in order to aid in laser induced fluorescence (LIF) detection at 488 nm of the acids.

Drange and Lundanes report the separation of long chain fatty acids up to $C_{26}$ using NACE with a mixed solvent system of acetonitrile and methanol [41]. The mixture of buffers was adjusted to determine the maximum resolution between electrophroetic peaks in the separation and it was found that baseline resolution was possible with a modest run time of less than 16 minutes. Significant difficulties were reported when fish oil acids were longer acids had poor resolution and reproducibility were poor. The authors attributed these problems to electrodispersion of the longer chain acids. Baseline stability was also observed to be poor when observing these biological samples. The acid concentration limits of detection in this study were determined to be 25 μM using indirect UV detection.

### 4.1.8 Detection limits

Detection in capillary electrophoresis is similar to HPLC detection discussed above, and offers similar challenges. Detection of fatty acids after electrophoretic separation is commonly accomplished by the use of indirect UV detection. Unfortunately, this only leads to modest detection limits of $10^{-5}$ M. The use of fluorescent tags can dramatically lower the detection limit to the $10^{-9}$ M range is common

[46]. Significant improvement can be made to the limits of detection by the use of laser induced fluorescence detection (discussed previously). Brando et al reported attomole level detection in mycobacteria fatty acids by capillary electrophoresis using laser induced fluorescence detection (CE-LIF) [47]. Their separation method was only able to analyze shorter chain lengths and polyunsaturated acids due to the 70:30 aqueous buffer : acetonitrile mixture. Gallaher and Johnson developed a separation technique for the separation and detection of a series of fatty acids ranging from $C_6$ to $C_{22}$ [40]. Non-aqueous solvent was used with TEAC as a background electrolyte. While the limit of detection was not sought, baseline separations at acid concentrations of 10 nM for C16-20 and 2 nM for C22 were reported.

Building on the work done by Gallagher and Johnson, a separation technique was developed (see Chapter Two). The limits of detection in an ideal system were found (see Chapter Three) and fatty acids were extracted from a biological sample to be analyzed. Capillary electrophoresis with the capillary having a successive multiple ionic layer (SMIL) coating was used to reduce the problems described by Drange and Lundanes and to reduce analyte, and contaminant, adsorption on the capillary walls. A simple and robust method of separation was developed for use in biological free fatty acid analysis that is able to avoid both critical pairs found in HPLC and small molecule sample loss found in GC. LIF detection in the IR region was used to increase resolution and decrease background noise brought on by biological contaminants.

## 4.2 Experimental reagents and materials

Linear saturated and unsaturated fatty acids, C8 (caprylic), C10 (capric), C12 (lauric), C14 (myristic), C18 (steric), C18:$1^{9\text{-cis}}$ (oleic), C18:$1^{9\text{-trans}}$ (eladic), C18:$2^{9,12\text{-cis}}$ (linoleic), 18:$2^{9,12\text{-trans}}$ (linolenolic), 18:$1^{6\text{-cis}}$ (petroselenic), 18:$3^{9,12,15}$ (linolenic), 18:$1^{6\text{-trans}}$ (petroselaidic), and 18:$1^{11\text{-trans}}$ (vaccenic) as well as N,N-dicyclohexylcarbodiimide (DCC) and myristyltrimethylammonium bromide (MTAB) were all purchased from Acros Organics. Tetraethylammonium chloride (TEAC) originally from Eastman Kodak (Rochester, NY) was obtained from house stores. Polybrene® (hexadimethrine bromide) and dextran sulfate (avg. mol. wt. = 5000 D) were purchased from Aldrich Chemical Corporation (Milwaukee, WI, USA). Methanol and chloroform used as solvents were HPLC grade and purchased from Fisher Scientific (Fair Lawn, NJ).

### 4.2.1 Apparatus

Capillary electrophoresis was performed on fused silica capillaries with 50 μm internal diameter, 360 μm outer diameter, that were purchased from Polymicro Technologies (Phoenix, AZ, USA). A detection window of 1 cm was created by pyrolysis of the polyimide coating using a low intensity butane flame. The capillary was then fixed to a microscope slide using epoxy.

Voltage was applied during electrophoretic separations using a CZE 1000R (Spellman High Voltage Electronics Corporation, Plainview, NY). Injections were gravimetric injections at the cathode by raising the capillary 10 cm for 5 seconds (approximately 5 μl injection).

Detection was achieved using laser induced fluorescence using a laboratory-constructed epifluorescence microscope. Excitation was with a near-infrared laser operating at 785 nm (Sanyo DL7140-201 S). The beam was passed through a mica half-wave plate (Melles Griot) and a calcite Glan-Thompson polarizer (Karl Lambrecht, Chicago, IL) for polarization and control of light intensity. The collimated beam was reflected by a dichroic reflector (Omega, 810 DRLP) and focused into the capillary by a 40X, 0.85 NA microscope objective (Nikon Fluor 40, Nikon Corp, Tokyo). Fluorescence was collected by the same objective, passed through the dichroic, spatially filtered with an 600 μm pinhole, and spectrally filtered with an 810EFLP (Omega) long pass filter. The remaining fluorescence was focused with a pair of 24mm EFL achromats (Rolyn Optics, Covina, AC) onto the active area of a single photon counting avalanche photodiode (SPCM module, EG&G Canada, now PE Instruments). Data collection was performed with an MCS plug-in card (MCSII, Tennelec/Nucleus, Oak Ridge, TN), usually at a rate of 250 ms/MCS bin, residing in an AT bus PC.

Peak analysis was done with Igor Pro 4.02A (Wavemetrics, Eugene, OR) using multipeak fit package version 1.30. Electropherograms were fit to the Gaussian peak shape.

### 4.2.2 Fatty acid extraction protocol

In order to remove unwanted biological material from the fatty acids, a tissue sample (bovine omentum) was taken from sub-zero storage and a 1.00 g portion was removed and weighed. The weighed sample was placed in 20 ml of a 2:1 chloroform : methanol solvent system and homogenized in a silanized glass homogenizer. The sample was

centrifuged in a Beckman Coulter Centrifuge at 1500 g for 30 minutes at -4 $^0$C. The liquid portion of the sample was removed and aqueous 0.88% KCL was added to make 1/5 of the total volume. The sample was vortexed for 10 seconds and allowed to separate in a below 0 $^0$C freezer. The top portion (aqueous) was discarded while the non-aqueous portion was dried with a stream of nitrogen. Once dried 5 ml of hexane were added to the sample and it was stored in a -4 $^0$C freezer.

A silica SPE column was constructed by placing a frit at the bottom of a 3 ml polypropylene column. 0.5 g of silica was then placed in the column and a second frit was added to hold the silica in place. The column was wetted by passing 4 ml of hexane through it. 100 µl of the biological extract discussed above was placed in the column. A series of solvent mixtures were then run through the column and the solutions that resulted were collected in fractions. The first fraction collected was 4ml of hexane washing through the column. Fraction 2 was 1 ml of 99:1 hexane : acetic acid, fraction 3 was 90:10 hexane to ethyl acetate, and fraction 4 was 80:20 hexane to ethyl acetate. This final fraction was the fraction containing the free fatty acids. The fraction was dried under nitrogen and stored in the -4 $^0$C freezer.

### 4.2.3 Fatty acid derivatization protocol

The procedures for labeling the fatty acids with the near-infrared fluorescent probe, and for synthesizing the probe, have been modified from the procedure previously reported [48]. Stock solutions of various fatty acids and DCC were prepared in chloroform. A stock solution of the NIR fluorescent probe (Patonay 3, Chapter 3 Figure 2) was prepared in anhydrous dimethylformamide. Stock solutions were altered in order

to maintain reaction conditions necessary to retrieve kinetic data from the reactions. To perform a derivatization, a 100 μL aliquot of fatty acid solution was pipetted into a 2 mL glass reaction vial and stirred with a magnetic stirrer. A 100 μL aliquot of DCC stock was added and the mixture was allowed to stir for 30 seconds. A 100 μL aliquot of the labeling reagent was added and the reaction vessel was capped and allowed to react for several hours, while shielded from ambient light. 100 μL of extract was taken directly from the extraction method and mixed with 20 μl DCC stock solution and 100 μl label solution. The reaction was allowed to mix for 2 hours to complete the reaction.

At the end of the reaction period, precipitated dicyclohexylurea was filtered off using a 0.2 μm nylon syringe filter and aliquots of the reaction mixture were diluted in methanol for CE analysis. To create a mixture of fatty acids, aliquots of the various individual reactions were combined and subjected to an identical work up procedure. To ensure separation conditions were reproducible, IR 786 dye was added to the stock buffer and used as an internal marker.

### 4.2.4 Coating procedure

SMIL capillary coatings were utilized in the separations and have been described earlier in this volume (Chapter 2). Briefly, the coating utilized in the separations were made from flushing a 10% Polybrene® solution through the capillary at a rate of 6.9 μL/minute for 4 hours. The capillary was then evacuated and 10% dextran sulfate was flushed at the same rate for 4 hours. Finally, the capillary was evacuated a third time and the final coat of Polybrene® was flushed as described above for 4 hours. The capillary was then evacuated and allowed to sit overnight.

The extraction separation was completed in a longer capillary (total length 100 cm) with a final Polybrene® coat of 1 hour.

## 4.3 Results and discussion

When developing a strategy to separate a biological mixture it is important to note that the mixture will contain many different compounds that may or may not contribute a signal to any detection method used. To mitigate the difficulty that these contaminants cause, selective labeling with a fluorescently active dye was used (the development of the method used is described earlier in this volume (chapter 3)). While attachment of a fluorescent label will greatly reduce the problem associated with contaminants, it will not eliminate it. Detection will only occur when a fluorescently active analyte migrates through the detection area, but nonselective binding of contaminants to dye can cause an increase in background and reduce signal to noise ratios. Due to the complexity of biological extracts, selective binding can occur when the reaction takes place if an acid group on any biomolecule in the sample is activated by DCC. This can cause problems as the fatty acid identification being pursued could become complicated when additional peaks are observed in an electropherogram which do not correspond to the fatty acids being analyzed.

Reduction of the effect of nonselective binding and selective binding with unwanted contaminants was done through several methods. Much unwanted biomaterial is eliminated through the use of the initial extraction. Solid phase extraction (SPE) was the method used to remove many unwanted portions of the biological mixture. SPE separated the biological homogenate into several different portions which had similar

properties. The primary disadvantage of the SPE method is the need for relatively large amounts of solvent to extract a comparatively small amount of the analyte. Due to the solvent used, there is a loss in analyte due to the extraction. Both disadvantages are balanced by the relative ease in use and speed of the extraction method.

Analysis of biological fatty acids has shown that mammalian tissue primarily contains saturated and unsaturated acids with chain lengths that range from 16 to 22 carbons [7]. While other, larger and smaller, acids are potentially present they are not the primary acids of interest due to their relatively small concentrations. It is also well established that only acids with an even number of carbons in their chain are synthesized in mammals (discussed above). These are the acids that are of primary interest in this study.

In order to develop and extend the capabilities of the separation technique described in Chapter 2, the successive multiple ionic layer (SMIL) coat was utilized. Coating times were adjusted and capillary lengths were tested in order to increase the resolution between the acids while maintaining a reasonable run time (under 30 minutes). Through several trials it was apparent that the electrophoretic mobility (EP) of the acids should be opposite to the bulk electroosmotic flow (EOF) driving the separation. A series of capillaries were tested that differed in their final coating time, and therefore the EOF associated with the capillary charge (described in Chapter 2).

### 4.3.1 Separations of fatty acid series

Several different fatty acids were obtained and separation conditions were adjusted to find an optimal separation. Parameters that were adjusted included the

capillary coat, the applied voltage, and the ionic strength of the solvent system. It was apparent that although adjusting the applied voltage had the potential to increase or decrease the run time, it did not increase the resolution of the separations significantly. EOF and EP are both dependent on the electric field so unless Joule heating is a factor.

### 4.3.2 Ionic strength modification

In order to develop the resolution between peaks, adjustments were made to the ionic strength of the background electrolyte. Increasing or decreasing the ionic strength is advantageous to the separation in that the EP and EOF will not change at the same rates. If the analytes of interest have an EP that will change greatly with the altering of ionic strength then the separation will improve drastically. Small analytes that are highly charged would be affected by changes in the ionic strength greatly, but this did not appear to be the case for the fatty acids of interest due to the small charge.

Figure 1 shows a comparison of several electropherograms in which the ionic strength was modified. In this capillary the EOF dominated the separation and the EP was in the opposite direction to the EOF. As a result the increase in EOF found when the buffer ionic strength was decreased from 12.5 mM to 6.25 mM shows a decrease in the time of migration within the capillary. The decrease in intensity as the ionic strength decreased was thought to be degradation of the acid-dye complex over the time while in running buffer. This was not further investigated, but dilution into running buffer directly before injection caused the disappearance of this effect.

The change in resolution was monitored but found to be insufficient to be the primary factor that contributes to the overall resolution needed for separation. This is

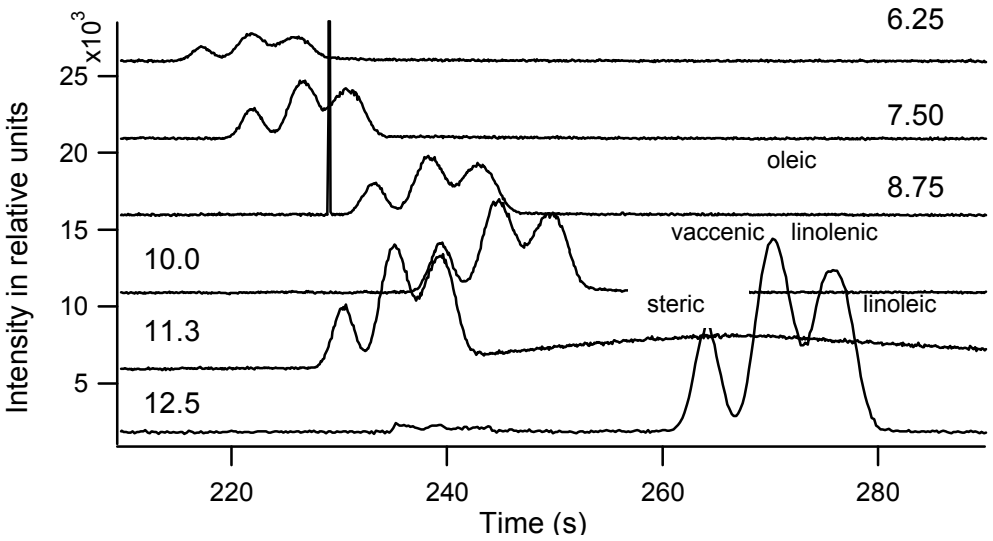


Figure 1. The effect of ionic strength on an injection of steric, linoleic, linolenic, oleic and vaccenic acids. Injections made at negative pole, ionic strengths given on each trace in mM. Capillary conditions; 50 µm ID, 360 µm OD, total length 35 cm, length to detection 18 cm, SMIL coat of 4 hour Polybrene®, 4 hour dextran sulfate, 4 hour Polybrene®. Subsequent traces are offset

believed to be due to analyte-wall interactions that become more of a problem when analytes interact with the capillary surface in longer separation times. Capillary conditions must be such that longer separation times are avoided. The SMIL capillary surface coating described in chapter 2, and utilized here, is able to reverse the EOF flow, and/or reduce it so that EP dominates the separation (Figure 1). Increasing buffer ionic strength will cause a decrease in the depth of the electronic double layer. This decrease will cause an increase in migration time in capillaries with a high EOF and a potential decrease in total migration time when EOF is low enough that EP will dominate the separation.

An increase in run time was detrimental to the separation and some attempts were made to increase the applied voltage to compensate for this increase. Two approaches to were taken in order to increase the applied voltage. The total length of the capillary was decreased from 65 cm to 35 cm, which increased the electric field without the need to

increase the applied voltage. While this approach found faster run times (Figure 2), the largest effect on the analyte mobility was more likely attributed to the coating procedure. Smaller capillaries will have less back pressure when the coat polymers are being deposited. The total amount of coating material and the nature of the coat itself as it pertains to the surface charge density is not easily determined (described in chapter 2). A direct comparison between a longer capillary and a shorter capillary must take this change in coat into account because the change in migration time due to the applied voltage is only one unknown variable along with the effect of the capillary coat. The speed of migration through the capillary can improve the separation only if the analyte EP is great enough to cause a separation in the amount of time it takes for the analytes to travel from the injection point to the detection point. When unsaturated acids were attempted in the shorter capillary it was found that the migration of the acids was too

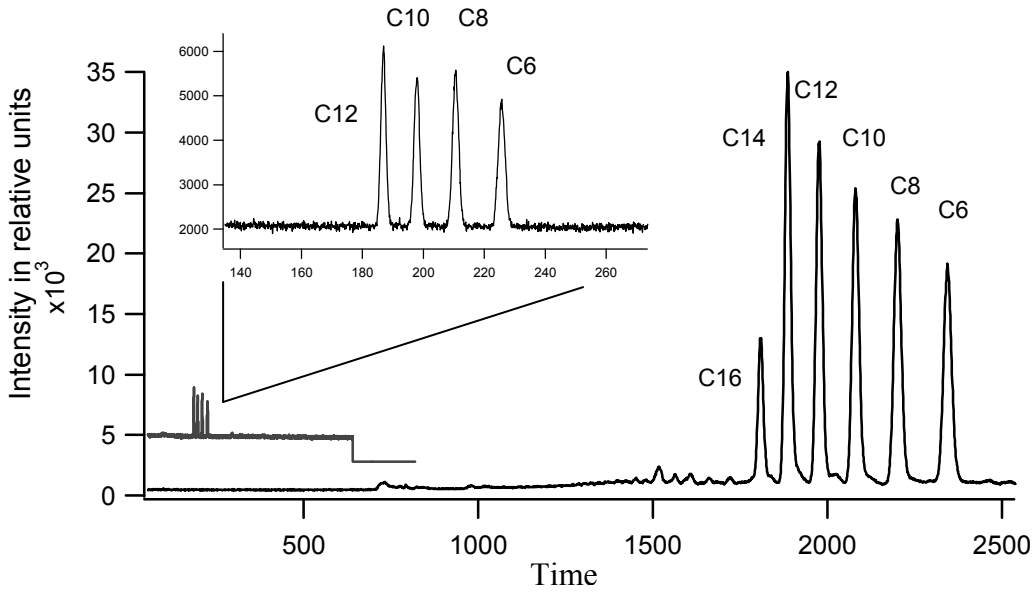


Figure 2. The effect of a shortened capillary. Bottom trace injection is C6, C8, C10, C12, C14, C16 with capillary length 65 cm, total dye concentration 700 nM. Top trace is C6, C8, C10, C12 with capillary length 35 cm, total dye concentration 50 nM. Both traces: 25 kV running voltage, ID 50 µm, 5 sec 15 kV injection.

great and the no reasonable separation was observed. To facilitate the separation, a longer capillary was coated with a SMIL coating. The procedure found in Chapter 2 was used with each coating time extended to 12 hours. This produced a negative overall charge on the capillary which caused EOF to travel from cathode to anode (separation discussed further below).

The second approach to limit the long run times was to increase the applied voltage. With the increase in applied voltage the EOF will increase accordingly and a shorter migration time should be apparent. Unfortunately, with the increase in applied voltage, the risk of Joule heating is much greater. When higher voltage was applied to the separation system, it was observed that the current was not stable. To avoid this problem the buffer ionic strength was decreased to limit the kinetic energy of buffer system. Current instability was found with any applied voltage over 30 kV and reproducibility was a major problem. Joule heating was likely the cause of this instability but the cause was not researched further.

### 4.3.3 Buffer additives

Exploration into buffer additives was also attempted to increase the resolution of the separations in each of the capillaries. This was done by adding surfactants to the buffer such as cholate, sodium dodecal sulfate (SDS) and lauric acid at concentrations that were known to be under the critical micelle concentration (CMC). While these buffer additives changed the appearance of the electropherograms, the resolution changes were not apparent and could be accounted for as changes in the ionic strength of the

buffer more than any other change. Reproducibility was also a problem and no reasonable conclusions could be drawn as to the effect of these surfactants on the acids.

Silver ion has been used in HPLC separations to bind to unsaturated bonds and increase resolution in separations. Both silver nitrate and silver triflоromethanesulfonate were used in order to increase the peak separation in the unsaturated acids. Silver nitrate was attempted using a partially aqueous buffer (50% aqueous, 50% MeOH) but it was found that solubility was a significant problem. Silver triflоromethanesulfonate was used with limited success, but had an adverse effect on the SMIL coating. The capillary coating was found to deteriorate within 1 run of using silver ion.

### 4.3.4 Extract separation

An extract of fatty acids from bovine omentum was collected and analyzed. The total identification of every acid was not determined but regions of acids with similar properties were found. Figure 3 shows the separation of the extract under the conditions determined above. The increase in background found early in the electropherogram may indicate non specific binding of the tag to biomolecules found in the extract mixture. The background signal improves, but longer chain acids at low concentration could potentially be obscured. Several areas of the electropherogram were found to have similar elution times to known acids and can constitute relative regions of the plot. The region adjacent to the large peak labeled ‘unreacted label’ is known to include the saturated, primary fatty acids from injections of standards. This region ranges from 8000 seconds to 6000 seconds. While some unsaturated acids could potentially be found in this region, the bulk of the saturated acids will be found here. The next region, between

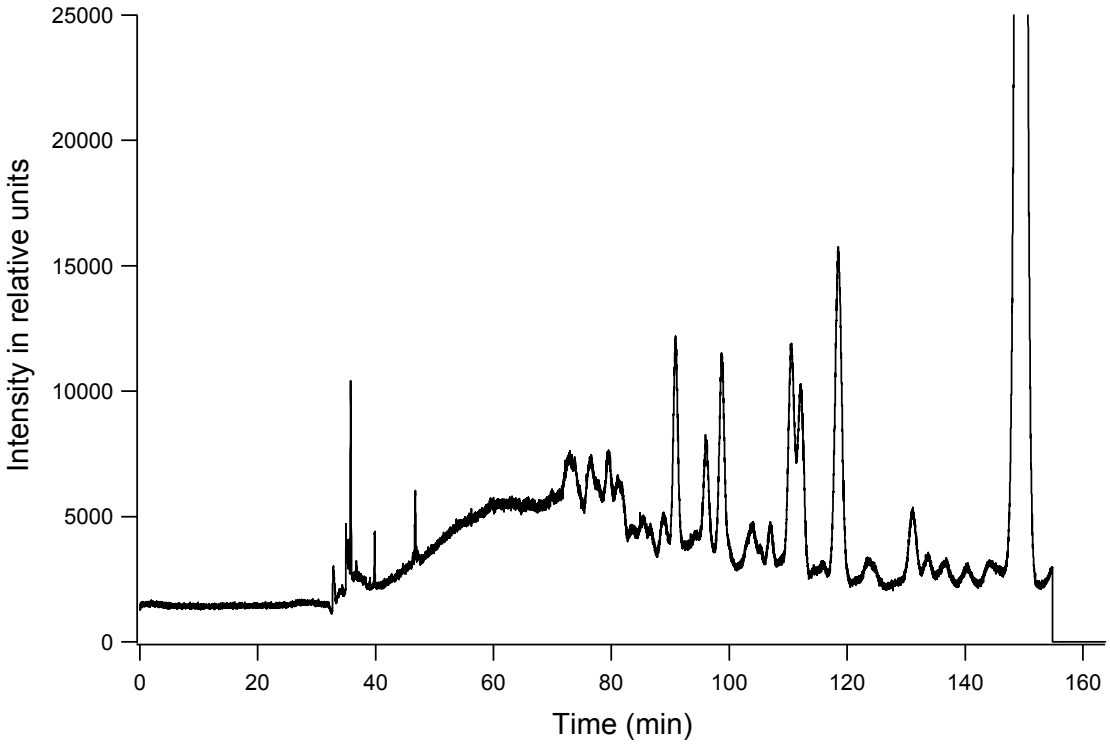


Figure 3: Injection of labeled fatty acid extract from bovine omentum. Injection at negative pole, running voltage 25kV, ID 50, I = 3.125 mM TEAC total SMIL capillary length 100 cm, length to detection 85 cm

5000 seconds and 4000 seconds is the region where the unsaturated 18 carbon species

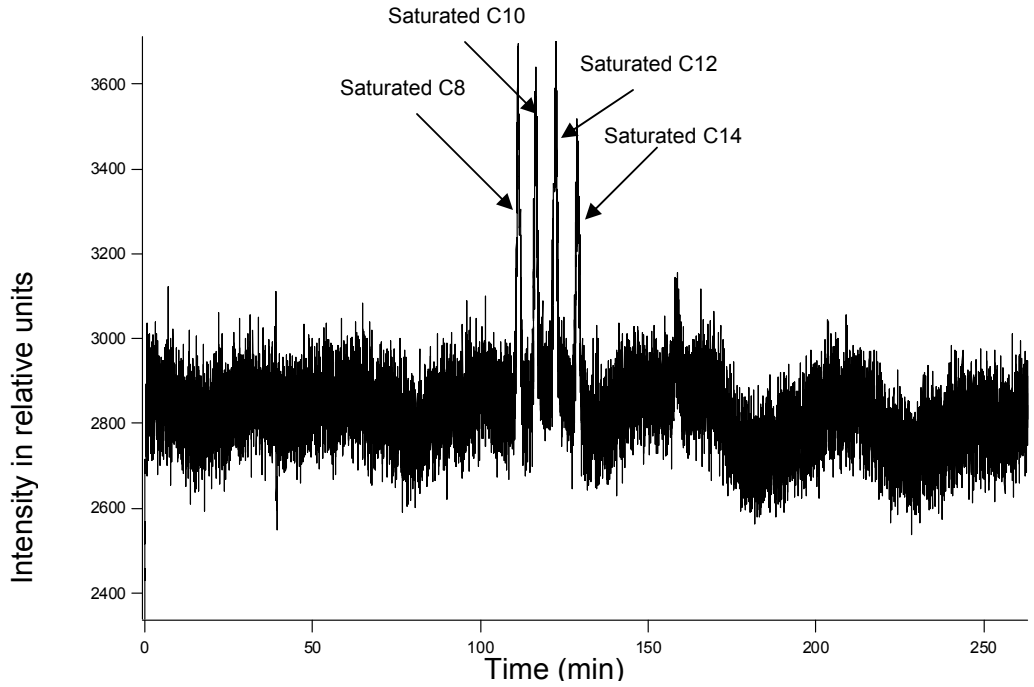


Figure 4: Labeled saturated fatty acids C8, C10, C12, C14 and unreacted label. Separations conditions identical to extraction injection. Injection at negative pole, running voltage 25kV, ID 50. Total SMIL capillary length 100 cm, length to detection 85 cm

would be found. Within the range between 5000 seconds and 4000 seconds the standard sample shows the presence of these acids. The region can be further subdivided into smaller regions. The first peaks to appear are those that correspond to acids with multiple unsaturation points and longer chain lengths. As the time of migration increases the acids with lower degree of unsaturation points and the smaller chain lengths will migrate to the detector. The divider between the regions is not a distinct line, but a continuum and without structural information on the acids it is difficult to determine the exact nature of each of the species. These regions were determined through the use of separations of standard acid samples shown in Figures 4 and 5. An attempt was made to spike the extract sample, but the complexity of the sample hindered the spiking experiment and conclusions could not be drawn due to these problems.

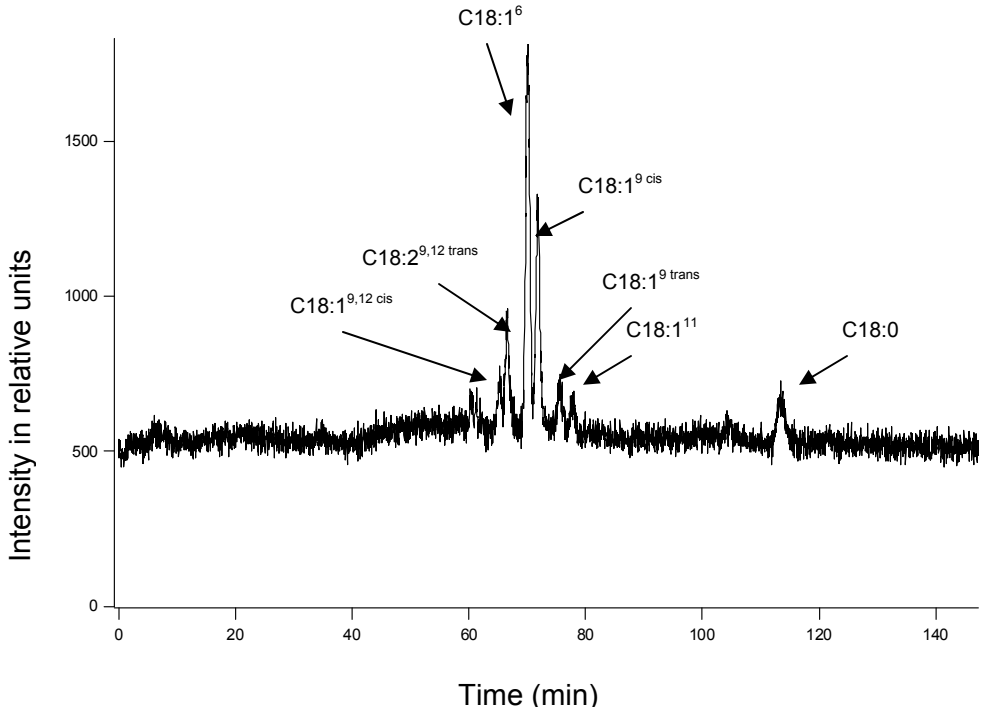


Figure 5: Injection of known acid mixture of C18:0, C18:$2^{9,12\ cis/trans}$, C18:$1^{9\ cis/trans}$, C18:$1^{11}$, C18:$1^{6}$. Injection at negative pole, running voltage 25 kV, ID 50 µm, I = 3.125 mM TEAC, total SMIL capillary length 100 cm, length to detection 85 cm

The direct comparison between the known standards (Figures 4 and 5) and the unknown extraction (Figure 3) shows that there is a significant amount of background interference in the region where the peaks corresponding to the longer (C22) chains would likely appear. This makes identification difficult and further pre-injection sample purification may be necessary.

Resolution between peaks is impossible to determine in the separation of the extract sample. Resolution values for the peaks in Figure 5 were determined (table 1). While this series of acids is limited in comparison to the full extract separation, the complexity of the extract separation makes resolution difficult to determine.

Although the concentration of the fatty acids in the extract was not able to be determined due to the complexity of the separation, some conclusions can be drawn from

the standard samples and the extract sample itself. The separation of the standard unsaturated fatty acid sample separated in the SMIL coated capillary (Figure 5) shows the separation of the cis and trans isomers of C18:$2^{9,12}$ and C18:$1^{9}$ with resolution that is 1.01 and 1.25 respectively (table 1).

Concentration of the acids when placed in the labeling reaction procedure is shown in table 2. The injection concentration was determined via the dye concentration which was at equal concentration in every reaction vial and at equal concentration to the acid concentration. The differences in peak area can be attributed to the reaction efficiency of the label to the acid in question (see Chapter 3).

Table 1. Theoretical plate height and average resolution

| Fatty acid | Average number of plates | Average plate height (μm) | Average resolution |
|---|---|---|---|
| C18:$2^{9,12\text{-cis}}$ | 51090 | 6.459 | |
| C18:$2^{9,12\text{-trans}}$ | 37308 | 8.845 | 1.01 |
| C18:$1^{6}$ | 44218 | 7.463 | 2.50 |
| C18:$1^{9\text{-cis}}$ | 45150 | 7.309 | 1.25 |
| C18:$1^{9\text{-trans}}$ | 31578 | 10.450 | 2.36 |
| C18:$1^{11}$ | 58527 | 5.638 | 1.43 |
| C18:0 | 30253 | 10.908 | 17.68 |

In order to determine the effect of the extraction sample on the capillary coat and to determine reproducibility within the separation system the extraction sample was allowed to set overnight in a -4 $^{o}$C freezer and then was injected into the system. This was repeated over the course of 4 days (Figure 6). A significant change can be observed in the electropherogram from the first and second day. This could possibly be attributed to the dye reacting with any remaining acid within the reaction vessel. The decrease in the peak attributed to the unreacted label between the first and second day also lends itself to this conclusion. There is a gradual loss of intensity that was observed within this

Table 2. Concentration and peak area

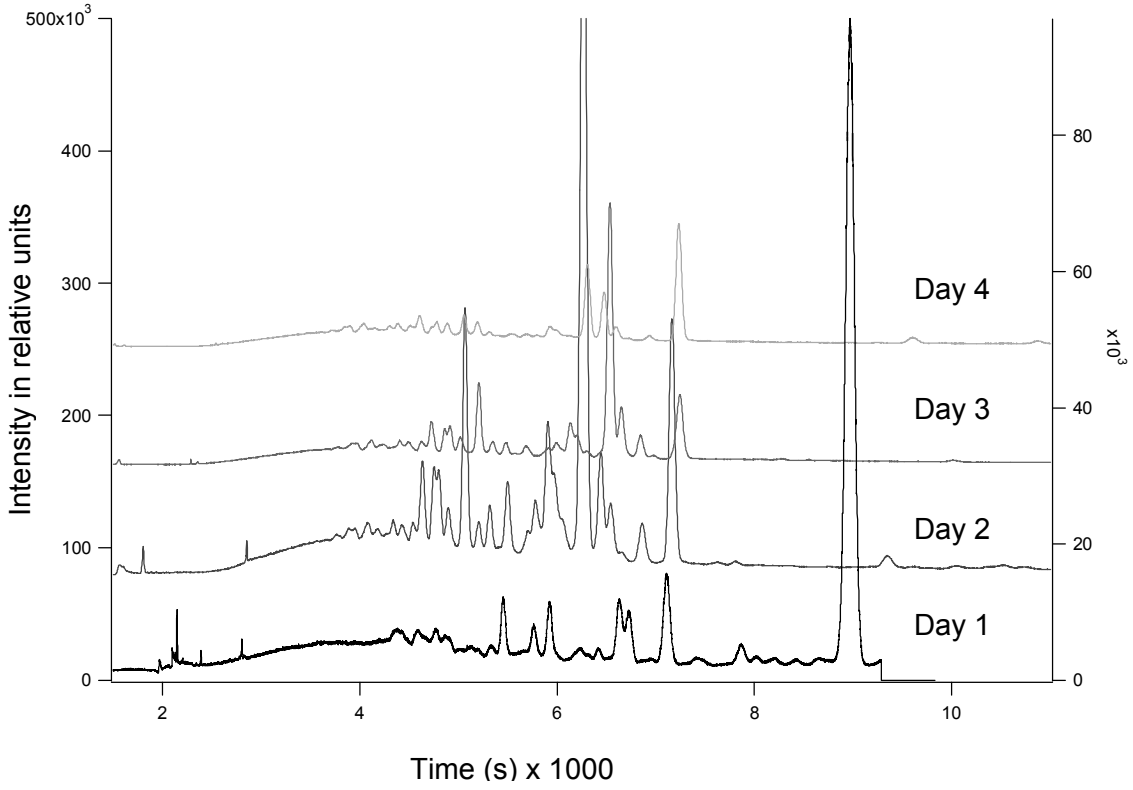


Figure 6. Effect of time on the extraction electropherogram Injection at negative pole, running voltage 25 kV, ID 50 μm, I = 3.125 mM TEAC total SMIL capillary length 100 cm, length to detection 85 cm. Subsequent traces are offset

timed trial. This intensity loss is likely due to a breakdown of the label, but further investigation into this was not sought.

| Fatty acid | Reaction concentration (μM) | Injection concentration (nM) | Integrated peak area (relative scale) |
|---|---|---|---|
| $C18:2^{9,12\text{-cis}}$ | 15.8 | 2.21 | 694.4 |
| $C18:2^{9,12\text{-trans}}$ | 29.4 | 2.21 | 1360.0 |
| $C18:1^{6}$ | 11.4 | 2.21 | 3552.6 |
| $C18:1^{9\text{-cis}}$ | 14.9 | 2.21 | 2301.5 |
| $C18:1^{9\text{-trans}}$ | 11.4 | 2.21 | 898.3 |
| $C18:1^{11}$ | 11.3 | 2.21 | 651.6 |
| C18:0 | 18.7 | 2.21 | 1428.3 |

## 4.4 Conclusion

Free fatty acids were extracted from bovine omentum and labeled with a fluorescent dye. These acids were separated into regions but a total separation into individual acids proved complicated. Structural information and relative concentrations of the sample could prove key in the total analysis of fatty acids present. While resolution in the SMIL coated capillary proved to be inferior to a previously reported TMS coated capillary coat [40] the detection limit was reduced an order of magnitude. The SMIL capillary also appeared to be resistant to analyte adsorption onto its surface, although a loss in intensity was observed when extract samples were tested over a period of several days.

The manipulation of EOF through the use of the capillary coating has proven to be a valuable tool in the separation of fatty acids. The resistance that the SMIL coat to analyte and contaminant adsorption and the stabilization of EOF improved the separation of standards and made possible the separation of bovine omentum free fatty acid extract. Further improvement to the capillary coating could potentially yield a full separation and potentially identification of free fatty acids within the extract, but further study into the surface charge density and the effect of non-aqueous solvent on the capillary surface is needed.

# REFERENCES


1. Siguel, E., *Diagnosis of essential fatty acid deficiency.* 1998: p. 2580.

2. Jones, R.; Fennessey, P.; Tjoa, S.; Goodman, S.; Fiore, S.; Burlina, A.; Rinaldo, P.; Boriack, R.; Bennett, M., *Improved stable isotope dilution-gas chromatography-mass spectrometry method for serum or plasma free 3-hydroxy-fatty acids and its utility for the study of disorders of mitochondrial fatty acid beta oxidation.* Clinical Chemistry, 2000. **46**(2): p. 149-155.

3. Costa, L.; Holwerda, U.; Almeida, I.; Poll-The, B.; Jakobs, C.; Duran, M., *Simultaneous analysis of plasma free fatty acids and their 3-hydroxy analogs in fatty acid beta oxidation disorders.* Clinical Chemistry, 1998. **44**(3): p. 463-471.

4. Hall, Geoffrey W.; Hjelm, M., *Ratios for very long chain fatty acids in plasma of subjects with peroxisomal disorders, as determined by HPLC and validated by gas chromatography-mass spectrometry.* Clinical Chemistry, 1988. **34**(6): p. 1041-1045.

5. Greenspan, E., *Separation and detection of neutral lipids and free fatty acids in a liver extract by high-performance liquid chromatography.* Analytical Biochemistry, 1982. **127**: p. 441-448.

6. Ikeda, K.; Sakaguchi, T., *High-performance liquid chromatographic determination of free fatty acids with 1-naphthylamine.* Journal of Chromatography, 1983. **272**: p. 251-259.

7. Gutnikov, G., *Fatty acid profiles of lipid samples.* Journal of Chromatography B, 1995. **671**: p. 71-89.

8. Puttmann, H.; Ochsenstein, E.; Kattermann, R., *Fast HPLC determination of serum free fatty acids in the picomole range.* Clinical Chemistry, 1993. **39**(5): p. 825-832.

9. Mehta, A.; Carlson, M., *Rapid quantitation of free fatty acids in human plasma by high performance liquid chromatography.* Journal of Chromatography B, 1998. **719**: p. 9-23.

10. Brown, J.; Turcotte, J., *The separation and the characterization of long chain fatty acids and their derivatives by reversed phase high performance liquid chromatography.* Analytical Chemistry, 1989. **21**(3): p. 193-208.

11. Chen, Y., *Analysis of fatty acids by column liquid chromatography.* Analytica Chimica Acta, 2002. **465**: p. 145-155.

12. Smith, R., *Recent advances in the high-performance liquid chromatography of fatty acids.* Journal of Pharmaceutical and biomedical analysis, 1983. **1**(2): p. 143-151.

13. Blau, K., *Handbook of derivatives for chromatography*, ed. King. 1977, London: Heyden & Sons.

14. Miwa, H., *High-performance liquid chromatographic determination of free fatty acids and esterified fatty acids in biological materials as their 2-nitrophenylhydrazides.* Analytica Chimica Acta, 2002. **465**: p. 237-255.

15. Sajiki, J., *Determination of free polyunsaturated fatty acids and their oxidative metabolites by high-performance liquid chromatography (HPLC) and mass spectrometry (MS).* Analytica Chimica Acta, 2002. **465**: p. 417-426.

16. Obert, D.; Sorenson, W.; McCann, M.; Ridley, W., *A quantitative method for the determination of cyclopropenoid fatty acids in cottonseed, cottonseed meal, and cottonseed oil (Gossypium hirsutum) by high-performance liquid chromatography.* Journal of Agricultral and Food Chemistry, 2007. **55**: p. 2062-2067.

17. Lin, J., Thomas A.; Stafford, Allan E., *Gradient reversed-phase high performance liquid chromatography of saturated, unsaturated and oxygenated free fatty acids and their methyl esters.* Journal of Chromatography A, 1995. **699**: p. 85-91.

18. Akasaka, H.; Meguro, H., *Determination of carboxylic acids by high-performance liquid chromatography with 2(2,3-anthracenedicarboximido)ethyl trifluoromethanesulfonate as a highly sensitive fluorescent labeling reagent.* Analyst, 1993. **118**(7): p. 765-768.

19. Lin, C.; McKeon, T., *Non-aqueous reversed-phase high-performance liquid chromatography of synthetic triacylglycerols and diacylglycerols.* Journal of Chromatography A, 1997. **782**: p. 41-48.

20. Heinig, F.; Martin, S.; Vogt, C., *Separation of saturated and unsaturated fatty acids by capillary electrophoresis and HPLC.* American Laboratory, 1998. **30**(10): p. 24-29.

21. Miwa, M., *High-performance liquid chromatographic analysis of serum short-chain fatty acids by direct derivatization.* Journal of Chromatography, 1987. **421**: p. 33-41.

22. Vekey, K., *Mass spectrometry and mass-selective detection in chromatography.* Journal of Chromatography A, 2001. **921**: p. 227-236.

23. Yang, M.; Paik, M.; Yoon, H.; Chung, B., *Gas chromatographic-mass spectrometric determination of plasma saturated fatty acids using pentafluorophenyldimethylsilyl derivatization.* Journal of Chromatography B, 2000. **742**: p. 37-46.

24. Vreken, A.; Bootsma, A.; Overmars, H.; Wanders, R.; Gennip, A., *Rapid stable isotope dilution analysis of very-long-chain fatty acids, pristanic acid and phytanic acid using gas chromatography-electron impact mass spectrometry.* Journal of Chromatography B, 1998. **713**: p. 281-287.

25. Moldovan, E.; Bayona, J., *Gas chromatographic and mass spectrometric methods for the characterization of long-chain fatty acids application to wool wax extracts.* Analytica Chimica Acta, 2002. **465**: p. 359-278.

26. Griffiths, W., *Tandem mass spectrometry in the study of fatty acids, bile acids, and steroids.* Mass Spectrometry Reviews, 2003. **22**: p. 81-152.

27. Gaskell, S., *Electrospray: Principles and practice.* Journal of Mass Spectrometry, 1997. **32**: p. 677-688.

28. Rezanka, J., *Chromatography of very long-chain fatty acids from animal and plant kingdoms.* Analytica Chimica Acta, 2002. **465**: p. 273-297.

29. Ohman, H.; Hamberg, M.; Blomberg, L., *Separation of conjugated linoleic acid isomers and parinaric fatty acid isomers by capillary electrophoresis.* Journal of Separation Sciences, 2002. **25**: p. 499-506.

30. Schmitz, S., *Separation of unsaturated fatty acids and related isomeric hydroperoxides by micellar electrokinetic chromatography.* Journal of Chromatography A, 1997. **781**: p. 215-221.

31. Schmitz, S., *Separation of isomeric hydroperoxides of unsaturated fatty acids by capillary electrophoresis.* Journal of Chromatography A, 1997. **767**: p. 249-253.

32. Desauziers, M.; Fanlo, J., *Simple analysis of odorous fatty acids in distillery effluents by capillary electrophoresis.* Analusis, 2000. **28**: p. 163-167.

33. *Handbook of Capillary Electrophoresis*. 2 ed, ed. J.P. Landers. 1997, New York: CRC Press.

34. Jussila, S.; Hopia, A.; Makinen, M.; Riekkola, M., *Separation of linoleic acid oxidation products by micellar electrokinetic capillary chromatography and nonaqueous capillary electrophoresis.* Electrophoresis, 1999. **20**: p. 111-117.

35. Wan, L.; Hamberg, M., *Highly efficient separation of isomeric epoxy fatty acids by micellar electrokinetic chromatography.* Electrophoresis, 1999. **20**: p. 132-137.

36. Melchior, S., *Simultaneous micellar electrokinetic chromatographic determination of isomeric fatty acid hydroperoxides and corresponding hydroxy fatty acids.* Journal of Chromatography A, 2000. **894**: p. 145-155.

37. Collet, P., *Micellar electrokinetic chromatography of long chain saturated and unsaturated free fatty acids with neutral micelles Considerations regarding selectivity and resolution optimization.* Journal of Chromatography A, 1997. **792**: p. 165-177.

38. Huang, J.; Gordon, M.; Zare, R., *Quantitative analysis of low molecular weight carboxylic acids by capillary zone electrophoresis / conductivity detection.* Analytical Chemistry, 1989. **61**: p. 766-770.

39. Arellano, S.; Roques, C.; Couderc, F.; Puig, P., *Capillary electrophoresis and indirect UV detection as a fast and simple analytical tool for bacterial taxonomy.* Journal of Chromatography A, 1997. **781**: p. 497-501.

40. Gallaher, D.; Johnson, M., *Nonaqueous capillary electrophoresis of fatty acids derivatized with a near-infared fluorophore.* Analytical Chemistry, 2000. **72**: p. 2080-2086.

41. Drange, E., *Determination of long-chained fatty acids using non-aqueous capillary electrophoresis and indirect UV detection.* Journal of Chromatography A, 1997. **771**: p. 301-309.

42. Oliveira, G.; Bruns, R.; Tavares, M., *Factorial design of electrolyte systems for the separation of fatty acids by capillary electrophoresis.* Journal of Chromatography A, 2001. **924**: p. 533-539.

43. Zuriguel, E.; Bounery,J.; Nouadje, G.; Simeon, N.; Nertz, M.; Salvayre, R.; Couderc, F., *Short chain fatty acids analysis by capillary electrophoresis and indirect UV detection or laser-induced fluorescence.* Journal of Chromatography A, 1997. **781**: p. 233-238.

44. Collet, J.P., G., *Capillary zone electrophoretic separation of C14 - C18 linear saturated and unsaturated free fatty acids with indirect UV detection.* Journal of Capillary Electrophoresis, 1996. **3**(2): p. 77-82.

45. Roldan-Assad, R., *Capillary zone electrophoretic determination of C2-C18 linear saturated free fatty acids with indirect absorbance detection.* Journal of Chromatography A, 1995. **708**: p. 339-350.

46. Breadmore, R.; Fakhari, A.; Macka, M.; Haddad, P., *Separation of Nile Blue-labeled fatty acids by CE with absorbance detection using a red light-emitting diode.* Electrophoresis, 2007. **28**: p. 1252-1258.

47. Brando, C.; Prandi, J.; Puzo, G., *Analysis of aminofluorescein-fatty acid derivatives by capillary electrophoresis with laser-induced fluorescence detection at the attomole level: application to mycobacterial fatty acids.* Journal of Chromatography A, 2002. **973**: p. 203-210.

48. Gallaher, D; Johnson, M., *Development of near-infrared fluorophoric labels for the determination of fatty acids separated by capillary electrophoresis with diode laser induced fluorescence detection.* The Analyst, 1999. **124**: p. 1541-1546.